Overlooked effect of ordinary inorganic ions on polyaluminum-chloride coagulation treatment

Yize Chen [a], Yoshihiko Matsui [b, *], Tsutomu Sato [b], Nobutaka Shirasaki [b], Taku Matsushita [b]

[a] *Graduate School of Engineering, Hokkaido University, N13W8 Sapporo 060-8628 Japan*

[b] *Faculty of Engineering, Hokkaido University, N13W8 Sapporo 060-8628 Japan*

ABSTRACT

Application of poly-aluminum chloride (PACl) coagulant is a popular mode of water treatment worldwide because of the high capacity of PACl to neutralize charge. The manufacture and use of PACls with various basicities in different regions around the world suggest that the characteristics of the raw water are important determinants of the efficacy of PACl application. However, attention has not been fully paid to the effects of water quality other than the substances to be removed. In this study, two typical PACls with different basicities were used to investigate why the performance of PACls depends on the characteristics of the raw water. We focused on the concentrations of inorganic ions in the raw water. Use of high-basicity PACl (HB-PACl) with a high content of polymeric-colloidal species (Al_b+Al_c) resulted in very slow floc formation and little turbidity removal in raw water with low concentrations of sulfate ions. The performance of the HB-PACl was inferior to that of normal-basicity PACl (NB-PACl), although the charge-neutralization capacity of the HB-PACl was higher. Rates of floc formation were strongly correlated with the rate of aluminum precipitation by hydrolysis reaction, which was identified as an indicator for evaluating the compatibility of raw water with PACl treatment. Among the common ions in natural water, the sulfate ion had the greatest ability to hydrolyze and precipitate PACl because of its divalency and tetrahedral structure. This conclusion followed from experimental results showing similar effects for selenate and chromate ions as for sulfate ions and somewhat smaller effects for thiosulfate ions. Bicarbonate ions and natural organic matter affected PACl hydrolysis-precipitation, but chloride ions, nitrate ions, and cations had little effect on PACl hydrolysis-precipitation. Interestingly, the abilities of sulfate ions to hydrolyze HB-PACl and NB-PACl were very similar, but bicarbonate ions were less effective in hydrolyzing HB-PACl than NB-PACl, and bicarbonate ions contributed little to the hydrolysis-precipitation of HB-PACl in raw water with normal alkalinity. Therefore, sufficient

coagulation with HB-PACl therefore usually requires a certain concentration of sulfate ions in water to be treated. The implication is that which anions are most influential to the hydrolysis-precipitation of PACl, and thus to PACl's coagulation ability depends on the constituents of the PACl.

Keywords:
Hydrolysis
Basicity
Sulfate ion
Additive effect
Floc
PACl

1. Introduction

Coagulation–flocculation is a fundamental process in water treatment and is applied worldwide as a pretreatment not only for traditional sedimentation–rapid sand filtration but also for membrane filtration (Edzwald, 2011). At the beginning of coagulation–flocculation, coagulant is dosed to destabilize particles during coagulation, which plays an important role in the formation of floc particles and particle removal in subsequent processes such as sedimentation and filtration (Bratby, 2016). Among various types of inorganic coagulants, polyaluminum chloride (PACl), which was first used as a coagulant in Japan, has been applied and is popular in water treatment worldwide. The aluminum species in PACl is pre-hydrolyzed and is produced in a way that gives it a high capacity for charge neutralization. The fact that the interaction between PACl and substances to be removed can proceed effectively (Bratby, 2016) leads to superior coagulation performance. Recently, high-basicity (basicity 70%), sulfated PACl has been developed and has rapidly become popular in Japan because its use results in lower aluminum residuality in treated water, higher removal efficiencies of natural organic matter (NOM), and long-term stability without the formation of precipitates during storage (Kimura et al., 2013). Furthermore, compared with normal-basicity (50%), sulfated PACl, high-basicity PACl can attenuate transmembrane pressure rise more when it is applied in coagulation pretreatment before microfiltration (Kimura et al., 2015). The market share of high-basicity PACl indicates that it is becoming popular, but for some raw water, high-basicity PACl may fail to outperform normal-basicity PACl (personal communication, Taki Chemical Co., Ltd., 2019). In other countries and regions, types of PACl similar to those used in Japan are not always used. The implication is that the PACl best suited for a local area depends on the characteristics of the raw water in that area. However, little attention has been focused on

73 the relationship between PACl and raw water quality, especially the concentrations of
74 substances not targeted for removal.

75 On the other hand, thorough studies of PACl coagulation performance have been conducted
76 on the effects of the amount of PACl added (Hendricks, 2016; Letterman and Yiacoumi, 2010)
77 and the mixing intensity after addition (Lin et al., 2013; Kan et al., 2002; and Nakazawa et al.,
78 2018). There has also been a great deal of research on the properties of various types of PACls,
79 including their basicity and chemical composition. In the case of non-sulfated PACls, the focus
80 has been on aluminum polynuclear species (Kong et al., 2021; Lin et al., 2008; Liu et al., 2021;
81 Matsui et al., 1998; Qu and Liu, 2004; Tang et al., 2015; Wu et al., 2007; Yan et al., 2007).
82 These studies have led to the common understanding that PACls with high basicity contain Al_{13}
83 and/or Al_{30} species and are excellent coagulants because of the high charge neutralization
84 capacities of these species. However, it is unclear whether this conclusion is true for all types
85 of raw waters, and the compatibility of PACls and raw water quality is not yet well understood,
86 with the exception of the compounds targeted in coagulation treatment. Because PACl and the
87 conventional coagulant alum are hydrolyzing aluminum salts, it is commonly understood that
88 alkalinity is required for their hydrolysis and that hydrolysis produces the aluminum
89 polynuclear species needed for coagulation. High alkalinity of raw water therefore increases
90 the efficiency of removal via coagulation with alum (Letterman et al., 1979; Yan et al., 2008).
91 In contrast, Saxena et al. (2019) have reported that high alkalinity in water has little effect on
92 particle removal via coagulation with high-basicity PACl, though they do not discuss the
93 mechanism responsible for this phenomenon. It has been reported that Kegging-type e-Al_{13}
94 polycation, which is said to be the active species in PACl, needs to be hydrolyzed prior to
95 interacting with colloidal particles to be removed by coagulation–flocculation (An et al., 2021).

Among other anions commonly found in natural waters, the effect of sulfate ions on alum coagulation was studied long ago (Miller, 1925). It is known that the pH range of aluminum precipitation and the sweep coagulation of aluminum sulfate extends to more acidic side than those of aluminum chloride, which attributed to the complexing of sulfate with aluminum (Hanna et al., 1970; Matijević and Stryker, 1966). Letterman (2010) reports that sulfate ion of a certain concentration in water is required for coagulation at pH 6, while no sulfate ion is needed at pH 7.5. It is explained that sulfate ion destabilizes positively charged aluminum hydroxide possibly by surface ionization and site-specific, complex formation reactions (Edzwald, 2011). The effect of sulfate ion on aluminum precipitation and is also reported elsewhere (Duan et al., 2014). Other researchers reports that sulfate ion in raw water increases the rate of floc formation (Snodgrass et al., 1984; Sricharoenchaikit and Letterman, 1987; Xiao et al., 2010). These studies have focused on conventional aluminum coagulants such as alum, but there have been a limited number of studies related to the effect inorganic anions on PACl coagulation, although it is known that sulfate ion content in PACl besides basicity influence the property and coagulation performance of PACl (Gao and Yue, 2005; Nakazawa et al., 2018; Wang et al., 2002) . Chu et al (2008) investigate the effect of sulfate ion on floc formation by PACl and report that floc formation is enhanced at low sulfate concentrations, but is reduced at high sulfate concentrations. However, the conclusions was not clearly confirmed because of very limited experiments. Chen et al. (2020) have examined the role of sulfate ions in removing superfine powdered activated carbon particles from water by coagulation, sedimentation, and sand filtration. They have pointed out that the coagulation performance of high-basicity PACl is highly dependent on the sulfate concentration in the raw water. However, the relevant mechanism and the effects of PACl types have not been fully studied.

The effect of ions other than sulfate in natural waters on PACl coagulation performance has not been fully investigated. Just as nitrate ions have little effect on coagulation by aluminum nitrate except at high concentrations (Hanna et al., 1970), monovalent ions possibly have no effect on coagulation by PACl at normal concentrations in natural surface waters. It is well known that phosphate forms precipitates with aluminum (Hanna et al., 1970), and therefore the efficiency of removal via aluminum coagulation declines as the phosphate concentration increases (Cheng et al., 2004). However, the concentration of phosphate is rarely high enough in sources of drinking water to influence removal by an aluminum coagulant. The effects of cations have rarely been investigated, but Long et al. (2021) have pointed out that the binding affinity of Ca^{2+} and Al^{3+} facilitates formation of large flocs by PACl.

In summary, although inorganic ions are the main dissolved species in natural waters, their effects on the performances of PACls with different basicity and polymerization degree, have not been systematically investigated. Because the concentrations of inorganic ions in surface waters are highly dependent on the type of soil and rock from which the minerals dissolved and entered a body of water (Nikanorov and Brazhnikova, 2009), they vary greatly worldwide, and it is necessary to figure out compatibility between PACl and raw water.

The main objective of this study was to unravel the relationships between the concentrations of inorganic ions, PACl precipitation by hydrolysis (hydrolysis-precipitation), and coagulation performance. Specifically, we investigated the effects of sulfate ions on the hydrolysis-precipitation of two PACls with different basicities and the mechanism responsible for those effects. Measurements of hydrolysis-precipitation rates were used to study the effects on PACl hydrolysis-precipitation of common ions and NOM, as well as their combined effects. Natural waters were used to verify the relationship between ion concentrations in natural waters and coagulation performance.

2. Materials & methods

2.1 Coagulants

We used sulfated PACl coagulants with high basicity (HB, 70%) and normal basicity (NB, 50%) (Taki Chemical Co., Ltd., Hyogo, Japan) in this study. We designated these as HB-PACl and NB-PACl, respectively. They were produced by the dissolution method described in Sato and Matsuda (2009). Briefly, NB-PACl was produced by heating a mixture of $AlCl_3$, $Al_2(SO_4)_3$, and $Al(OH)_3$. HB-PACl was producing from NB-PACl by adding a sodium carbonate solution to raise the basicity to 70% at a temperature <85 °C. Table S1 in the Supplementary Information (SI) lists the basic properties of the PACl coagulants. The characteristics of the PACl were analyzed by ferron assay, colloid titration, and ^{27}Al-NMR analysis (Fig. S1, SI). The details of these analytical methods are described in Text S1 (SI) (Chen et al., 2020). Stock PACls were diluted to 0.1 mol-Al/L using ultrapure water (Milli-Q water) produced by an ultrapure lab water system (Milli-Q Advantage; Merck KGaA, Darmstadt, Germany) before they were used in the experiments.

2.2 Water

Waters tested in this study were given 15 designations. Table S2, Table S3, and Table S4 (SI) show the water characteristics. Waters designated Y-1, J-1, M-1, and T-1 (Table S2, SI) were natural waters sampled from the Kuromorigawa Reservoir (Akita, Japan), Jyoganji River

(Toyama, Japan), Toyohira River (Hokkaido, Japan), and Jyoganji River, respectively. Waters J-1 and T-1 were sampled from the same river on different dates. Waters designated Y-2–6, J-2, M-2, and T-2 were prepared by adding Na_2SO_4 and $NaHCO_3$ to the respective natural water.

Series of Na_2SO_4, $NaHCO_3$, NaCl, $NaNO_3$, K_2SO_4, $MgSO_4$, $CaSO_4$, Na_2SeO_4, $Na_2S_2O_3$, and Na_2CrO_4 were prepared by dissolving Na_2SO_4, $NaHCO_3$, NaCl, $NaNO_3$, K_2SO_4, $MgSO_4$, $Ca(OH)_2$ (99.9%), Na_2SeO_4, $Na_2S_2O_3 \cdot 5H_2O$, and $Na_2CrO_4 \cdot 4H_2O$ (FUJIFILM Wako Pure Chemical Corporation., Osaka, Japan), respectively, into pure water (Elix water, Elix Advantage; Merck KGaA, Darmstadt, Germany) slightly buffered with bicarbonate (0.24 mmol/L, 12 mg/L as $CaCO_3$). SRNOM series water was prepared by dissolving Suwannee River Natural Organic Matter (International Humic Substances Society, FUJIFILM Wako Pure Chemical Corporation) into pure water slightly buffered with bicarbonate. The water was then filtered through a polytetrafluoroethylene (PTFE) membrane filter (Φ90 mm, 0.45-μm pore size; Toyo Roshi Kaisha, Ltd., Tokyo, Japan).

These waters were stored at 4 °C prior to experiments, which were begun after the temperature of the waters had returned to room temperature (~20 °C). Concentrations of ions in the water were measured by ion chromatography (Integrion and ICS-1100; Thermo Scientific, Bremen, Germany). At the experimental pH of 7.0, almost all the alkalinity is associated with bicarbonate ions. The alkalinity was measured by titration with sulfuric acid (0.01 M H_2SO_4, FUJIFILM Wako Pure Chemical Corporation), and then the concentration of bicarbonate ions was determined from the alkalinity. For measurements of dissolved organic carbon (DOC) and ultraviolet (UV) light absorbance, a water sample was filtered through a membrane filter (0.45-μm pore size; Toyo Roshi Kaisha, Ltd., Tokyo, Japan). The DOC was measured with a TOC analyzer (TOC900; GE Analytical Instruments, Inc., Boulder, CO, USA). The UV absorbance was measured at 260 nm (UV260 value) with a spectrophotometer (UV-

1800; Shimadzu, Kyoto, Japan). Turbidity was measured with a turbidity meter (WA7700; Nippon Denshoku Industries Co., Ltd; Tokyo, Japan).

2.3 Coagulation experiment

Coagulation experiments (including flocculation and sedimentation processes) were performed in a rectangular plastic beaker. Four liters of raw water were placed in the beaker, and a predetermined volume of HCl or NaOH (0.1N) was added to the water to bring the coagulation pH to 7.0 or 7.5. After 30 min of mixing, PACl was added. Rapid mixing conducted at a G value of 600 s^{-1} for 40 s was followed by three stages of slow mixing at G values (in chronological order) of 50 s^{-1} for 170 s, 20 s^{-1} for 170 s, and 10 s^{-1} for 320 s. During the rapid and slow mixing, portions of water were withdrawn from the beaker and filtered through a 10-μm pore size membrane filter (Chen et al., 2020). Aluminum concentrations in the filtered water were measured with an inductively coupled plasma mass spectrometer (ICPMS, 7700x; Agilent Technologies, Inc., Santa Clara, CA, USA). The time required to reduce the Al concentration fourfold from the initial concentration (calculation method explained in Text S2, SI), and this one-quarter concentration time was used as the index of the rate of PACl hydrolysis-precipitation (the one-quarter concentration was chosen because it was considered important that most of the aluminum be hydrolyzed and precipitated). After mixing, the water was allowed to stand for 1 h for sedimentation. The turbidities of the raw water and the supernatant after sedimentation were measured with a turbidity meter. The zeta potentials of the water sampled after rapid mixing were measured with a zeta potential meter (Zetasizer Nano ZS; Malvern Panalytical Ltd., Almelo, Netherlands) using a dip cell.

Floc particle size was measured by using a particle-size analyzer (Microtrac MT3300EXII; MicrotracBEL Corp., Osaka, Japan). Throughout the time of mixing, water in the beaker was introduced into the analyzer by a peristaltic pump at a flow rate of 0.5 mL/s (a sufficiently slow speed to avoid floc breakage). The outflow from the analyzer was discarded directly without circulation. As an index of floc formation speed, we used the time until the D50 (median diameter) of floc particles grew to 500 μm. Because the maximum D50 values were approximately 1 mm, the size was set to 0.5 mm. The time until the D50 grew to 500 μm and its 95% confidence interval were determined from the model-fit (Chassagne, 2021) by using Minitab (Minitab, LLC, Pennsylvania, USA).

3. Results and discussion

3.1 Hydrolysis-precipitation rate as a performance index of coagulation and flocculation

A previous study has revealed that the removability of superfine powdered activated carbon (SPAC) particles by coagulation and sedimentation varies greatly as a function of the basicity of PACl and the sulfate ion concentration of the raw water (J-1 water and J-2 water, Fig. S2, SI) (Chen et al., 2020). For HB-PACl, the residual turbidity of the supernatant water was high in J-1 water (low sulfate ion concentration), but the residual turbidity was very low in J-2 water (high sulfate ion concentration). In contrast, when NB-PACl was applied, the residual turbidity was low in both J-1 and J-2 water. To confirm the universality of this phenomenon for the turbidity components (not SPAC), we conducted experiments using Y-, M-, and T-series waters (because the J-series water was consumed), and we varied the amount of PACl added and the

coagulation pH. In addition to measuring the turbidity of the supernatant after sedimentation, we measured floc particle size during rapid and slow mixing (Fig. S3 and Fig. S4).

Because the sulfate ion concentrations in the Y-1 and T-1 waters used in the experiment were low (< 0.06 mmol-SO_4^{2-}/L), coagulation with HB-PACl in these waters took more than 11 min to form floc particles with a D50 > 500 μm or did not form floc particles > 500 μm (Fig. 1). As a result, the rate of removal of turbidity after sedimentation was also generally low (Fig. 1). However, because floc formation was faster in M-1 water with higher sulfate ion concentrations, turbidity removal rates were higher. When sufficient sulfate ions were added to the Y-1 water, which had the lowest concentration of ions, to increase the concentration of sulfate ions to greater than 0.1 mmol/L, floc formation was faster, and the rate of turbidity removal was higher. In the case of NB-PACl, flocs with a D50 of 500 μm or greater were formed within 7 min in raw water with low as well as high sulfate ion concentrations, and the turbidities of the supernatants were low. On the weak alkaline side of pH 7.5, the coagulation pH at which PACls of high basicity excel (Kimura et al., 2013), floc formation was faster than at pH 7.0, but floc formation still required a longer time if the sulfate ion concentration in the water was low (0.04 mmol/L) than with the NB-PACl (Fig. S5A, SI). Furthermore, even when the dose was increased for HB-PACl, floc particles did not form in raw water with low sulfate ion concentrations, and the rate of turbidity removal was low (Fig. S6A,B, SI). Therefore, the reason why coagulation-flocculation by HB-PACl does not work well in raw water with low sulfate ion concentrations does not appear to be the insufficiency of its dose. In contrast, when the sulfate ion concentration in the raw water was high, the rate of floc formation also increased with an increase of PACl dose (Fig. S6C, SI), as is normally observed.

Because aluminum coagulants such as PACl consume alkalinity in the coagulation reaction, bicarbonate ions may also have an effect on PACl coagulation and floc formation. In NB-PACl,

floc formation was faster in raw water with bicarbonate ion concentrations greater than 0.2 mmol/L than in raw water with bicarbonate ion concentrations less than 0.2 mmol/L, and floc particles with D50s of 500 μm or more were formed in a shorter time (Fig. 2B). The effect of bicarbonate ion concentration was not clearly apparent in HB-PACl (Fig. 2A). Overall, the rate of floc formation depended on the raw water, and in raw water with low concentrations of sulfate ions, the rate of floc formation with HB-PACl was inferior to that with NB-PACl.

Conventional indices of coagulant properties include the ferron distribution of Al species, the colloid charge, and ^{27}Al nuclear magnetic resonance (NMR). The analytical results for the two PACls used in this study are shown in Fig. S1(SI). The ferron distribution (Panel A) indicated that HB-PACl had a higher content of Al_b + Al_c, which are generally regarded as the aluminum species with the highest charge-neutralization capacity (Yan et al., 2008). The colloid charge was actually higher for HB-PACl than for NB-PACl (Panel B). The peak at 62.5 ppm in the ^{27}Al-NMR spectrum (Panel C) indicated that the concentration of Kegging-type e-Al_{13} polycations, which have relatively high charge neutralization ability (Chen et al., 2007; Parker and Bertsch, 1992; Sposito, 1995), was higher in HB-PACl than in NB-PACl. This superior charge neutralization ability of HB-PACl suggests that it should be a better coagulant than NB-PACl.

The zeta potential has commonly been used as an indicator of whether the neutralization of the particle charge necessary for coagulation is sufficient. In our experiments, we measured the zeta potential of the floc particles after rapid mixing for coagulation. The zeta potentials of floc particles seemed closer to zero when they were formed by HB-PACl than by NB-PACl (Panel A of Fig. S7, SI), and the former particles were better destabilized because of the higher charge-neutralization capacity of the HB-PACl, but HB-PACl coagulation removed less turbidity than NB-PACl coagulation. Even when HB-PACl reduced the zeta potential of the flocs closer to

285 zero than NB-PACl, floc formation took a longer time (Panel A). The zeta potential could
286 therefore not explain why the coagulation performance of HB-PACl and NB-PACl depended
287 on the raw water, and it was unclear why the charge neutralization mechanism was unrelated
288 to the inferior coagulation performance of HB-PACl compared with NB-PACl when raw water
289 with a low concentration of sulfate ions was treated. In contrast, moderate correlations were
290 apparent between the zeta potential and turbidity removal for each HB-PACl and NB-PACl
291 (Panel B of Fig. S7, SI). However, the rates of turbidity removal by HB-PACl and NB-PACl
292 were very different, even when the zeta potentials were the same. Although charge
293 neutralization as measured by the zeta potential is still a necessary requirement for coagulation
294 by HB-PACl and NB-PACl, comparison of the turbidity removal abilities of HB-PACl and NB-
295 PACl is not possible based on zeta potential alone.

296 A previous study dealing with coagulation of superfine powdered activated carbon particles
297 (Chen et al., 2020) mentions an Al hydrolysis-precipitation reaction and proposes that the
298 change of dissolved Al concentration, which is related to the polymerization of aluminum
299 species, is a key property, besides charge-neutralization capacity, for proper coagulation,
300 including formation of large floc particles. Chu et al (2008) indicate that zeta potential is not
301 the only indicator for the coagulant efficiency when aluminum precipitation significantly
302 improves coagulation. An et al. (2021) also mention the importance of hydrolysis and have
303 reported that Al_{13} polycation hydrolyzes while retaining its structure. In this study, we used
304 one-quarter concentration time (the time required to reduce the soluble—precisely 10 μm or
305 less in particle size—Al concentration fourfold from the initial concentration, as described in
306 Section 2.3) as the index of the rate of PACl hydrolysis-precipitation. As shown in Fig. 3, when
307 the rate of floc formation was slow (a long time was required for the floc to grow to a size of
308 500 μm), the one-quarter concentration time was long (the rate of PACl hydrolysis-

309 precipitation was slow). The rates of floc formation, which depended on the type of coagulant
310 (HB-PACl or NB-PACl) and dose, water quality (sulfate and bicarbonate ion concentrations),
311 and pH, were correlated to the rates of PACl hydrolysis-precipitation (R^2 = 0.614). The
312 correlation became somewhat stronger (R^2 = 0.672) when we omitted the datum associated
313 with the lowest dose (1.5 mg/L), which resulted in low particle charge neutralization (Fig. S8,
314 SI). Hydrolysis of aluminum was therefore found to be an important factor for floc formation.
315 The rate of turbidity removal was also measured, and the results are shown in Fig. S9 (SI). Low
316 turbidity removal (< 70%) was observed when the rates of PACl hydrolysis-precipitation were
317 slow (the one-quarter concentration time exceeded 30 s) or the zeta potential was lower than
318 −5 mV (Fig. S7B, SI). In summary, the dependence of coagulation performance on PACl type
319 and water quality (sulfate ion concentration) was related to the hydrolysis-precipitation of
320 aluminum species in the PACl. The rate of hydrolysis-precipitation was identified as an
321 indicator that could be used to evaluate the compatibility of the raw water with high-basicity
322 PACl. Furthermore, the fact that there was no difference in the hydrolysis of PACl when looking
323 at solubility/insolubility around 1 μm, which is usually used, or at 0.1 μm in the colloidal region
324 (Chen et al., 2020), and that the hydrolysis-precipitation index by concentration passing 10 μm
325 was valid in this study, suggests that the effect of aluminum hydrolysis-precipitation on floc
326 formation is different from that of charge neutralization by colloidal aluminum polymers. The
327 former is probably a main indicator of sweep flocculation, while the latter is that of charge-
328 neutralization coagulation. Therefore, even though the aluminum distribution by the ferron
329 assay, which is an indicator of the amount of highly charge-neutralizing poly-nuclear species
330 contained in PACl, are the same, the difference in hydrolysis-precipitation (Chen et al., 2020)
331 is due to the fact that the charge-neutralization and the hydrolysis-precipitation are looking at
332 different properties of PACl.

333

334 *3.2 Effects of inorganic ions and natural organic matter*

335

336 We investigated the effect on PACl hydrolysis-precipitation of inorganic ions commonly
337 found in natural water, including sulfate and bicarbonate ions, by using artificial waters
338 containing one major anion and one major cation each. The time for the Al concentration in the
339 filtrate to decrease to one-fourth of the original concentration (one-quarter concentration time)
340 was calculated from the experimental data and used as an index of the rate of hydrolysis-
341 precipitation, as in Section 3.1. If the rates of hydrolysis-precipitation were very slow in the
342 waters with monovalent ions and the one-quarter concentration time was not obtainable, the
343 one-quarter concentration time was calculated from the one-half concentration time by using
344 the linear relationship between the one-half concentration time and one-quarter concentration
345 time (Text S2 and Fig. S10, SI). Figure 4 shows the one-quarter concentration times of PACl
346 hydrolysis-precipitation plotted against anion concentrations. Bicarbonate ions hydrolyzed
347 both HB-PACl and NB-PACl at higher concentrations than sulfate ions. Much higher
348 concentrations of chloride and nitrate ions were required to hydrolyze HB-PACl and NB-PACl.
349 The concentrations of sulfate, bicarbonate, chloride, and nitrate ions required for a one-quarter
350 concentration time of 60 s for hydrolysis-precipitation of HB-PACl were approximately 0.174,
351 2.20, 34, and 42 mmol/L. Those of NB-PACl were 0.168, 1.00, 14, and 12 mmol/L, respectively
352 (Table 1). Because such high chloride and nitrate ion concentrations are not normally found in
353 natural river waters, nitrate and chloride ions do not have a substantial effect on the hydrolysis-
354 precipitation of PACl in river water. The bicarbonate ion concentration of 1.0 mmol/L
355 (corresponding to an alkalinity of 1 meq/L) required for hydrolysis-precipitation of NB-PACl
356 was similar to the concentrations sometimes observed in natural surface waters. The

357 bicarbonate concentration required for hydrolysis-precipitation of HB-PACl (2.20 mmol/L)
358 was relatively high. Therefore, the bicarbonate ion concentration of ~0.1–0.8 mmol/L
359 (corresponding to an alkalinity of 0.1–0.8 meq/L) observed in the natural surface waters we
360 used would contribute to the hydrolysis-precipitation of NB-PACl but contribute to a much
361 lesser extent to the hydrolysis-precipitation of HB-PACl. This conclusion explains why the
362 effect of bicarbonate was more clearly apparent in the formation of floc particles by NB-PACl
363 than HB-PACl (Fig. 2 in Section 3.1).

364 The concentrations of sulfate ions required for hydrolysis-precipitation of NB-PACl and
365 HB-PACl also differed, but the difference (0.174 vs. 0.168 mmol/L) was not large compared
366 with the difference of bicarbonate ion concentrations (2.20 vs. 1.00 mmol/L). Therefore, the
367 reason for the poor performance of HB-PACl in water with low sulfate ion concentrations was
368 partly the high concentration of sulfate ions required for the hydrolysis-precipitation of HB-
369 PACl but mainly the small contribution of bicarbonate ions to the hydrolysis-precipitation of
370 HB-PACl. Conversely, because bicarbonate ions contribute to the hydrolysis-precipitation of
371 NB-PACl, hydrolysis-precipitation proceeds satisfactorily, even in water with a low
372 concentration of sulfate ions, and NB-PACl is a better coagulant than HB-PACl in water with
373 a low concentration of sulfate ions (Section 3.1). Furthermore, a review of previous data (Chen
374 et al., 2020) revealed that PACl produced by high-temperature heating and base-titration
375 requires 3 times the concentration of sulfate ions for hydrolysis-precipitation and floc
376 formation than HB-PACl produced by the widely and commercially applied dissolution method
377 even at the same basicity. This difference suggests that the effect of anions on the hydrolysis-
378 precipitation of PACl (i.e., which ion hydrolyzes each component in the PACl) influences the
379 suitability of PACl for raw water. This study revealed that HB-PACl, which contains a larger
380 amount of Al_b+Al_c and thus have has a high charge-neutralization capacity than NB-PACl, is

not easily hydrolyzed by bicarbonate ions and requires a higher concentration of sulfate ions than NB-PACl. If various types of PACl are manufactured, sold, and used around the world (Jiang, 2001; X. Wang et al., 2017; Zouboulis and Tzoupanos, 2010), and if each of them is suitable for a region, the diversity of PACls may be related to the anion concentrations in the raw water.

Bicarbonate ions were about 11 times more effective than nitrate and chloride ions in promoting hydrolysis-precipitation. Because the concentration of carbonate ions is 1% of the concentration of bicarbonate ions at the experimental pH of 7.0, its effect would be small compared to that of bicarbonate. Because the hydrolysis-precipitation of PACl consumes alkalinity, bicarbonate ions play a role as a source of alkalinity (Bratby, 2016; Dousma and de Bruyn, 1978), and their influence is thus likely to be greater than that of monovalent ions such as chloride ions. The sulfate ion was ~200 times more effective than chloride and nitrate ions in hydrolyzing PACl. It was also >6 times more effective than the bicarbonate ion. This difference was not eliminated by basing the calculations on ionic strengths rather than molar concentrations. The effect of the sulfate ion on aluminum coagulant (including PACl) performance is explained by its capacity to neutralize the positive charge of hydrolyzing colloids of aluminum (Edzwald, 2011). However, there is roughly a 60-fold difference in the relative effectiveness of charge neutralization by divalent ions compared with monovalent ions according to the Schulze–Hardy rule (Bratby, 2016) but less than a 60-fold difference according to the modified Schulze–Hardy rules by the DLVO theory of the electric double layer (Rakshit et al., 2021). The relative effectiveness on the critical coagulation concentration has been reported to be around 60 or less (Nowicki and Nowicka, 1994). These values are still smaller than the observed relative effectiveness of PACl hydrolysis-precipitation (~200). The charge

404 neutralization mechanism on the basis of these rules is therefore insufficient to explain the
405 effect of sulfate, chloride, and nitrate ions on PACl hydrolysis-precipitation.

406 The effects of cations were also investigated by using waters containing sulfate ion as the
407 major counter anion. As shown in Fig. S11 (SI), the rate of hydrolysis-precipitation was not
408 influenced by whether the counter cation was Na^+ or Ca^{2+}. K^+ and Mg^{2+} slightly retarded the
409 rate of hydrolysis-precipitation of HB-PACl compared with Na^+ or Ca^{2+}, whereas K^+, Mg^{2+},
410 Na^+, and Ca^{2+} did not have any effect on the rate of hydrolysis-precipitation of NB-PACl.
411 Because K^+ and Mg^{2+} are not as abundant as Na^+ or Ca^{2+} in normal natural river water and the
412 effects of cation type are much smaller than those of anion type, the types of cations would not
413 be expected to substantially affect PACl hydrolysis-precipitation.

414 Because it is commonly known that NOM affects coagulation performance, we investigated
415 its role in PACl hydrolysis-precipitation. We conducted a test of hydrolysis-precipitation rates
416 by using artificial waters with the same NOM (SRNOM) and different DOC concentrations.
417 The results for HB-PACl and NB-PACl are shown in Fig. S12 (SI). Rates of hydrolysis-
418 precipitation were slower in waters with lower NOM concentration, and the presence of NOM
419 accelerated the hydrolysis-precipitation of PACl. These results may be related to the fact that
420 NOM is a target compound for coagulation treatment and reacts with PACl coagulants to form
421 precipitates. At the same DOC concentration, HB-PACl was hydrolyzed at a slower rate (longer
422 one-quarter concentration time) than NB-PACl, a trend consistent with the results for anions,
423 including sulfate ions (Section 3.1). Although the DOC concentrations required for hydrolysis-
424 precipitation were not very high (~1.5 mg/L and ~1.0 mg/L for HB-PACl and NB-PACl,
425 respectively, for a one-quarter concentration time of 60 s), surface waters with DOC
426 concentrations lower than 1.0 mg/L are not uncommon in Japan. For such water, the ionic
427 composition required for PACl hydrolysis-precipitation is key for floc formation when HB-

PACl is applied. In contrast, the influence of the nature of the NOM must not be forgotten. Chromophoric NOM with high specific ultraviolet absorbance values is removed by aluminum coagulation, but non-chromophoric NOM is less amenable to removal (Archer and Singer, 2006; Edwards, 1997; Edzwald, 2011; Ou et al., 2014). Therefore, UV absorbance is considered more suitable than the concentration of DOC as a metric of the concentration of NOM that affects the rate of PACl hydrolysis-precipitation: this is discussed further in section 3.4.

The mechanisms responsible for the effects of NOM and anions on the hydrolysis-precipitation of PACl would be expected to differ. The correlation between the one-half and the one-quarter concentration times regardless of anion species suggests that anions accelerate the rate of hydrolysis-precipitation of PACl by the same mechanism (Al concentration vs. time, Fig. S10, SI). In contrast, the hydrolysis-precipitation of PACl by NOM followed a different trend from hydrolysis-precipitation by anions because the relationship between the half-lives and one-quarter concentration times in the case of hydrolysis-precipitation by NOM differed significantly from the relationship for hydrolysis-precipitation by anions (Fig. S13, SI). The fact that the initial rate of the hydrolysis-precipitation reaction was very rapid in the presence of NOM compared with the rate in the absence of NOM (Text S2) was probably due to the direct reaction of NOM with PACl (Barrett et al., 2000; Bratby, 2016; Edzwald, 1993; Yue et al., 2021). This study did not examine in depth the detailed properties of NOM and its stoichiometric relationship to hydrolysis-precipitation because such an examination would have been beyond the scope of this study (Hussain et al., 2013; Li et al., 2021; Su et al., 2017), but it should definitely be a subject of future research.

3.3 Effect of sulfate ions and its mechanism

To further clarify the mechanism by which sulfate ions accelerate PACl hydrolysis-precipitation and improve coagulation performance, we selected three other oxo anions (the selenate ion [SeO_4^{2-}], thiosulfate ion [$S_2O_3^{2-}$], and chromate ion [CrO_4^{2-}]) that have the same valency and/or similar structure to sulfate ion, and we investigated their abilities to accelerate PACl hydrolysis-precipitation. Figure 5 shows the relationship between the one-quarter concentration times and the concentrations of anions in raw water. For the rates of hydrolysis-precipitation of both HB-PACl and NB-PACl, water containing chromate ions or selenate ions was as effective as water containing sulfate ions (Panel B in Fig. 5). The effect of thiosulfate ions was somewhat smaller than that of sulfate ions, but the difference was much smaller than the difference between sulfate ions and monovalent ions (chloride, nitrate, and bicarbonate ions). The main reason for the effect of sulfate ions on the hydrolysis-precipitation of PACl therefore seemed to be its divalency, but the effect was not explained solely by the electric double layer theory that divalent ions are more effective, as mentioned in Section 3.2.

The difference between the effects of sulfate ions and thiosulfate ions on the rate of hydrolysis-precipitation indicates that the effect of sulfate ions is not due only to their divalency. There is another property of sulfate ions that affects PACl hydrolysis-precipitation. A possible explanation is related to their pKa2, which reflects the tendency of the ion to keep a proton, H^+. A lower pKa2 value means that the ion tends to donate a proton. Among the four anions, the thiosulfate ion, which had the least effect on PACl hydrolysis-precipitation, has the lowest pKa2. However, the chromate ion has the largest pKa2 but had an effect on PACl hydrolysis-precipitation similar to that of the sulfate and selenate ions (Fig. S14, SI). Sulfate, selenate, and chromate ions have a similar structure consisting of a central atom surrounded by four equivalent oxygen atoms in a tetrahedral arrangement, whereas the thiosulfate ion is a sulfate ion with one oxygen replaced by sulfur. The effect on hydrolysis-precipitation may therefore

476 be related not only to the valence but also to the structure of the anion. Duan et al. (2014) have
477 mentioned that sulfate ions chemically bound to an Al precipitate increase its negative surface
478 charge and thereby prompt the aggregation of precipitates. Because of their structure, sulfate
479 ions would chemisorb onto colloidal aluminum species and thereby effectively neutralize their
480 charge and promote further hydrolysis-precipitation and the formation of coarse aluminum
481 colloidal aggregates. This supports the possibility that sulfate ions form complexes with
482 aluminum (Hanna et al., 1970; Matijević and Stryker, 1966). This process could result in sulfate
483 ions' promoting hydrolysis-precipitation of PACl more efficiently than the Schulze–Hardy rule
484 predicted by DLVO theory.
485
486 *3.4 Effect of sulfate and bicarbonate ions and NOM mixture*
487
488 The simultaneous effects of anions and NOM in water need to be considered because
489 natural waters contain a variety of ions, not just cation–anion pairs as described in Section 3.2.
490 Because sulfate ions, bicarbonate ions, and NOM had the largest effects on PACl hydrolysis-
491 precipitation, we investigated their synergistic/additive effects. Chloride and nitrate ions were
492 omitted from this study because they affected PACl hydrolysis-precipitation only at
493 concentrations much higher than those found in surface waters. The fact that increasing the
494 concentration of either sulfate ions, bicarbonate ions, or NOM shortened the one-quarter
495 concentration time of hydrolysis-precipitation (Figs. S15 and S16, SI) indicated that the rate of
496 hydrolysis-precipitation had increased. Increasing the concentrations of both sulfate and
497 bicarbonate ions led to a much shorter one-quarter concentration time than increasing the
498 concentration of sulfate or bicarbonate ions separately. We therefore analyzed the experimental
499 data on the assumption that the effects of sulfate and bicarbonate ions and NOM were additive.

Table 1 summarizes the concentrations required for a one-quarter concentration time of 60 s (see Section 3.2). If the effects of sulfate ion, bicarbonate ion, and NOM are additive, the total concentration of the components affecting the hydrolysis-precipitation rate can be expressed in terms of the sulfate ion concentration by the following equation.

$$C_{SE} = C_S + aC_{BC} + bC_{NOM} \quad (1)$$

Here, C_{SE} is the sulfate-ion-equivalent concentration for the overall effect of sulfate ions, bicarbonate ions, and NOM (mmol/L). C_S, C_{BC}, and C_{NOM} are the concentrations of sulfate ions (mmol/L), bicarbonate ions (mmol/L), and NOM (cm^{-1}). UV absorbance at 260 nm was used as a measure of the NOM that reacts with PACl. The parameter *a* is the ratio of the effects of bicarbonate ions to sulfate ions, and *b* is the corresponding ratio of the effects of NOM to sulfate ions. Table 1 shows the values of *a* and *b*.

We then obtained Fig. 6 by plotting the one-quarter concentration times for PACl hydrolysis-precipitation versus the C_{SE} values of the water. Despite the various concentrations of sulfate ions, bicarbonate ions, and NOM, the data appear to reflect a single relationship (the values for one-quarter concentration times of less than 5 s were scattered and imprecise because the aluminum concentrations decreased rapidly). The results shown in Fig. 6 indicate that the effects of sulfate ion, bicarbonate ion, and NOM on the hydrolysis-precipitation of PACl vary greatly, but the interactions between the effects are additive. The graph shows that the rate of hydrolysis-precipitation begins to decrease when the C_{SE} falls below 0.2 mmol/L. Incidentally, when the DOC concentration was used instead of UV260 as the metric of the NOM concentration, the functional relationship shown in Fig. 6 was not obtained (Fig. S17, SI). This

confirms that UV260 is more appropriate as the concentration of NOM that reacts with PACl and promotes hydrolysis-precipitation.

Using the *a* and *b* values, we analyzed the contributions of sulfate and bicarbonate ions and NOM to C_{SE} and the hydrolysis-precipitation of HB-PACl and NB-PACl in T-1 and T-2 waters (Fig. 7). The reciprocal of the one-quarter concentration times for hydrolysis-precipitation when HB-PACl was added to the T-1 water was 0.007 s^{-1}. Sulfate ions, bicarbonate ions, and NOM were estimated to contribute 47%, 21%, and 32%, respectively, to the hydrolysis-precipitation. In T-2 water, in which the concentrations of sulfate and bicarbonate ions were higher, the reciprocal one-quarter concentration time was 0.063 s^{-1} for HB-PACl, and the contributions of sulfate ions, bicarbonate ions, and NOM to hydrolysis-precipitation were 58%, 24%, and 18%, respectively. In contrast, when NB-PACl was added to the T-1 water, the reciprocal one-quarter concentration was 0.043 s^{-1}, and the contributions of sulfate ions, bicarbonate ions, and NOM to the hydrolysis-precipitation were estimated to be 35%, 34%, and 31%, respectively. In T-2 water, the reciprocal one-quarter concentration time for NB-PACl was 0.22 s^{-1}, and the corresponding contributions to hydrolysis-precipitation were 44%, 39%, and 17%, respectively. The much larger reciprocal one-quarter concentration times for NB-PACl versus HB-PACl indicated that the former was much more effective than the latter. Use of Eq. (1) enabled us to determine the contribution of each component to the hydrolysis-precipitation and thus to coagulation as well as how the contributions varied with the components in the raw water.

The main substances in the water that affected PACl hydrolysis-precipitation were sulfate ions, bicarbonate ions, and NOM. These substances interacted additively to enhance the hydrolysis-precipitation of PACl. This additive interaction may have led to better PACl coagulation performance. But the enhancement depended on whether the PACl was a HB-PACl

or NB-PACl. We then used natural waters (Y series) containing different concentrations of sulfate ions, bicarbonate ions, and NOM to verify that the effects on coagulation, flocculation, and sedimentation were in all cases additive. The flocculation time (the time for the D50 of floc particles to reach 500 μm) was strongly correlated with the sulfate-ion-equivalent concentration for the overall effect of sulfate ions, bicarbonate ions, and NOM (by UV260) as shown in Fig. 8 (note: as shown in Fig. 18S, no correlations were obtained for $C_{\mathrm{SE}}(\mathrm{DOC})$, which supports that some NOM sensitive to UV is more effective for hydrolysis-precipitation of PACl than the entire NOM measured by DOC). The C_{SE} was therefore a useful metric of the effectiveness of a PACl coagulant.

In this study, it was shown that high-basicity PACl, in which the polymerization of aluminum is more advanced than that of normal-basicity PACl, is difficult to hydrolyze, and therefore, PACl hydrolysis is important for the coagulation-flocculation by the PACl, in addition to neutralizing the charge on the particles to be removed. Anions such as sulfate ion are important for the hydrolysis of PACl. On the other hand, it has been reported that mixing intensity during rapid mixing for coagulation process is important for high-basicity PACl (Nakazawa et al., 2018), so it is also important to study how physical condition, such as mixing intensity and water temperature, affect PACl hydrolysis-precipitation. We feel the high-intensity mixing promote the hydrolysis-precipitation of PACl.

4. Conclusion

This study comprehensively investigated the ability of ions commonly found in natural surface waters to increase the rate of hydrolysis-precipitation of PACls and thereby reduce turbidity by enhancing coagulation and the formation of floc particles.

The rates of floc formation by PACls with different basicities and polymerization (HB-PACl and NB-PACl) varied as a function of the characteristics of the raw water. Those variations were related to the hydrolyzability of the PACls. Floc formation rates were strongly correlated with the rates of PACl hydrolysis-precipitation.

Hydrolysis-precipitation of PACls was enhanced by sulfate, selenate, chromate, thiosulfate, and bicarbonate ions, and NOM. Sulfate, selenate, and chromate ions had >200 times greater ability to hydrolyze and precipitate PACl than chloride ions and nitrate ions. This greater ability was attributable to both the divalency and tetrahedral structure of the sulfate ion, which supports the possible mechanism of the complexing of sulfate with aluminum. Cations in the water had little effect on the rate of PACl hydrolysis-precipitation. The ability of bicarbonate ions to hydrolyze PACls was more than tenfold that of chloride and nitrate ions but much less than that of sulfate ions.

HB-PACl was hydrolyzed more slowly than NB-PACl. In particular, HB-PACl was very slowly hydrolyzed by bicarbonate ions. The hydrolysis-precipitation of HB-PACl needed for sufficient flocculation performance therefore required a certain concentration of sulfate ions in natural surface water. In contrast, because NB-PACl was hydrolyzed to some extent by bicarbonate ions, the concentration of sulfate ions required for hydrolysis-precipitation was low and in practice was rarely insufficient.

Sulfate ions, bicarbonate ions, and NOM affected the rate of hydrolysis-precipitation of PACl in an additive manner. The rates of PACl hydrolysis-precipitation were therefore described rather well by sulfate-ion-equivalent concentrations, which represent the additive

effects of sulfate ions, bicarbonate ions and NOM. The rate of floc formation was low when the sulfate-ion-equivalent concentration in the raw water was low.

In this study, it was found that hydrolysis-precipitation of PACl, beside charge neutralization, is necessary for coagulation-flocculation. Sulfate ion, bicarbonate ion, and NOM accelerate the hydrolysis-precipitation, but their effects are different depending on the type of PACl. The effectiveness of PACl, which has a high charge-neutralization capacity due to its high content of Alb and AlC, has been demonstrated in a number of papers. However, such PACl is difficult to hydrolyze in raw water with low sulfate ion concentrations, resulting in poor coagulation-flocculation. Since PACl is composed of a variety of aluminum polymeric species, clarifying which aluminum species is hydrolyzed by which anion or NOM and at what rate will undoubtedly be an important research theme in the future.

Acknowledgments

This work was supported by a Japan Society for the Promotion of Science Grant-in-Aid for Scientific Research S (no. 16H06362) and A (no. 21H04567). The authors gratefully acknowledge Taki Chemical for providing PACl coagulants, and we thank Sapporo Waterworks Bureau, the Waterworks Division of Yurihonjo City, and the Water and Wastewater Works Bureau of Toyama City for water sampling.

References

An, G., Yue, Y., Wang, P., Liu, L., Demissie, H., Jiao, R., Wang, D., 2021. Deprotonation and aggregation of Al13 under alkaline titration: A simulating study related to

617 coagulation process. Water Res. 203, 117562.
618 https://doi.org/10.1016/j.watres.2021.117562
619 Archer, A.D., Singer, P.C., 2006. Effect of SUVA and enhanced coagulation on removal of
620 TOX precursors. Journal-American Water Work. Assoc. 98, 97–107.
621 Barrett, S.E., Krasner, S.W., Amy, G.L., 2000. Natural organic matter and disinfection by-
622 products: Characterization and control in drinking water—an overview.
623 Bratby, J., 2016. Coagulation and flocculation in water and wastewater treatment. IWA
624 publishing.
625 Chassagne, C., 2021. A simple model to study the flocculation of suspensions over time.
626 Chem. Eng. Res. Des. 172, 302–311. https://doi.org/10.1016/j.cherd.2021.06.006
627 Chen, Y., Nakazawa, Y., Matsui, Y., Shirasaki, N., Matsushita, T., 2020. Sulfate ion in raw
628 water affects performance of high-basicity PACl coagulants produced by Al(OH)3
629 dissolution and base-titration: Removal of SPAC particles by coagulation-flocculation,
630 sedimentation, and sand filtration. Water Res. 183, 116093.
631 https://doi.org/10.1016/j.watres.2020.116093
632 Chen, Z., Luan, Z., Fan, J., Zhang, Z., Peng, X., Fan, B., 2007. Effect of thermal treatment on
633 the formation and transformation of Keggin Al13 and Al30 species in hydrolytic
634 polymeric aluminum solutions. Colloids Surfaces A Physicochem. Eng. Asp. 292, 110–
635 118. https://doi.org/10.1016/j.colsurfa.2006.06.005
636 Cheng, W.P., Chi, F.H., Yu, R.F., 2004. Effect of phosphate on removal of humic substances
637 by aluminum sulfate coagulant. J. Colloid Interface Sci. 272, 153–157.
638 https://doi.org/10.1016/j.jcis.2003.08.074

639 Chu, Y., Gao, B., Yue, Q., Wang, Y., 2008. Investigation of dynamic processing on
640 aluminum floc aggregation: Cyclic shearing recovery and effect of sulfate ion. Sci.
641 China, Ser. B Chem. 51, 386–392. https://doi.org/10.1007/s11426-007-0129-2
642 Dousma, J., de Bruyn, P.L., 1978. Hydrolysis-precipitation studies of iron solutions. II.
643 Aging studies and the model for precipitation from Fe(III) nitrate solutions. J. Colloid
644 Interface Sci. 64, 154–170. https://doi.org/10.1016/0021-9797(78)90345-4
645 Duan, J., Wang, J., Guo, T., Gregory, J., 2014. Zeta potentials and sizes of aluminum salt
646 precipitates - Effect of anions and organics and implications for coagulation
647 mechanisms. J. Water Process Eng. 4, 224–232.
648 https://doi.org/10.1016/j.jwpe.2014.10.008
649 Edwards, M., 1997. Predicting DOC removal during enhanced coagulation. Journal-
650 American Water Work. Assoc. 89, 78–89.
651 Edzwald, J., Association, A.W.W., 2011. Water quality & treatment: a handbook on drinking
652 water. McGraw-Hill Education.
653 Edzwald, J.K., 1993. Coagulation in drinking water treatment: Particles, organics and
654 coagulants. Water Sci. Technol. 27, 21–35. https://doi.org/10.2166/wst.1993.0261
655 Gao, B., Yue, Q., 2005. Effect of SO42-/Al3+ratio and O-/Al3+value on the characterization
656 of coagulant poly-aluminum-chloride-sulfate (PACS) and its coagulation performance in
657 water treatment. Chemosphere 61, 579–584.
658 https://doi.org/10.1016/j.chemosphere.2005.03.013
659 Hanna, Rubin, A.J., 1970. Effect of Sulfate and Other Ions in Coagulation With
660 Aluminum(Iii. J. / Am. Water Work. Assoc. 62, 315–321.
661 https://doi.org/10.1002/j.1551-8833.1970.tb03912.x

Hendricks, D.W., 2016. Fundamentals of Water Treatment Unit Processes: Physical, Chemical, and Biological. CRC Press.

Hussain, S., van Leeuwen, J., Chow, C., Beecham, S., Kamruzzaman, M., Wang, D., Drikas, M., Aryal, R., 2013. Removal of organic contaminants from river and reservoir waters by three different aluminum-based metal salts: Coagulation adsorption and kinetics studies. Chem. Eng. J. 225, 394–405. https://doi.org/10.1016/j.cej.2013.03.119

Jiang, J.Q., 2001. Development of coagulation theory and pre-polymerized coagulants for water treatment. Sep. Purif. Methods 30, 127–141. https://doi.org/10.1081/SPM-100102986

Kan, C., Huang, C., Pan, J.R., 2002. Time requirement for rapid-mixing in coagulation. Colloids Surfaces A Physicochem. Eng. Asp. 203, 1–9. https://doi.org/10.1016/S0927-7757(01)01095-0

Kimura, M., Matsui, Y., Kondo, K., Ishikawa, T.B., Matsushita, T., Shirasaki, N., 2013. Minimizing residual aluminum concentration in treated water by tailoring properties of polyaluminum coagulants. Water Res. 47, 2075–2084. https://doi.org/10.1016/j.watres.2013.01.037

Kimura, M., Matsui, Y., Saito, S., Takahashi, T., Nakagawa, M., Shirasaki, N., Matsushita, T., 2015. Hydraulically irreversible membrane fouling during coagulation-microfiltration and its control by using high-basicity polyaluminum chloride. J. Memb. Sci. 477, 115–122. https://doi.org/10.1016/j.memsci.2014.12.033

Kong, Y., Ma, Y., Ding, L., Ma, J., Zhang, H., Chen, Z., Shen, J., 2021. Coagulation behaviors of aluminum salts towards humic acid: Detailed analysis of aluminum speciation and transformation. Sep. Purif. Technol. 259, 118137. https://doi.org/10.1016/j.seppur.2020.118137

686 Letterman, R.D., Tabatabaie, M., Jr, R.S.A., 1979. The Effect of the Bicarbonate Ion
687 Concentration on Flocculation With Aluminum Sulfate. J. Am. Water Works Assoc. 71,
688 467–472. https://doi.org/10.1002/j.1551-8833.1979.tb04395.x
689 Letterman, R.D., Yiacoumi, S., 2010. Coagulation and flocculation, in: Edzwald, J.K. (Ed.),
690 Water Quality and Treatment A Handbook on Drinking Water. McGrawHill, pp. 8.1-
691 8.81.
692 Li, M., Cheng, J., Zou, F., Zhang, C., Wang, M., Li, Y., Gu, J., Yan, M., 2021. Effects of pre-
693 oxidation on residual dissolved aluminum in coagulated water: A pilot-scale study.
694 Water Res. 190, 116682. https://doi.org/10.1016/j.watres.2020.116682
695 Lin, J.L., Chin, C.J.M., Huang, C., Pan, J.R., Wang, D., 2008. Coagulation behavior of
696 Al13aggregates. Water Res. 42, 4281–4290.
697 https://doi.org/10.1016/j.watres.2008.07.028
698 Lin, J.L., Pan, J.R., Huang, C., 2013. Enhanced particle destabilization and aggregation by
699 flash-mixing coagulation for drinking water treatment. Sep. Purif. Technol. 115, 145–
700 151. https://doi.org/10.1016/j.seppur.2013.05.013
701 Liu, L., Lu, S., Demissie, H., Yue, Y., Jiao, R., An, G., Wang, D., 2021. Formation of Al30
702 aggregates and its correlation to the coagulation effect. Chemosphere 278, 130493.
703 https://doi.org/10.1016/j.chemosphere.2021.130493
704 Long, Y., Yu, G., Dong, L., Xu, Y., Lin, H., Deng, Y., You, X., Yang, L., Liao, B.Q., 2021.
705 Synergistic fouling behaviors and mechanisms of calcium ions and polyaluminum
706 chloride associated with alginate solution in coagulation-ultrafiltration (UF) process.
707 Water Res. 189, 116665. https://doi.org/10.1016/j.watres.2020.116665

708 Matijević, E., Stryker, L.J., 1966. Coagulation and reversal of charge of lyophobic colloids
709 by hydrolyzed metal ions. III. Aluminum Sulfate. J. Colloid Interface Sci. 22, 68–77.
710 https://doi.org/10.1016/0021-9797(66)90068-3
711 Matsui, Y., Yuasa, A., Furuya, Y., Kamei, T., 1998. Dynamic analysis of coagulation with
712 alum and PACl. Journal-American Water Work. Assoc. 90, 96–106.
713 Miller, L.B.., 1925. A Study of the Effects of Anions upon the Properties of " Alum Floc ".
714 Public Health Rep. 40, 351–367.
715 Nakazawa, Y., Matsui, Y., Hanamura, Y., Shinno, K., Shirasaki, N., Matsushita, T., 2018.
716 Minimizing residual black particles in sand filtrate when applying super-fine powdered
717 activated carbon: Coagulants and coagulation conditions. Water Res. 147, 311–320.
718 https://doi.org/10.1016/j.watres.2018.10.008
719 Nikanorov, A.M., Brazhnikova, L. V, 2009. Water Chemical Composition of Rivers, Lakes
720 and Wetlands, Encyclopedia of Life Support Systems (EOLSS).
721 Nowicki, W., Nowicka, G., 1994. Verification of the Schulze-Hardy rule - A colloid
722 chemistry experiment. J. Chem. Educ. 71, 624–626. https://doi.org/10.1021/ed071p624
723 Ou, H.-S., Wei, C.-H., Deng, Y., Gao, N.-Y., 2014. Principal component analysis to assess
724 the efficiency and mechanism for ultraviolet-C/polyaluminum chloride enhanced
725 coagulation of algae-laden water. Water Sci. Technol. Water Supply 14, 493–503.
726 Parker, D.R., Bertsch, P.M., 1992. Identification and Quantification of the “Al13”
727 Tridecameric Aluminum Polycation Using Ferron. Environ. Sci. Technol. 26, 908–914.
728 https://doi.org/10.1021/es00029a006
729 Qu, J., Liu, H., 2004. Optimum conditions for Al13 polymer formation in PACl preparation
730 by electrolysis process. Chemosphere 55, 51–56.
731 https://doi.org/10.1016/j.chemosphere.2003.10.058

Rakshit, A.K., Naskar, B., Moulik, S.P., 2021. Performance of modified Schulze-Hardy rule on the stability of nano, micro, and macro colloidal dispersions: A comprehensive account. Colloids Surfaces A Physicochem. Eng. Asp. 626, 127084. https://doi.org/10.1016/j.colsurfa.2021.127084

Sato, F., Matsuda, S., 2009. Novel Basic Aluminum Chloride, Its Manufacturing Method and Its Application. Japanese Patent, Appl.

Saxena, K., Brighu, U., Choudhary, A., 2019. Coagulation of humic acid and kaolin at alkaline pH: Complex mechanisms and effect of fluctuating organics and turbidity. J. Water Process Eng. 31, 100875. https://doi.org/10.1016/j.jwpe.2019.100875

Snodgrass, W.J., Clark, M.M., O'Melia, C.R., 1984. Particle formation and growth in dilute aluminum(III) solutions. Characterization of particle size distributions at pH 5.5. Water Res. 18, 479–488. https://doi.org/10.1016/0043-1354(84)90157-X

Sposito, G., 1995. The Environmental Chemistry of Aluminum, Second Edition. Taylor & Francis.

Sricharoenchaikit, P., Letterman, R.D., 1987. Effect of Al(III) and sulfate ion on flocculation kinetics. J. Environ. Eng. -ASCE 113, 1120–1138. https://doi.org/10.1061/(ASCE)0733-9372(1987)113:5(1120)

Su, Z., Liu, T., Yu, W., Li, X., Graham, N.J.D., 2017. Coagulation of surface water: Observations on the significance of biopolymers. Water Res. 126, 144–152. https://doi.org/10.1016/j.watres.2017.09.022

Tang, H., Xiao, F., Wang, D., 2015. Speciation, stability, and coagulation mechanisms of hydroxyl aluminum clusters formed by PACl and alum: A critical review. Adv. Colloid Interface Sci. 226, 78–85. https://doi.org/10.1016/j.cis.2015.09.002

Wang, D., Tang, H., Gregory, J., 2002. Relative importance of charge neutralization and precipitation on coagulation of kaolin with PACI: Effect of sulfate ion. Environ. Sci. Technol. 36, 1815–1820. https://doi.org/10.1021/es001936a

Wang, X., Tang, X., Feng, P., Li, X., Zhao, C., Chen, W., Zheng, H., 2017. A novel preparation method of polyaluminum chloride/polyacrylamide composite coagulant: Composition and characteristic. J. Appl. Polym. Sci. 134, 1–6. https://doi.org/10.1002/app.44500

Wu, X., Ge, X., Wang, D., Tang, H., 2007. Distinct coagulation mechanism and model between alum and high Al 13 -PACl 305, 89–96. https://doi.org/10.1016/j.colsurfa.2007.04.046

Xiao, F., Yi, P., Pan, X.R., Zhang, B.J., Lee, C., 2010. Comparative study of the effects of experimental variables on growth rates of aluminum and iron hydroxide flocs during coagulation and their structural characteristics. Desalination 250, 902–907. https://doi.org/10.1016/j.desal.2008.12.050

Yan, M., Wang, D., Ni, J., Qu, J., Chow, C.W.K., Liu, H., 2008a. Mechanism of natural organic matter removal by polyaluminum chloride: Effect of coagulant particle size and hydrolysis kinetics. Water Res. 42, 3361–3370. https://doi.org/10.1016/j.watres.2008.04.017

Yan, M., Wang, D., Qu, J., He, W., Chow, C.W.K., 2007. Relative importance of hydrolyzed Al(III) species (Ala, Alb, and Alc) during coagulation with polyaluminum chloride: A case study with the typical micro-polluted source waters. J. Colloid Interface Sci. 316, 482–489. https://doi.org/10.1016/j.jcis.2007.08.036

Yan, M., Wang, D., Yu, J., Ni, J., Edwards, M., Qu, J., 2008b. Enhanced coagulation with polyaluminum chlorides: Role of pH/Alkalinity and speciation. Chemosphere 71, 1665–1673. https://doi.org/10.1016/j.chemosphere.2008.01.019

Yue, Y., An, G., Liu, L., Lin, L., Jiao, R., Wang, D., 2021. Pre-aggregation of Al13 in optimizing coagulation for removal of humic acid. Chemosphere 277, 130268. https://doi.org/10.1016/j.chemosphere.2021.130268

Zouboulis, A.I., Tzoupanos, N., 2010. Alternative cost-effective preparation method of polyaluminium chloride (PAC) coagulant agent: Characterization and comparative application for water/wastewater treatment. Desalination 250, 339–344. https://doi.org/10.1016/j.desal.2009.09.053

Research Highlights

- Hydrolysis explains the dependence of coagulation on type of PACl and raw water
- Hydrolysis and coagulation depend on type of PACl and the anions in the raw water
- Effects of sulfate, bicarbonate, and NOM in raw water on PACl hydrolysis are additive
- Hydrolysis of high-basicity PACl by bicarbonate is slow and hence needs sulfate ions
- Large hydrolysis power of sulfate is due to its divalency and tetrahedral structure

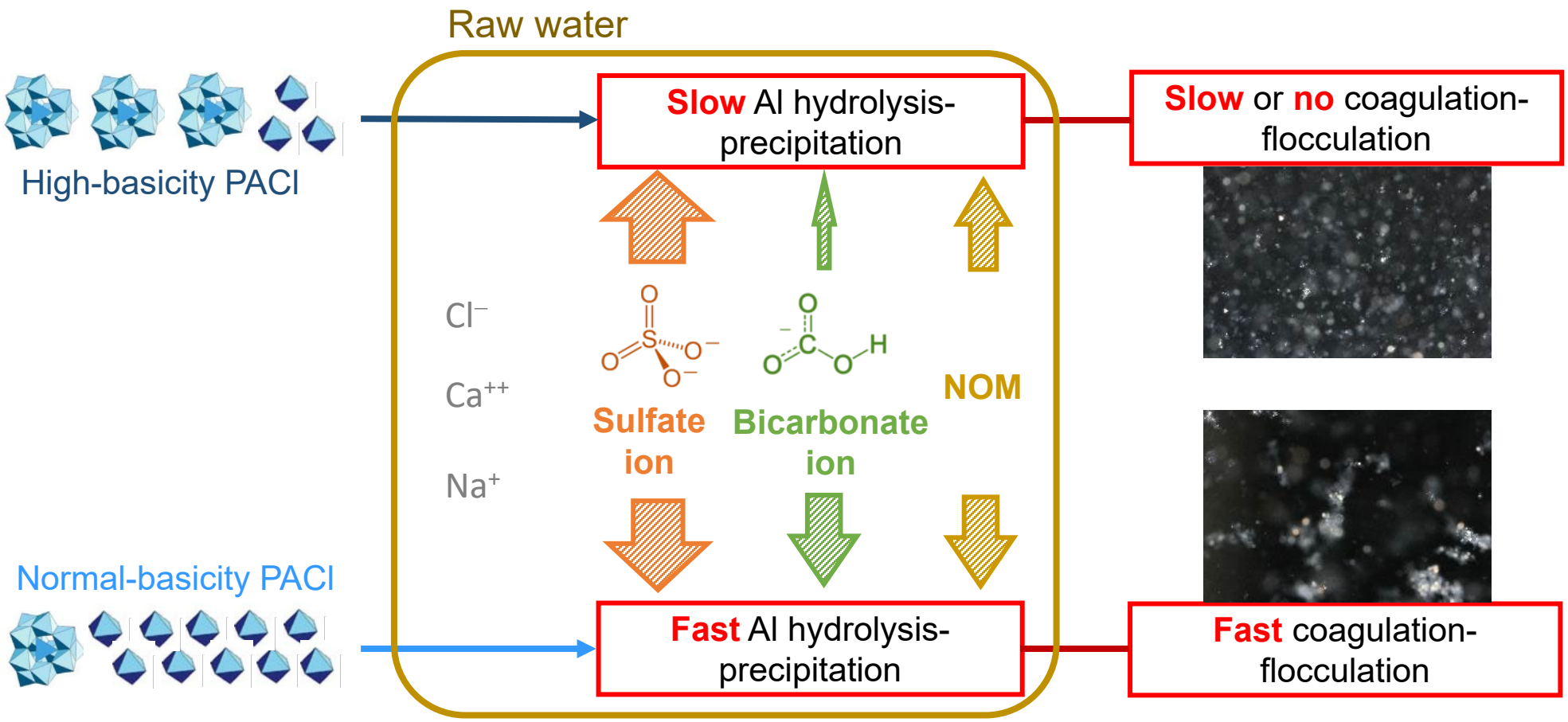
Raw water
High-basicity PACl
Normal-basicity PACl
Slow Al hydrolysis-precipitation
Fast Al hydrolysis-precipitation
Cl⁻
Ca⁺⁺
Na⁺
Sulfate ion
Bicarbonate ion
NOM
Slow or no coagulation-flocculation
Fast coagulation-flocculation

Table 1

Concentrations required for one-quarter concentration times of 60 s and relative intensities for PACl hydrolysis.

		Sulfate ion	Bicarbonate ion	Chloride ion	Nitrate ion	DOC	UV260
Concentrations required for a one-quarter concentration time of 60 s	HB-PACl	0.174 mmol/L	2.20 mmol/L	34.3 mmol/L	41.8 mmol/L	N/A	N/A
		16.7 mg-SO_4^{2-}/L	134 mg-HCO_3^-/L	1220 mg-Cl^-/L	2590 mg-NO_3^-/L	1.46 mg-C/L	0.088 cm^{-1}
	NB-PACl	0.168 mmol/L	1.00 mmol/L	14.5 mmol/L	11.5 mmol/L	N/A	N/A
		16.1 mg-SO_4^{2-}/L	61 mg-HCO_3^-/L	514 mg-Cl^-/L	714 mg-NO_3^-/L	0.99 mg-C/L	0.066 cm^{-1}
Intensity for PACl hydrolysis relative to the intensity of sulfate ions	HB-PACl	1 mol/mol	0.079 [ah)] mol/mol	0.0051 mol/mol	0.0042 mol/mol	0.12 mol/(g-C)	1.97 [bh)] (mmol/L)/cm^{-1}
		1 g/g	0.12 (g-SO_4^{2-})/(g-HCO_3^-)	0.014 (g-SO_4^{2-})/(g-Cl^-)	0.0064 (g-SO_4^{2-})/(g-NO_3^-)	11.4 (g-SO_4^2)/(g-C)	190 (mg-SO_4^{2-}/L)/ cm^{-1}
	NB-PACl	1 mol/mol	0.17 [an)] mol/mol	0.012 mol/mol	0.015 mol/mol	0.17 mol/(g-C)	2.54 [bn)] (mmol/L)/cm^{-1}
		1 g/g	0.26 (g-SO_4^{2-})/(g-HCO_3^-)	0.031 (g-SO_4^{2-})/(g-Cl^-)	0.022 (g-SO_4^{2-})/(g-NO_3^-)	16.3 (g-SO_4^{2-})/(g-C)	244 (mg-SO_4^{2-}/L)/ cm^{-1}

Note: Because the waters used in the experiments for sulfate, chloride, and nitrate ions contained a slight bicarbonate, the effect of bicarbonate ions was subtracted from the apparent effective concentration for the one-quarter concentration time of 60 s.

The numbers with superscripts ah) and an) are the values of "a" in equation (1) for HB-PACl and NB-PACl, respectively.

The numbers with superscripts bh) and bn) are the values of "b" in equation (1) for HB-PACl and NB-PACl, respectively.

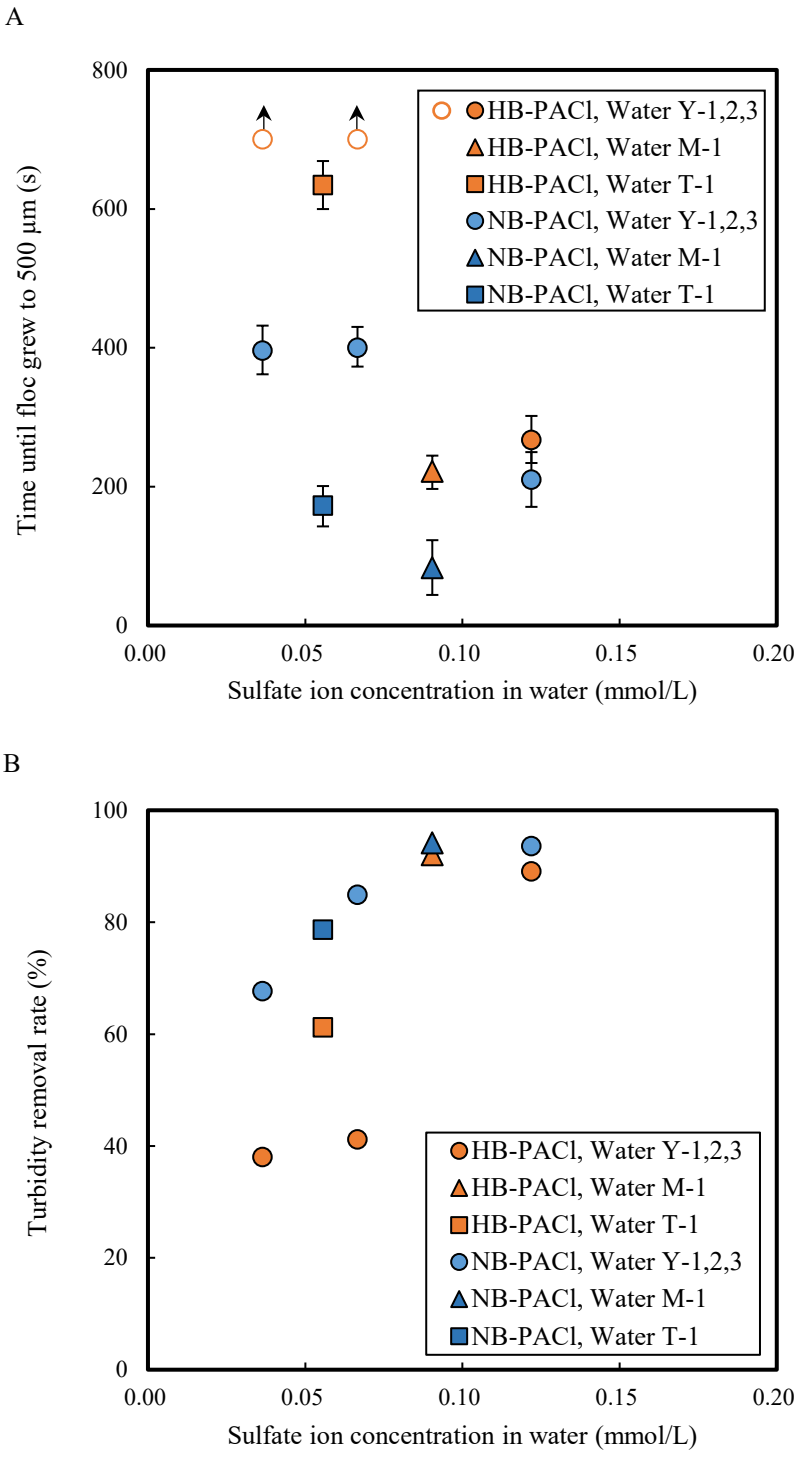

Fig. 1. Time until floc grew to 500 µm (Panel A) and the rate of turbidity removal (Panel B) of HB-PACl and NB-PACl in coagulation–flocculation experiments. Y-1–3, M-1, and T-1 waters were used in these experiments. The PACl dosage was 2.5 mg-Al/L. The coagulation pH was 7.0. Open circles with an arrow show data for HB-PACl in Y-1 and 2. In those experiments, no 500-µm floc formed by the end of mixing, therefore the y-axis values were above that point. Error bars in Panel A indicate 95% confidence intervals.

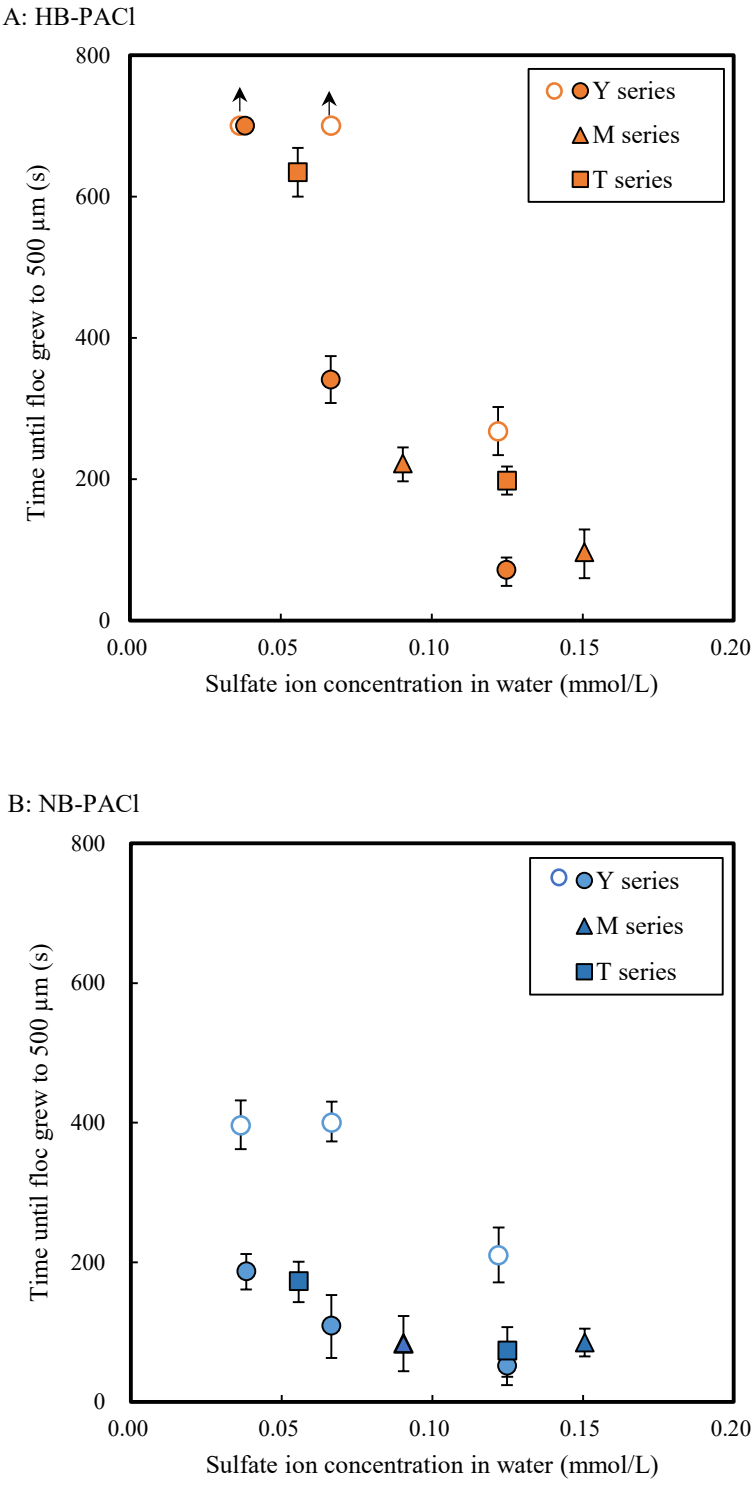

Fig. 2. Time until flocs of HB-PACl and NB-PACl grew to 500 µm in waters containing different concentrations of sulfate ions. Y series waters (Y-1–6), M-1,2, and T-1,2 waters were used in these experiments. The PACl dose was 2.5 mg-Al/L. The coagulation pH was 7.0. Open circles indicate that bicarbonate ion concentrations in the waters were lower than 0.2 mmol/L. Open circles with an arrow in Panel A indicate that no 500-µm floc formed by the end of mixing, therefore the y-axis values were above that point. Error bars indicate 95% confidence intervals.

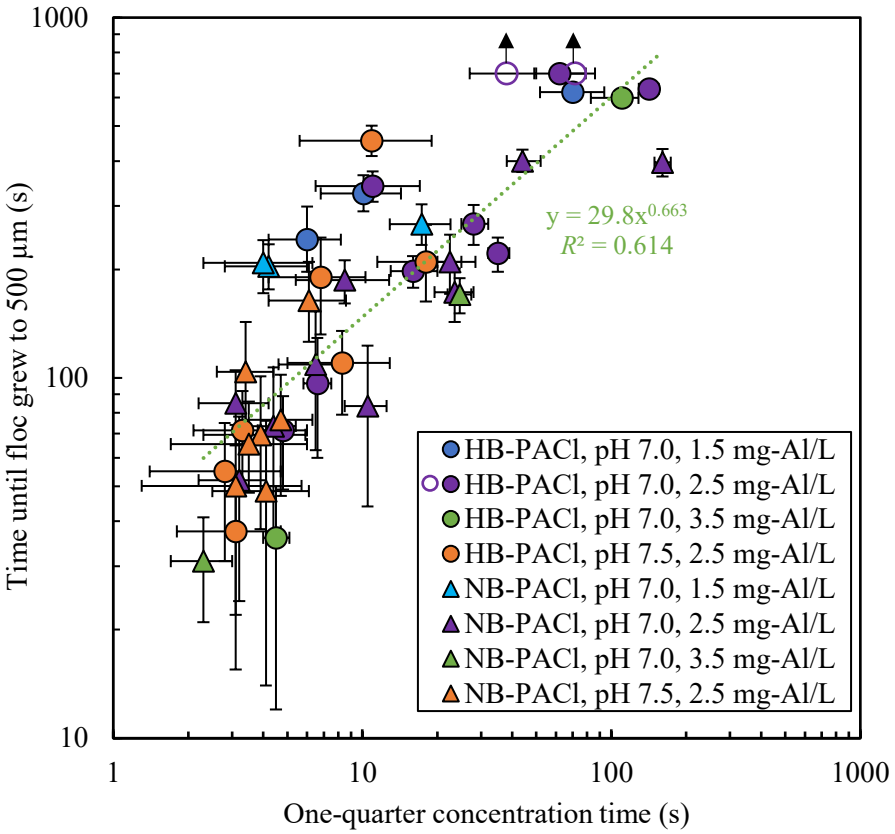

Fig. 3. Relationship between the time until floc grew to 500 µm and one-quarter concentration times in coagulation experiments. The results for HB-PACl and NB-PACl at pHs of both 7.0 and 7.5 are shown. Y-1–6, M-1,2, and T-1,2 waters were used in these experiments. The PACl doses were 1.5, 2.5, and 3.5 mg-Al/L. Open circles with an arrow indicate that floc size did not grow to 500 µm during flocculation, therefore the y-axis values were above that point. Error bars indicate 95% confidence intervals.

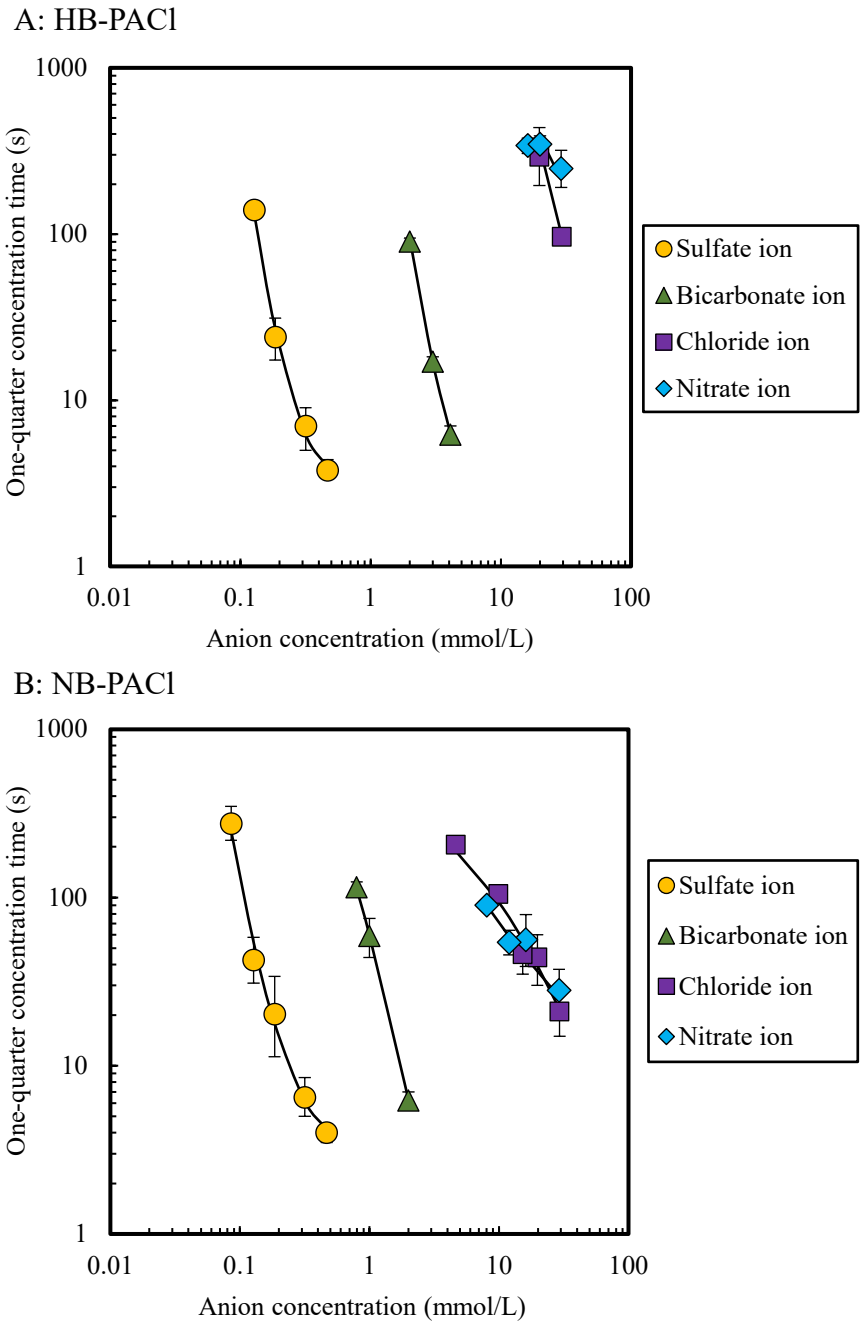

Fig. 4. Relationship between one-quarter concentration times and anion concentrations in tests of hydrolysis rates. Panel A shows the data for HB-PACl in Na_2SO_4-1–6, $NaHCO_3$-3,5,6, NaCl-8,9, and $NaNO_3$-1,3,4 waters. Panel B shows the data for NB-PACl in Na_2SO_4-2–4, $NaHCO_3$-1,5,7, NaCl-5,7–10, and $NaNO_3$-1,2,4,5 waters. The PACl dose was 2.5 mg-Al/L. The coagulation pH was 7.0. Error bars indicate 95% confidence intervals.

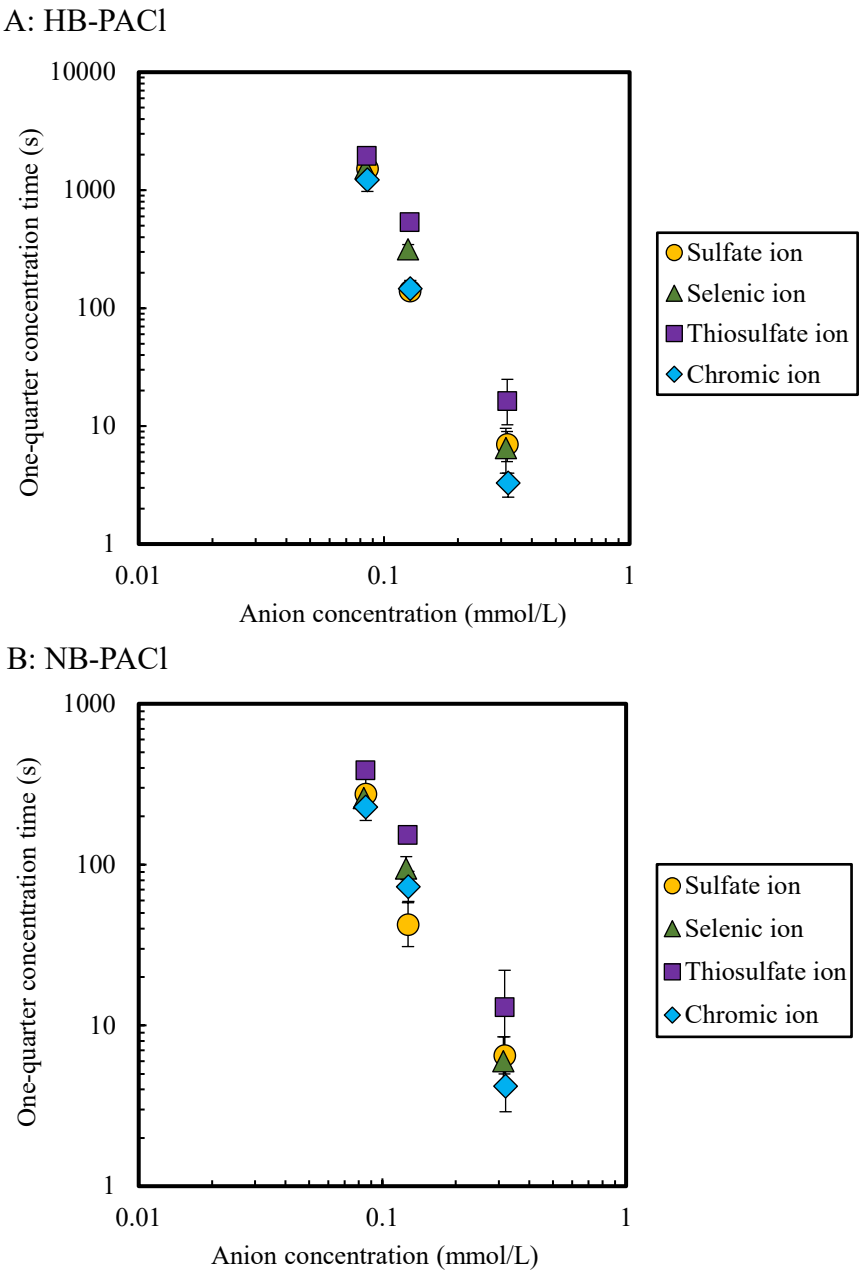

Fig. 5. Relationship between one-quarter concentration time and oxyanion concentration in tests of hydrolysis rates. Panel A shows the data for HB-PACl. Panel B shows the data for NB-PACl. Na_2SO_4-3,4,6, Na_2SeO_4-1–3, $Na_2S_2O_3$-1–3, and Na_2CrO_4-1–3 waters were used in these experiments. The PACl dose was 2.5 mg-Al/L. The coagulation pH was 7.0. Error bars indicate 95% confidence intervals.

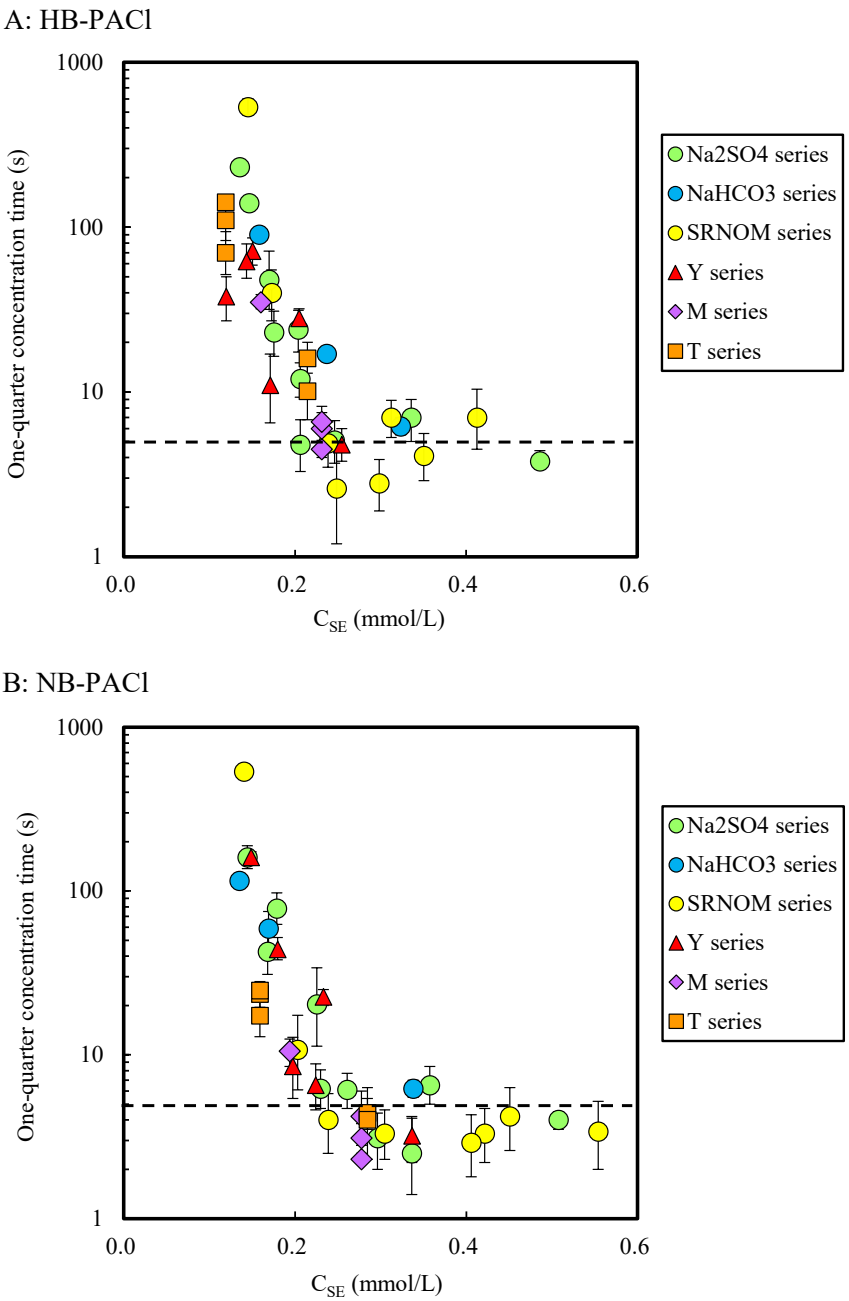

Fig. 6. One-quarter concentration times versus C_{SE} values. Panel A shows the data for HB-PACl in Na_2SO_4-1,2,4,6,8–13, $NaHCO_3$-3,5,6, SRNOM-3–10, Y-1–6, M-1,2, and T-1,2 waters, and Panel B shows the data for NB-PACl in Na_2SO_4-1,2,4,6,8–13, $NaHCO_3$-1,5,7, SRNOM-2–9, Y-1–6, M-1,2, and T-1,2 waters. The PACl dose was 2.5 mg-Al/L, but doses of 1.5 and 3.5 mg-Al/L were also used in the experiments with M-1,2 and T-1,2 waters. The coagulation pH was 7.0. Error bars indicate 95% confidence intervals.

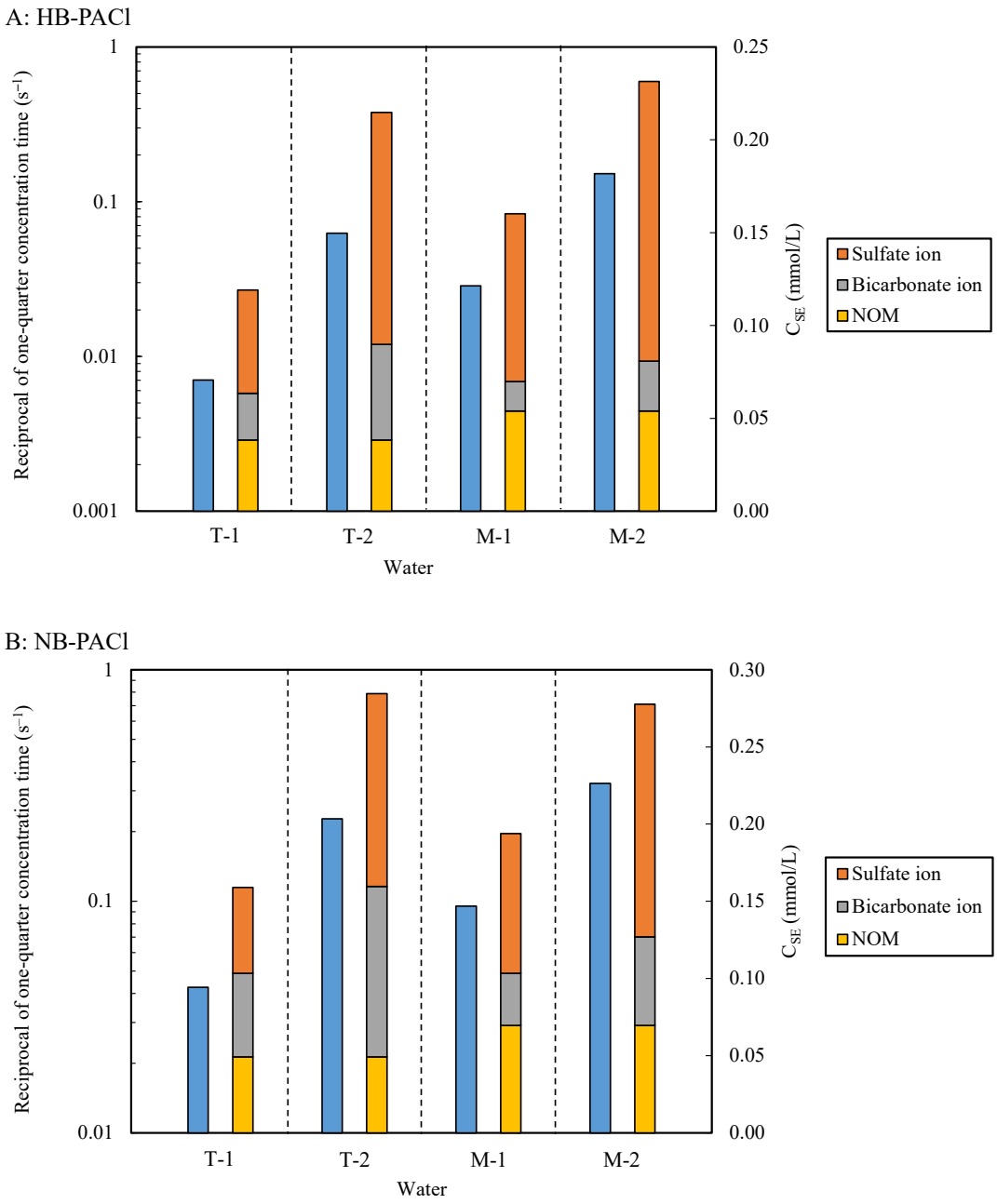

Fig. 7. The reciprocal of one-quarter concentration time and the contribution from sulfate ions, bicarbonate ions, and NOM in C_{SE} units. Blue bars show the reciprocal of one-quarter concentration time indicated by the left axis scale. Contributions of sulfate ion (orange bars), bicarbonate ion (grey bars), and NOM (yellow bars) to C_{SE} value are indicated by the right axis scale. Results of HB-PACl are shown in Panel A, and the results of NB-PACl are shown in Panel B. T-1,2 and M-1,2 waters were used.

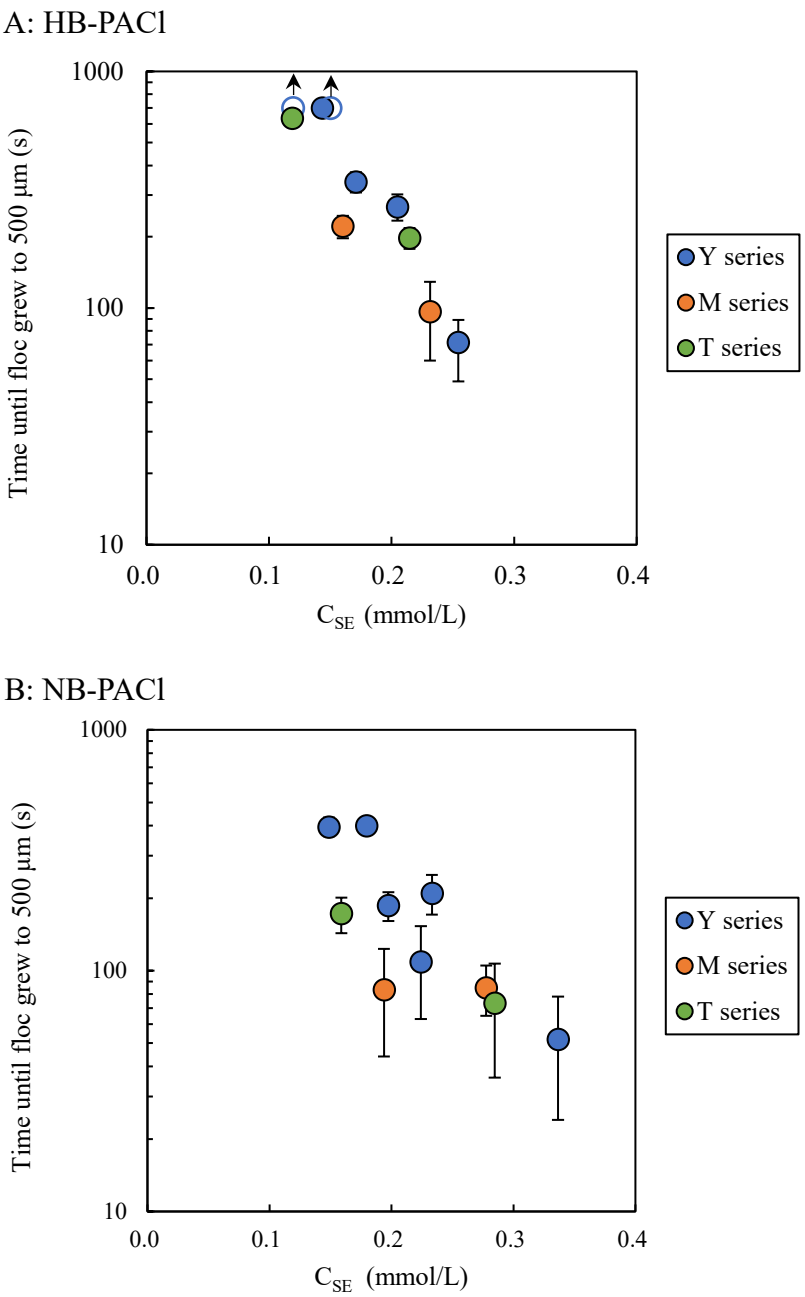

Fig. 8. Time until floc grew to 500 µm against C_{SE} values in coagulation experiments. Panels A and B show the data for HB-PACl and NB-PACl, respectively, in Y, M, and T series waters. The coagulation pH was 7.0. The PACl dose was 2.5 mg-Al/L. Open circles with an arrow in Panel A indicate that floc size did not increase to 500 µm during the experiment, therefore the y-axis values were above that point. Fig. S18 in the SI shows these relationships when DOC is used for the NOM concentration. Error bars indicate 95% confidence intervals.

Supplementary Information

Overlooked effect of ordinary inorganic ions on polyaluminum-chloride coagulation treatment

Yize Chen [a], Yoshihiko Matsui [b, *], Tsutomu Sato [b], Nobutaka Shirasaki [b], Taku Matsushita [b]

[a] Graduate School of Engineering, Hokkaido University.

N13W8 Sapporo 060-8628 Japan

[b] Faculty of Engineering, Hokkaido University

N13W8 Sapporo 060-8628 Japan

* Corresponding author. Phone: +81-11-706-7280.

E-mail address: matsui@eng.hokudai.ac.jp (Y. Matsui)

Text S1. Methods used to analyze PACl Characteristics

The ferron assay was conducted with HB-PACl and NB-PACl. Immediately after being diluted with Milli-Q water to a concentration of 0.1 mol-Al/L, PACls were added to the ferron reagent (8-hydroxy-7-indo-5-quinoline sulfonic acid; FUJIFILM Wako Pure Chemical Corporation) to initiate the reaction. The absorbance at 366 nm was then measured using an ultraviolet light meter (UV-1800; Shimadzu, Kyoto, Japan). Dilution of the PACls was acceptable because dilution has little effect on the distribution of ferron (Kimura et al., 2013; Wang et al., 2002). The aluminum species in the PACl were divided based on their reaction time with the ferron reagent into Al_a (monomeric species, within 30 s), Al_b (polymeric species, from 30 s to 120 min), and Al_c (colloidal species, did not react within 120 min) (Wang et al., 2004; Yan et al., 2007).

The colloid charges of the PACls were measured via colloid titration. A PACl was diluted with Milli-Q water to an Al concentration of 0.1 mol-Al/L and was titrated with a potassium polyvinyl sulfate titration solution (N/400, for colloidal titration; FUJIFILM Wako Pure Chemical Corporation) using an automatic titrator (COM-555; Hiranuma Sangyo Co., Inc., Ibaraki, Japan) (Matsui et al., 2017).

^{27}Al-NMR analysis was conducted with a JNM-ECA Series FT NMR (ECA 600; JEOL Ltd., Tokyo, Japan). A $NaAl(OH)_4$ (FUJIFILM Wako Pure Chemical Corporation) solution (0.01 mol-Al/L) was used as the internal standard. An $AlCl_3$ (FUJIFILM Wako Pure Chemical Corporation) solution (0.1 mol-Al/L) was used as the reference material. Parameters for the measurement were as follows: field strength, 14.09 T; frequency, 78247 Hz; resonance frequency, 156.39 MHz; number of scans, 8000; temperature 70 °C. The data and peaks were processed with the data-processing software provided with the instrument (Nakamura, 2009).

Text S2. Calculation method of one-half and one-quarter concentration times.

During hydrolysis rate test, samples were taken at pre-determined time and the Al concentration in the filtrate that passed through a 10-μm pore size membrane filter was measured by an inductively coupled plasma mass spectrometer (ICPMS, 7700x; Agilent Technologies, Inc., Santa Clara, CA, USA). The change of Al concentration with time is shown in Fig. S19– Fig. S30. Using Minitab (Minitab, LLC, Pennsylvania, USA), the experimental data were fitted to a model (initial exponential decrease followed by a plateau at a very low concentration) to determine the one-half concentration time, one-quarter concentration time (the time to reduce Al concentration to one-half and one-quarter, respectively, of the initial value) and their 95% confidence intervals. If no such change was observed (which was often the case for NOM water), the one-half concentration time and one-quarter concentration time were determined by interpolation of the experimental data.

Table S1.

Properties of the PACls used in this study

	HB-PACl	NB-PACl
Al content (mol/L)	2.5	2.5
SO_4^{2-}/Al (mole ratio)	0.11	0.14
Basicity (%)	70.8	49.8

Table S2.
Ion components, alkalinity, DOC, UV260, and turbidity of the Y, J, M, and T water series used in this study

Series	Water	Na^+	K^+	Mg^{2+}	Ca^{2+}	Cl^-	NO_3^-	SO_4^{2-}	Alkalinity (meq/L) ≈ HCO_3^- (mmol/L)	DOC	UV260	Turbidity	Source
		mmol/L	mmol/L	mmol/L	mmol/L	mmol/L	mmol/L	mmol/L		mg-C/L	cm^{-1}	NTU	
Y	Y-1	0.34	0.02	0.05	0.04	0.37	0.00	0.04	0.08	1.9	0.04	5.2	Kuromorigawa Reservoir
	Y-2	0.40	0.02	0.05	0.03	0.34	0.01	0.07	0.08	1.8	0.04	5.6	
	Y-3	0.51	0.02	0.05	0.04	0.33	0.01	0.12	0.08	1.8	0.04	5.4	
	Y-4	0.62	0.02	0.05	0.04	0.34	0.01	0.04	0.34	1.9	0.04	4.9	
	Y-5	0.68	0.02	0.05	0.04	0.34	0.00	0.07	0.34	1.8	0.04	5.1	
	Y-6	1.10	0.02	0.05	0.04	0.34	0.02	0.12	0.66	1.9	0.04	5.9	
J	J-1	0.08	0.01	0.04	0.16	0.05	0.01	0.04	0.32	0.5	NM	NM	Joganji River
	J-2	0.35	0.01	0.04	0.16	0.05	0.01	0.16	0.32	0.5	NM	NM	
M	M-1	0.24	0.02	0.05	0.14	0.19	0.01	0.09	0.20	0.4	0.03	3.2	Toyohira River
	M-2	0.45	0.04	0.09	0.23	0.37	0.02	0.15	0.34	0.4	0.03	1.1	
T	T-1	0.08	0.01	0.04	0.18	0.04	0.01	0.06	0.32	0.4	0.02	1.4	Jyoganji River
	T-2	0.55	0.01	0.04	0.18	0.04	0.01	0.12	0.66	0.4	0.02	1.6	

NM: Not measured.

Table S3.

Ion components, alkalinity, DOC, and UV260 values of waters used in this study

Series	Water	Na^+	K^+	Mg^{2+}	Ca^{2+}	Cl^-	NO_3^-	SO_4^{2-}	Alkalinity meq/L	DOC	UV260	Source
		mmol/L	mmol/L	mmol/L	mmol/L	mmol/L	mmol/L	mmol/L	$\approx HCO_3^-$ mmol/L	mg-C/L	cm^{-1}	
Na_2SO_4	Na_2SO_4-1	1.21	0.00	0.00	0.00	0.00	0.00	0.47	0.24	0.0	0.00	Elix water
	Na_2SO_4-2	0.60	0.00	0.00	0.00	0.00	0.00	0.18	0.24	0.0	0.00	
	Na_2SO_4-3	0.43	0.00	0.00	0.00	0.00	0.00	0.09	0.24	0.0	0.00	
	Na_2SO_4-4	0.52	0.00	0.00	0.00	0.00	0.00	0.13	0.24	0.0	0.00	
	Na_2SO_4-5	0.33	0.00	0.00	0.00	0.00	0.00	0.04	0.24	0.0	0.00	
	Na_2SO_4-6	0.88	0.00	0.00	0.00	0.00	0.00	0.32	0.24	0.0	0.00	
	Na_2SO_4-7	0.38	0.00	0.00	0.00	0.00	0.00	0.06	0.24	0.0	0.00	
	Na_2SO_4-8	1.37	0.00	0.00	0.00	0.00	0.00	0.17	1.00	0.0	0.00	
	Na_2SO_4-9	0.45	0.00	0.00	0.00	0.00	0.00	0.16	0.10	0.0	0.00	
	Na_2SO_4-10	0.95	0.00	0.00	0.00	0.00	0.00	0.16	0.61	0.0	0.00	
	Na_2SO_4-11	0.35	0.00	0.00	0.00	0.00	0.00	0.13	0.10	0.0	0.00	
	Na_2SO_4-12	0.87	0.00	0.00	0.00	0.00	0.00	0.13	0.61	0.0	0.00	
	Na_2SO_4-13	1.27	0.00	0.00	0.00	0.00	0.00	0.13	1.00	0.0	0.00	
	Na_2SO_4-14	2.04	0.00	0.00	0.00	0.62	0.00	0.17	1.00	0.0	0.00	
$NaHCO_3$	$NaHCO_3$-0	0.25	0.00	0.00	0.00	0.00	0.00	0.00	0.24	0.0	0.00	

	$NaHCO_3$-1	1.04	0.00	0.00	0.00	0.00	0.00	0.00	1.00	0.0	0.00
	$NaHCO_3$-2	0.62	0.00	0.00	0.00	0.00	0.00	0.00	0.60	0.0	0.00
	$NaHCO_3$-3	4.09	0.00	0.00	0.00	0.00	0.00	0.00	4.09	0.0	0.00
	$NaHCO_3$-4	8.20	0.00	0.00	0.00	0.00	0.00	0.00	8.20	0.0	0.00
	$NaHCO_3$-5	2.00	0.00	0.00	0.00	0.00	0.00	0.00	2.00	0.0	0.00
	$NaHCO_3$-6	3.00	0.00	0.00	0.00	0.00	0.00	0.00	3.00	0.0	0.00
	$NaHCO_3$-7	0.80	0.00	0.00	0.00	0.00	0.00	0.00	0.80	0.0	0.00
NaCl	NaCl-1	0.86	0.00	0.00	0.00	0.60	0.00	0.00	0.24	0.0	0.00
	NaCl-2	1.41	0.00	0.00	0.00	1.15	0.00	0.00	0.25	0.0	0.00
	NaCl-3	5.15	0.00	0.00	0.00	4.63	0.00	0.00	0.24	0.0	0.00
	NaCl-4	7.24	0.00	0.00	0.00	6.61	0.00	0.00	0.24	0.0	0.00
	NaCl-5	10.58	0.00	0.00	0.00	9.90	0.00	0.00	0.24	0.0	0.00
	NaCl-6	29.60	0.00	0.00	0.00	29.35	0.00	0.00	0.24	0.0	0.00
	NaCl-7	20.05	0.00	0.00	0.00	19.75	0.00	0.00	0.24	0.0	0.00
	NaCl-8	15.48	0.00	0.00	0.00	15.23	0.00	0.00	0.24	0.0	0.00
$NaNO_3$	$NaNO_3$-1	16.37	0.00	0.00	0.00	0.00	16.13	0.00	0.24	0.0	0.00
	$NaNO_3$-2	12.25	0.00	0.00	0.00	0.00	12.00	0.00	0.24	0.0	0.00
	$NaNO_3$-3	20.25	0.00	0.00	0.00	0.00	20.00	0.00	0.24	0.0	0.00
	$NaNO_3$-4	29.31	0.00	0.00	0.00	0.00	29.06	0.00	0.24	0.0	0.00
	$NaNO_3$-5	8.32	0.00	0.00	0.00	0.00	8.07	0.00	0.24	0.0	0.00
	$NaNO_3$-6	4.85	0.00	0.00	0.00	0.00	4.60	0.00	0.24	0.0	0.00

	$NaNO_3$-7	1.45	0.00	0.00	0.00	0.00	1.20	0.00	0.24	0.0	0.00
K_2SO_4	K_2SO_4-1	0.25	0.25	0.00	0.00	0.00	0.00	0.12	0.24	0.0	0.00
$MgSO_4$	$MgSO_4$-1	0.25	0.00	0.12	0.00	0.00	0.00	0.11	0.24	0.0	0.00
$CaSO_4$	$CaSO_4$-1	0.25	0.00	0.00	0.19	0.00	0.00	0.18	0.24	0.0	0.00
	$CaSO_4$-2	0.25	0.00	0.00	0.04	0.00	0.00	0.04	0.24	0.0	0.00
	$CaSO_4$-3	0.26	0.00	0.00	0.08	0.00	0.00	0.09	0.24	0.0	0.00
	$CaSO_4$-4	0.26	0.00	0.00	0.13	0.00	0.00	0.12	0.24	0.0	0.00
SRNOM	SRNOM-1	0.25	0.00	0.00	0.00	0.00	0.00	0.00	0.24	0.1	0.16
	SRNOM-2	0.26	0.00	0.00	0.00	0.00	0.00	0.00	0.24	0.5	0.04
	SRNOM-3	0.26	0.00	0.00	0.00	0.00	0.00	0.00	0.24	1.3	0.08
	SRNOM-4	0.40	0.00	0.00	0.00	0.00	0.00	0.07	0.24	1.3	0.08
	SRNOM-5	1.16	0.00	0.00	0.00	0.00	0.00	0.07	1.00	1.4	0.08
	SRNOM-6	0.59	0.00	0.00	0.00	0.00	0.00	0.16	0.24	1.4	0.09
	SRNOM-7	1.34	0.00	0.00	0.00	0.00	0.00	0.16	1.00	1.5	0.09
	SRNOM-8	1.38	0.00	0.00	0.00	0.00	0.00	0.14	1.00	0.5	0.04
	SRNOM-9	0.26	0.00	0.00	0.00	0.00	0.00	0.00	0.24	1.0	0.06
	SRNOM-10	0.26	0.00	0.00	0.00	0.00	0.00	0.00	0.24	2.0	0.12

Table S4.

Ion components and alkalinity of the Na_2SeO4, $Na_2S_2O_3$, and Na_2CrO_4 water series used in this study

Series	Water	Na^+	SeO_4^{2-}	$S_2O_3^{2-}$	CrO_4^{2-}	Alkalinity meq/L ≈ HCO_3^-	Source
		mmol/L	mmol/L	mmol/L	mmol/L	mmol/L	
Na_2SeO_4	Na_2SeO_4-1	0.89	0.31	0.00	0.00	0.24	Elix water
	Na_2SeO_4-2	0.50	0.13	0.00	0.00	0.24	
	Na_2SeO_4-3	0.42	0.08	0.00	0.00	0.24	
$Na_2S_2O_3$	$Na_2S_2O_3$-1	0.89	0.00	0.32	0.00	0.24	
	$Na_2S_2O_3$-2	0.50	0.00	0.13	0.00	0.24	
	$Na_2S_2O_3$-3	0.42	0.00	0.09	0.00	0.24	
Na_2CrO_4	Na_2CrO_4-1	0.89	0.00	0.00	0.32	0.24	
	Na_2CrO_4-2	0.51	0.00	0.00	0.13	0.24	
	Na_2CrO_4-3	0.42	0.00	0.00	0.09	0.24	

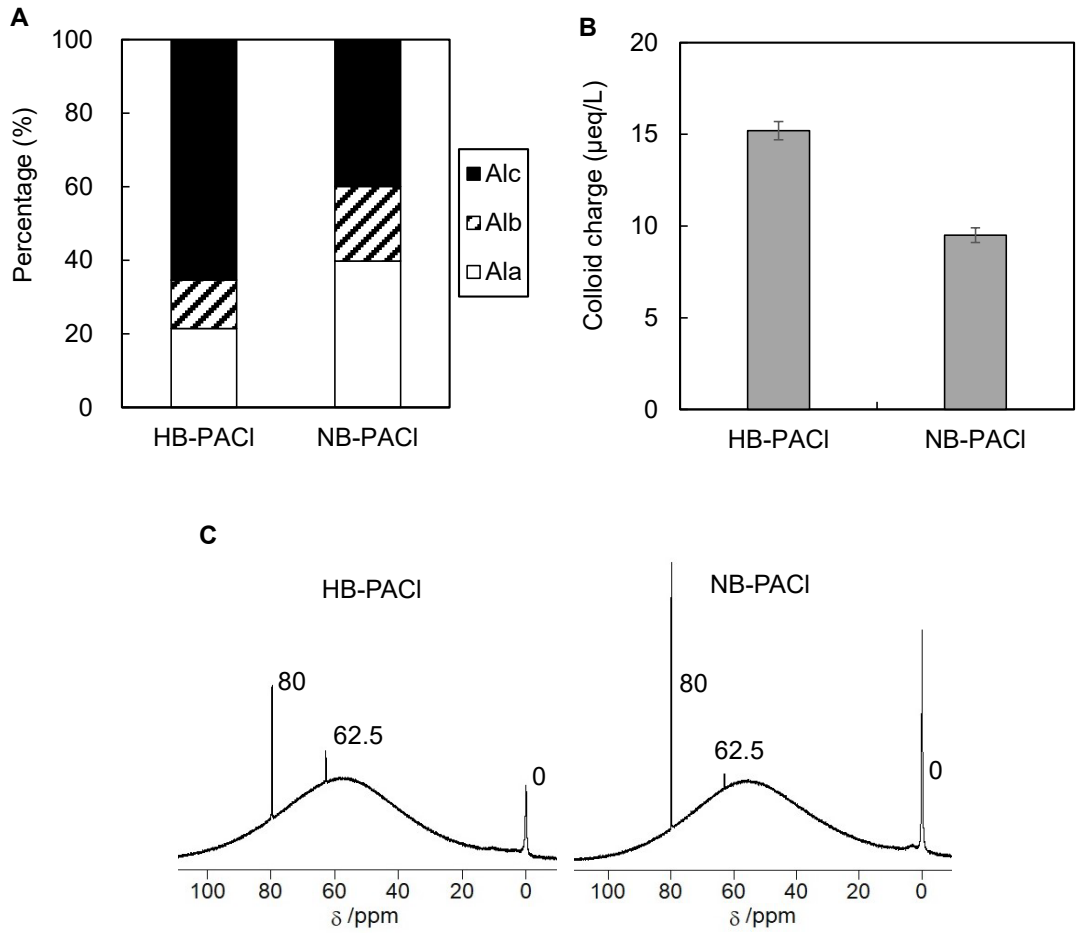

Fig. S1. Characteristics of HB-PACl and NB-PACl. Panel A: ferron distributions. Panel B: colloid charges. Panel C: ^{27}Al-NMR spectra. The peaks at δ = 80 ppm are due to the internal standard, $NaAl(OH)_4$.

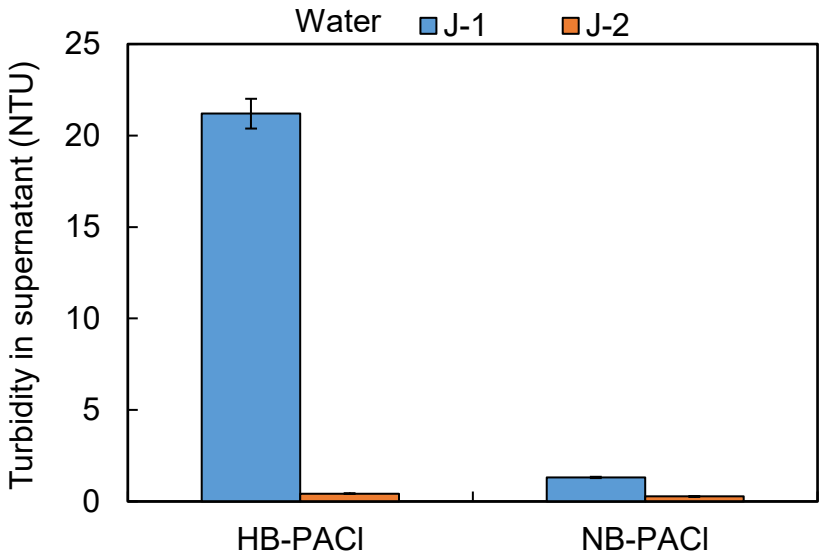

Fig. S2. The residual turbidities of supernatants. Waters J-1 and J-2 with sulfate ion concentrations of 4.0 mg/L and 15.3 mg/L, respectively, were used. Superfine powdered activated carbon was used as the removal target substance. HB-PACl and NB-PACl were used at a dose of 4.0 mg-Al/L. The coagulation pH was 7.0 (Chen et al., 2020).

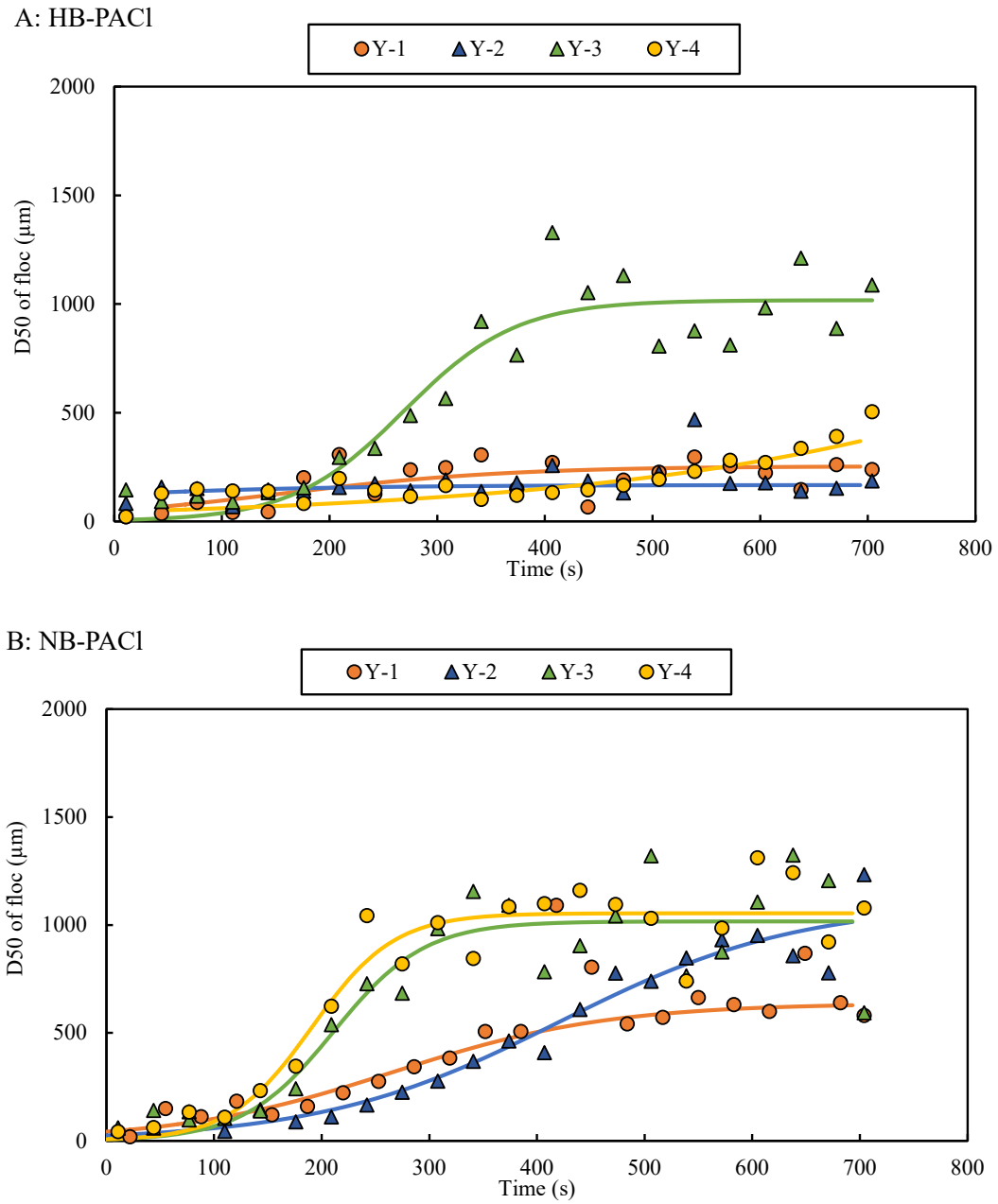

Fig. S3. Change of D50 of floc particles in coagulation experiments using HB-PACl (Panel A) and NB-PACl (Panel B). Particle size measurements were conducted every 10 s, and the average value of triplicate measurements is shown (plots). The lines are the fits to the semi-empirical model equation proposed by Chassagne (2021). The time until the D50 of floc particles grew to 500 μm was determined from the model-fit lines. Y series waters (Y-1–4) were used in these experiments. The PACl dose was 2.5 mg-Al/L. The coagulation pH was 7.0.

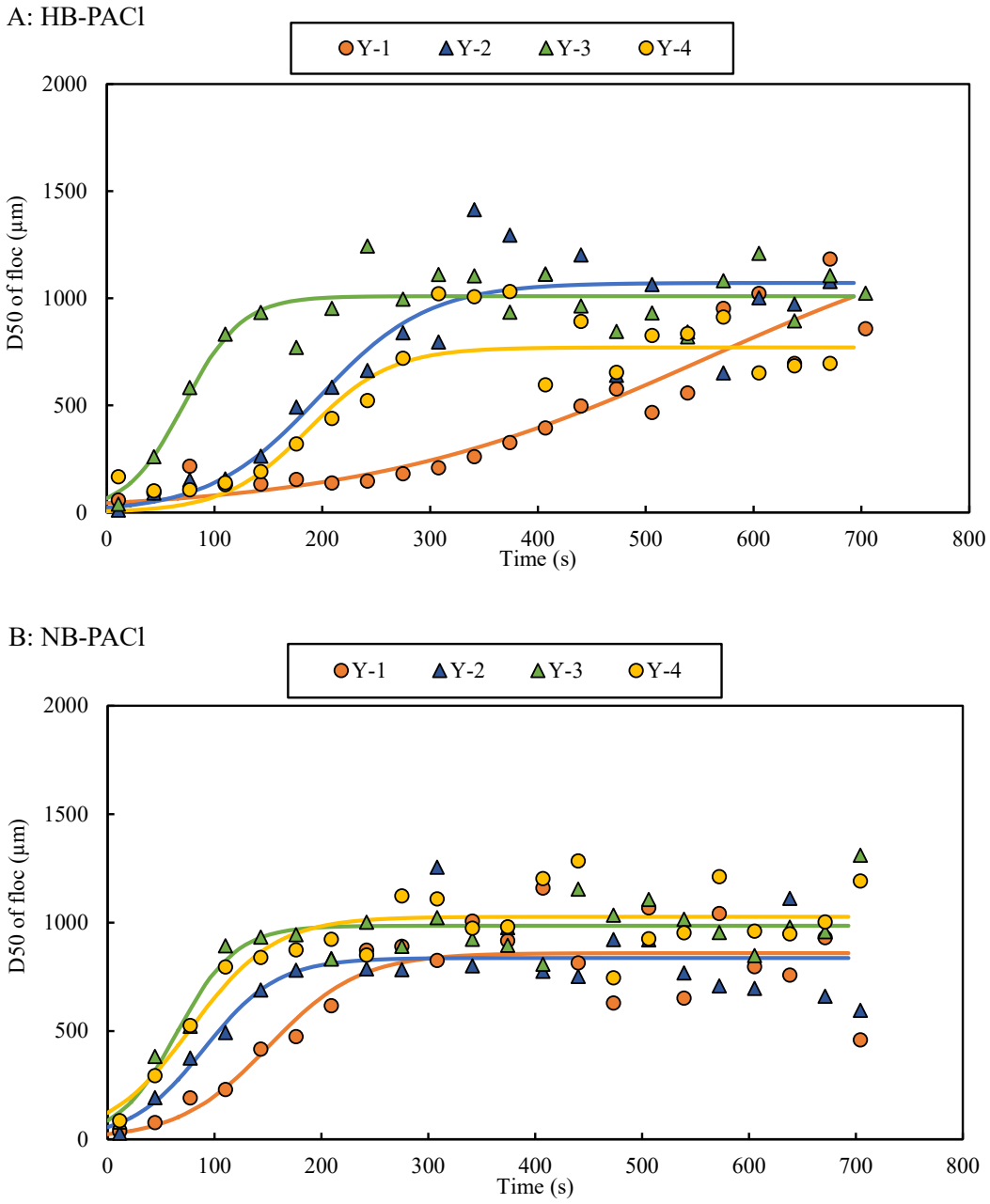

Fig. S4. Change of D50 of floc particles in coagulation experiments using HB-PACl (Panel A) and NB-PACl (Panel B). A particle size measurement was conducted every 10 s and the averages of triplicate measurements are shown (symbols). The lines are the fits to the semi-empirical model equation proposed by Chassagne (2021). The time until the D50 of the floc particles grew to 500 µm was determined from the model-fit lines. Y series waters (Y-1–4) were used in these experiments. The PACl dose was 2.5 mg-Al/L. The coagulation pH was 7.5.

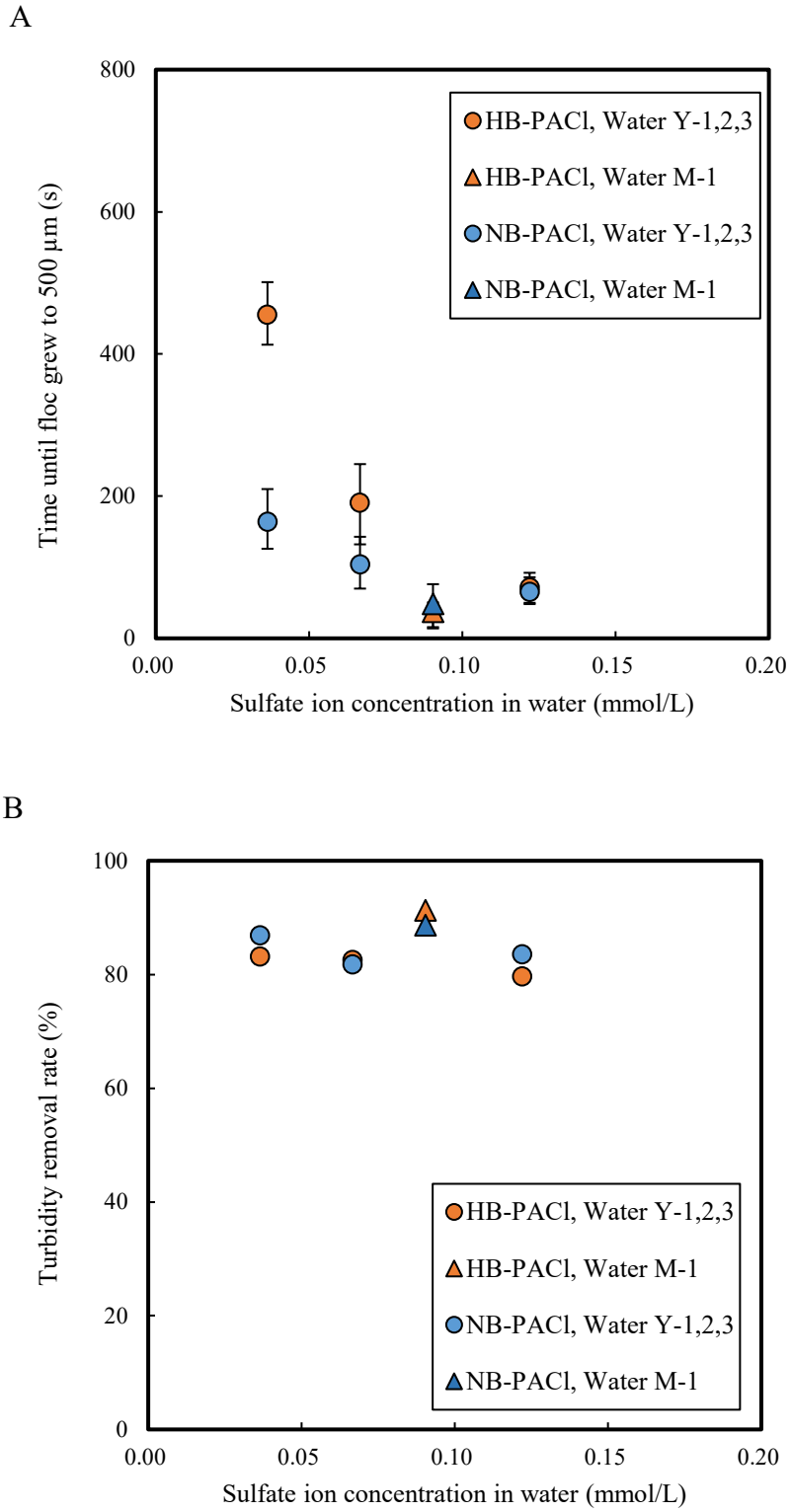

Fig. S5. Plots of the time until the floc grew to 500 µm (Panel A) and rate of turbidity removal (Panel B) against sulfate ion concentration. HB-PACl and NB-PACl were used. Y-1–3 and M-1 waters were used. The PACl dose was 2.5 mg-Al/L. The coagulation pH was 7.5. Error bars in Panel A indicate 95% confidence intervals.

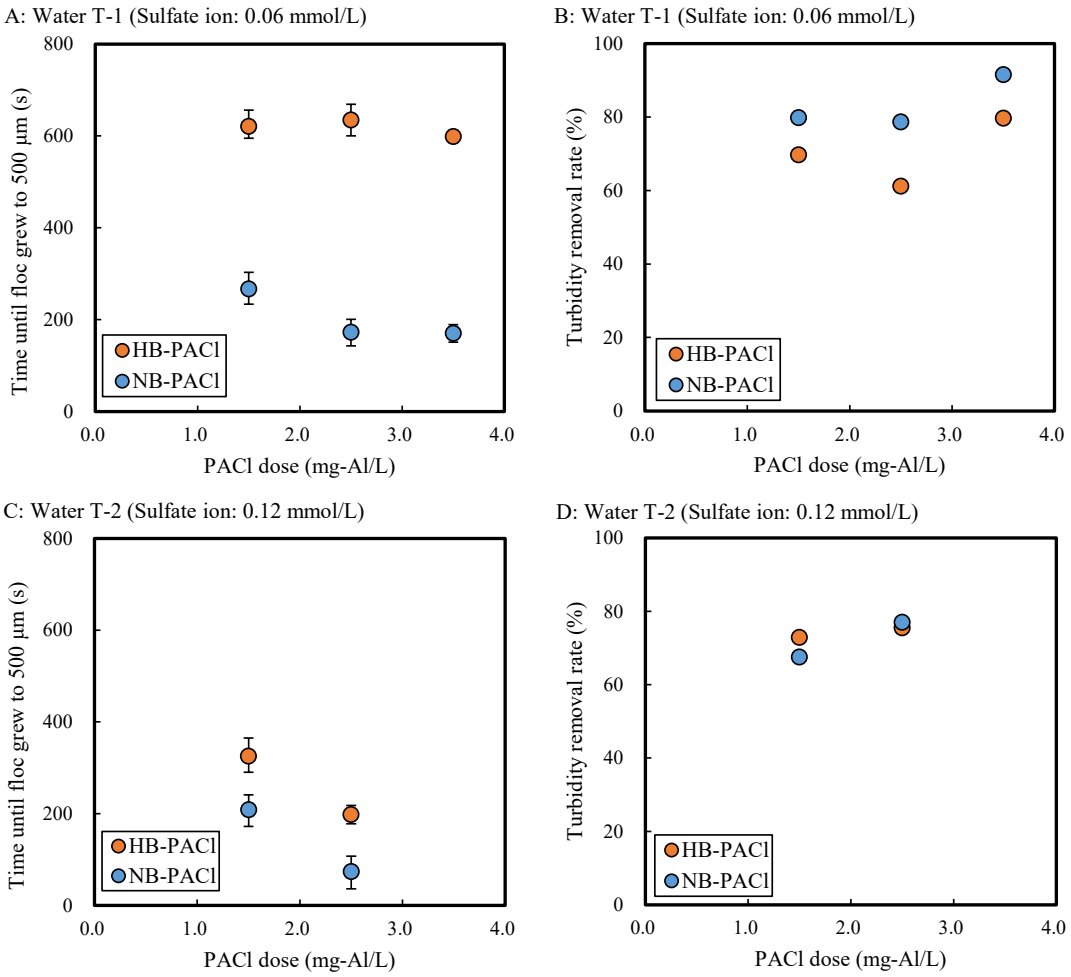

Fig. S6. Plots of the time till floc grew to 500 µm and rate of turbidity removal against PACl dose. Panels A and B show the data for HB-PACl and NB-PACl in water T-1. Panels C and D show the data in water T-2. The coagulation pH was controlled at 7.0. The PACls were 1.5, 2.5, and 3.5 mg-Al/L. Error bars in Panel A and C indicate 95% confidence intervals.

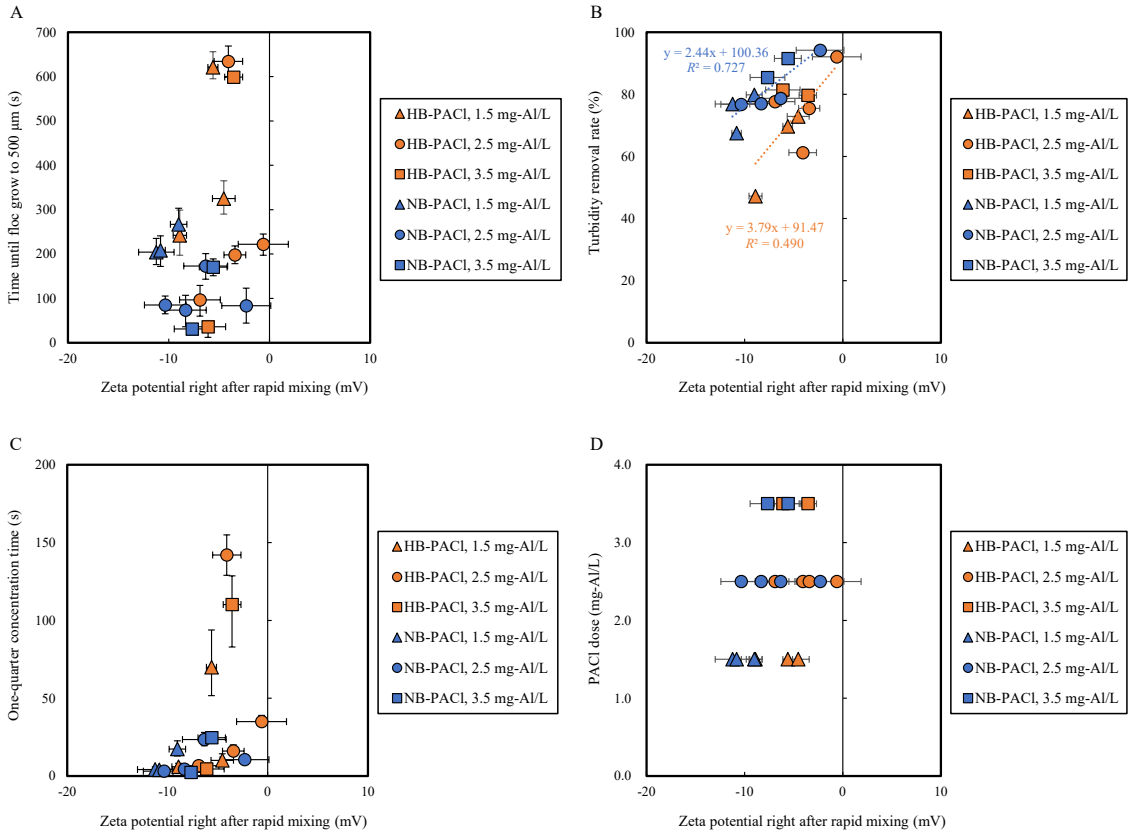

Fig. S7. Plots of the time until floc grow to 500 μm (Panel A), turbidity removal rate (Panel B), one-quarter concentration time in hydrolysis rate test (Panel C), and PACl dose (Panel D) against zeta potential right after rapid mixing. HB-PACl and NB-PACl were used. The PACl doses were 1.5, 2.5, and 3.5 mg-Al/L. Coagulation experiments were conducted in M and T series waters. The coagulation pH was 7.0. Error bars in *x*-axis indicate standard deviations. Error bars in *y*-axis in Panel A and C indicate 95% confidence intervals.

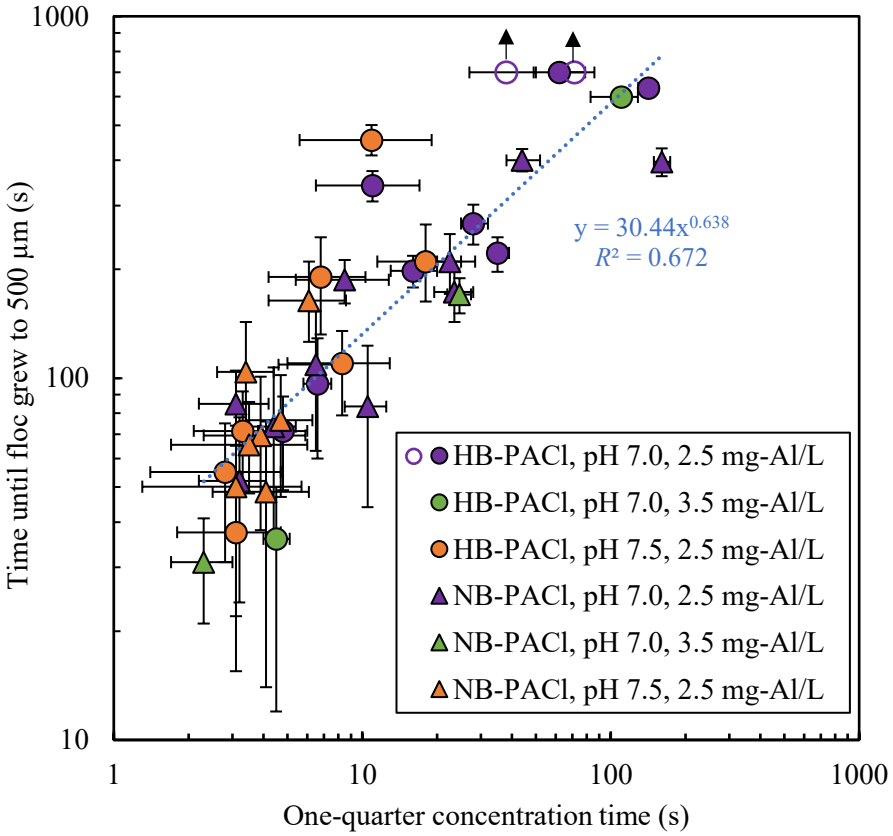

Fig. S8. Relationship between the time until floc grew to 500 µm and one-quarter concentration times in coagulation experiments. The results for HB-PACl and NB-PACl at pHs of both 7.0 and 7.5 are shown. Y-1–6, M-1,2, and T-1,2 waters were used in these experiments. Results for PACl doses of 2.5 and 3.5 mg-Al/L are shown. Open circles with an arrow indicate that floc size did not grow to 500 µm during flocculation, therefore the y-axis values were above that point. Error bars indicate 95% confidence intervals.

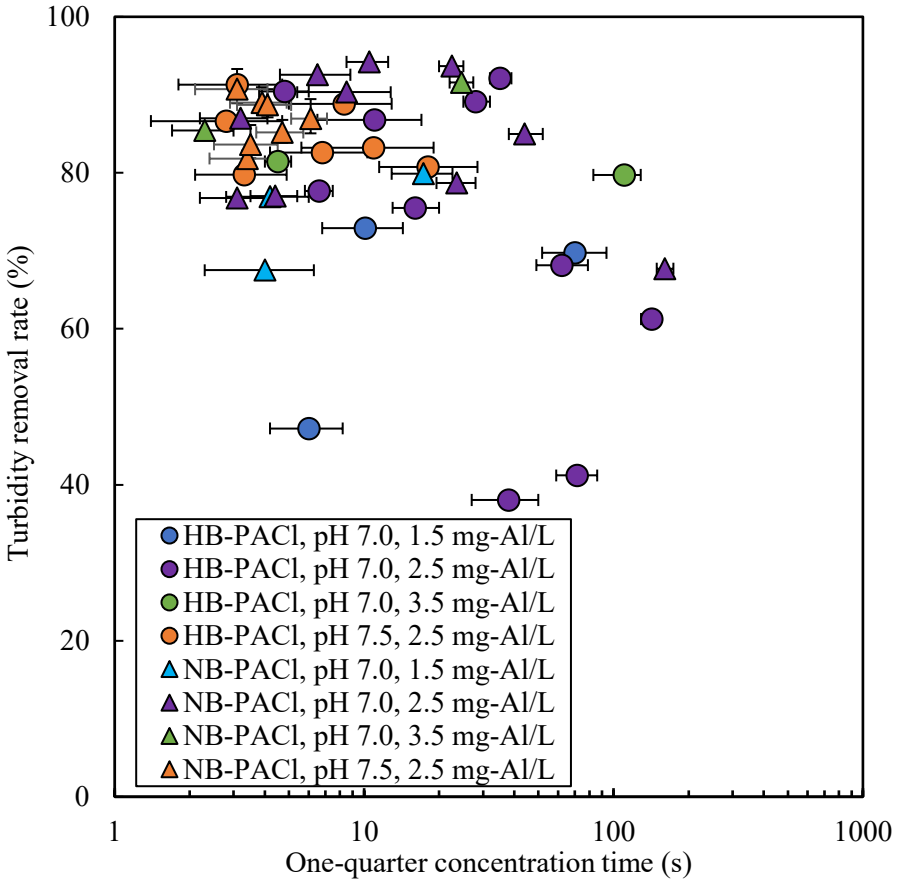

Fig. S9. Relationship between the rate of turbidity removal and the one-quarter concentration time. HB-PACl and NB-PACl were used. Y-1–6, M-1,2, and T-1,2 waters were used. The PACl doses were 1.5, 2.5, and 3.5 mg-Al/L. Coagulation pHs were 7.0 and 7.5. Error bars indicate 95% confidence intervals.

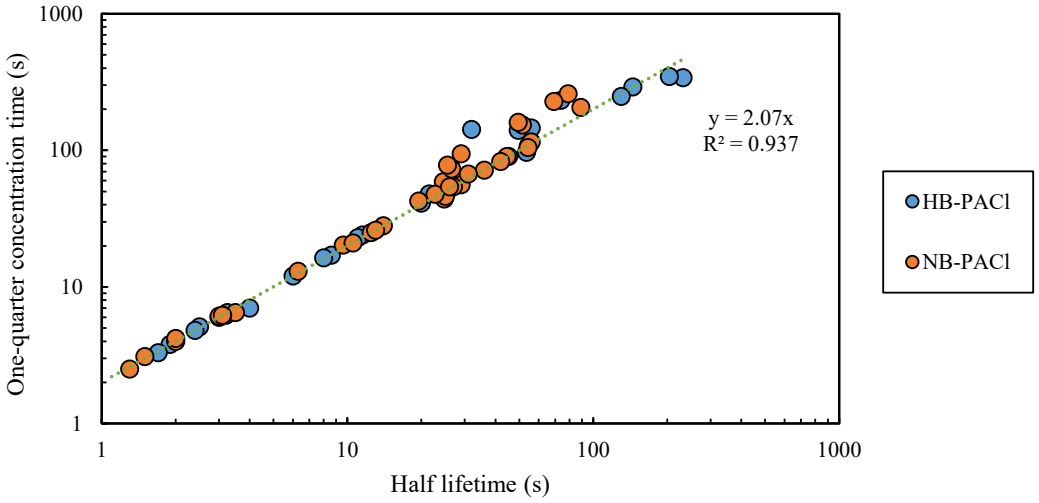

Fig. S10. The relationship between one-quarter concentration times and half lifetime. NOM-free waters (Na_2SO_4, $NaHCO_3$, NaCl, $NaNO_3$, K_2SO_4, $MgSO_4$, $CaSO_4$, Na_2SeO_4, $Na_2S_2O_3$, and Na_2CrO_4 series) were used. The PACl dose was 2.5 mg-Al/L. The coagulation pH was 7.0. Error bars indicate 95% confidence intervals.

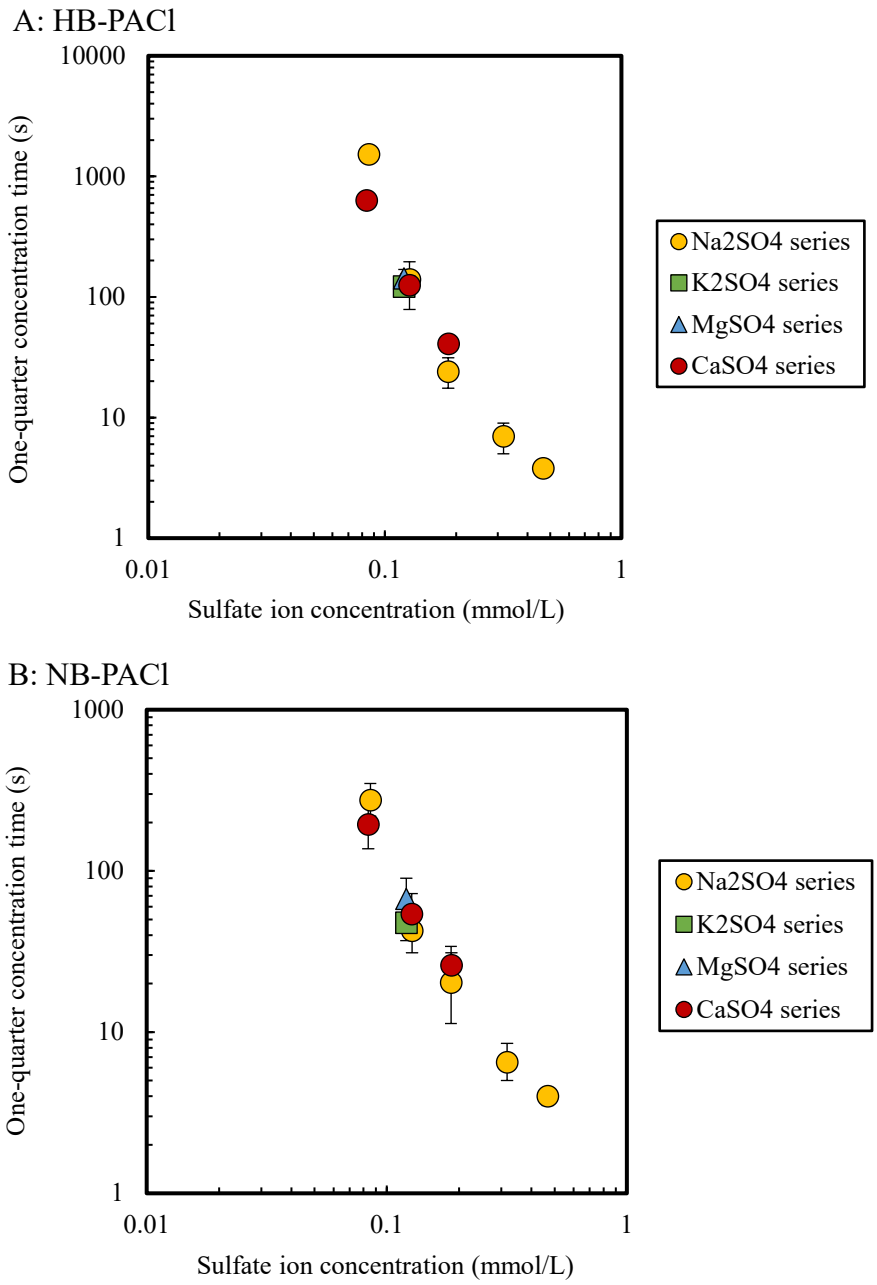

Fig. S11. Plots of one-quarter concentration times against sulfate ion concentrations with different counter cations. Panel A shows the data for HB-PACl in Na_2SO_4-1–4,6 and $CaSO_4$-1,3,4 waters. Panel B shows the data for NB-PACl in Na_2SO_4-2–4 and $CaSO_4$-1,3,4 waters. The PACl dose was 2.5 mg-Al/L. The coagulation pH was 7.0. Error bars indicate 95% confidence intervals.

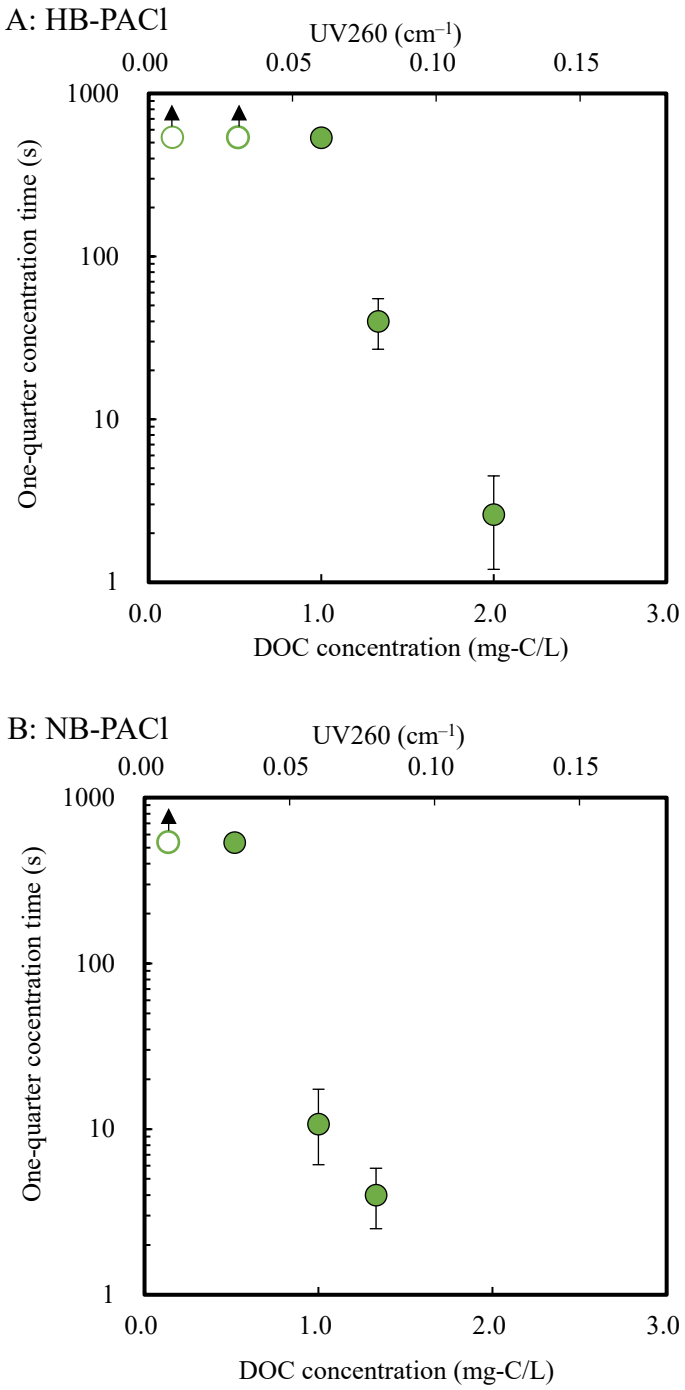

Fig. S12. Plots of one-quarter concentration times against DOC concentrations. Panel A shows the data for HB-PACl in SRNOM-1–3,9,10 waters. Panel B shows the data for NB-PACl in SRNOM-1–3,9 waters. The PACl dose was 2.5 mg-Al/L. The coagulation pH was 7.0. Open circles with an arrow indicate that one-quarter concentration times exceeded 540 s. Error bars indicate 95% confidence intervals.

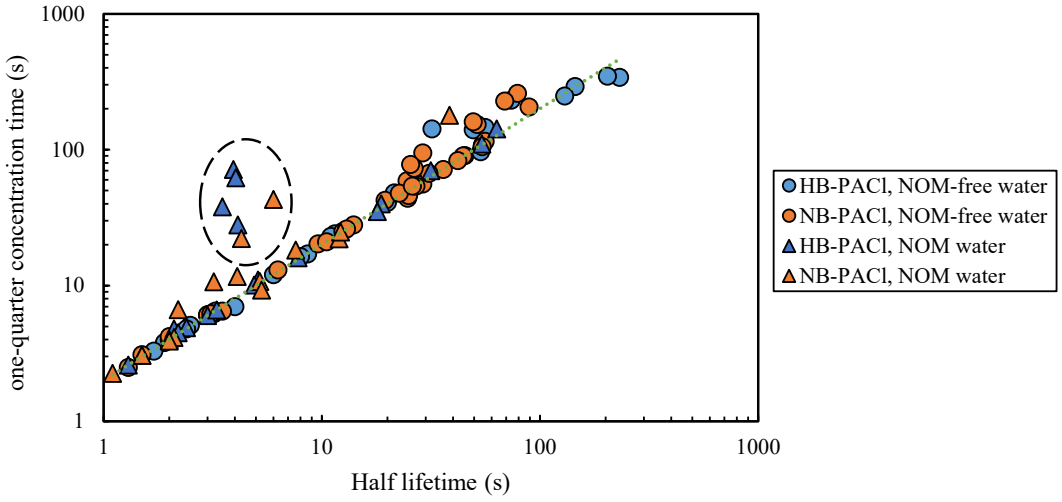

Fig. S13. Relationship between one-quarter concentration times and half lifetimes. NOM-free water (Na_2SO_4, $NaHCO_3$, NaCl, $NaNO_3$, K_2SO_4, $MgSO_4$, $CaSO_4$, Na_2SeO_4, $Na_2S_2O_3$, and Na_2CrO_4 series) and NOM water (SRNOM, Y, M, T series) were used. The PACl doses were 1.5, 2.5, and 3.5 mg-Al/L. The coagulation pH was 7.0. Error bars indicate 95% confidence intervals.

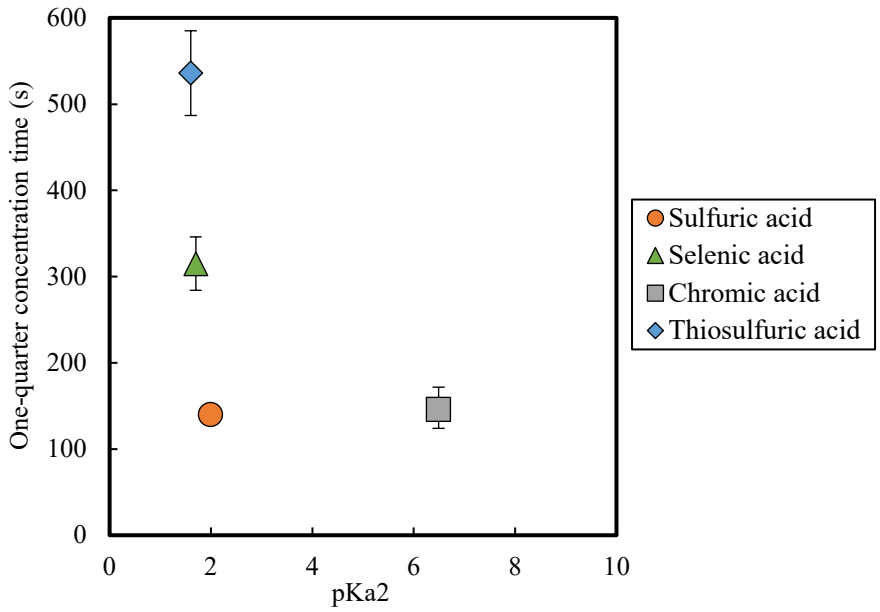

Fig. S14. Plots of one-quarter concentration times in waters that contained sulfate ions, selenate ions, chromate ions, or thiosulfate ions against the pKa2 value of these ions. Na_2SO_4-4, Na_2SeO_4-2, Na_2CrO_4-1, and $Na_2S_2O_3$-2 waters were used. The PACl dose was 2.5 mg-Al/L, and the coagulation pH was 7.0. The pKa2 data for sulfuric acid, selenic acid, and chromic acid are from Lide (2004). The pKa2 data for thiosulfuric acid are from Macintyre et al. (1992). Error bars indicate 95% confidence intervals.

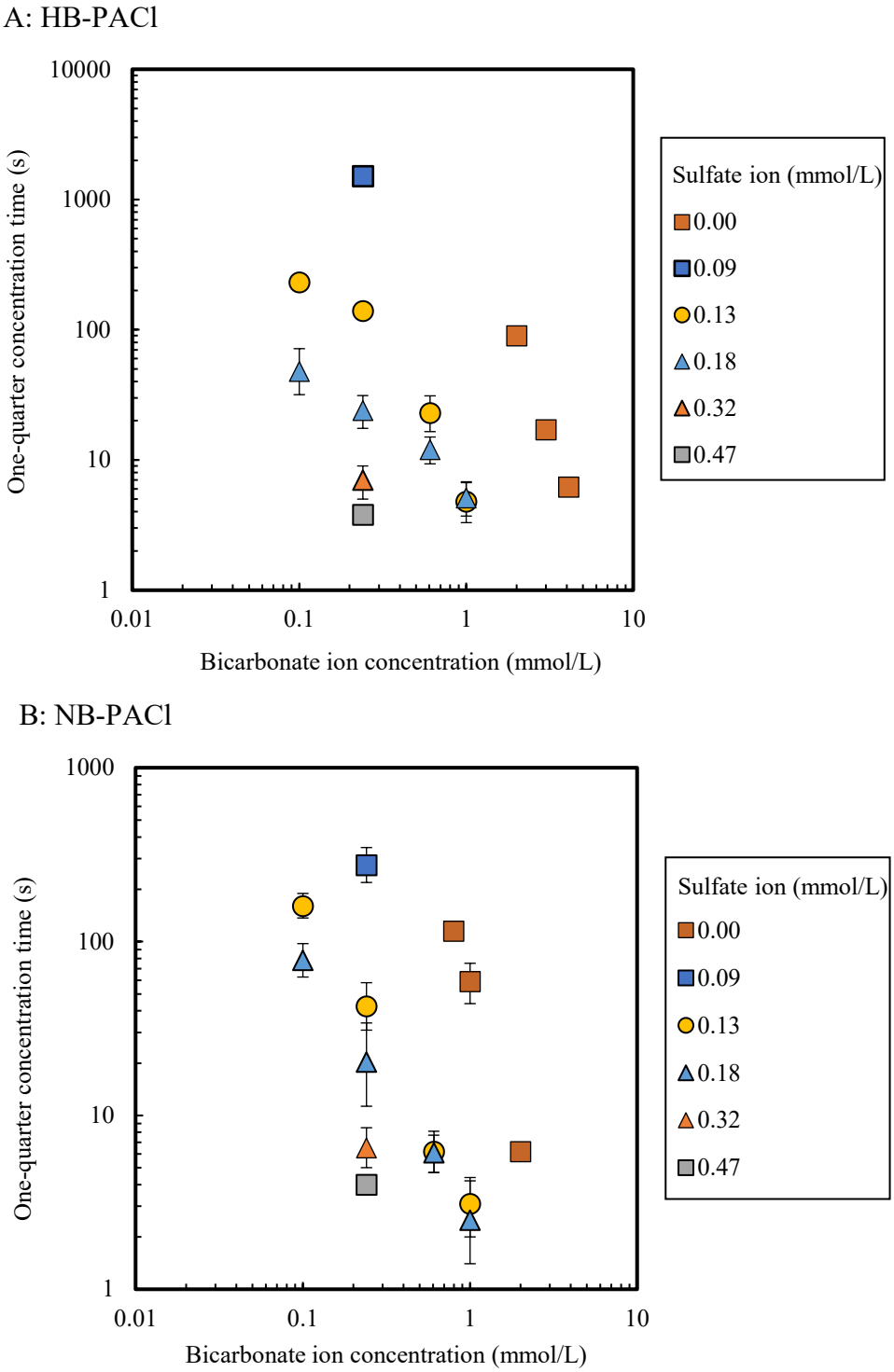

Fig. S15. One-quarter concentration times for various bicarbonate and sulfate ion concentrations. Panel A: HB-PACl was used in waters Na_2SO_4-1–3,6,8–13, and $NaHCO_3$-3,5,6 waters. Panel B: NB-PACl was used in Na_2SO_4-1–4,6,8–13, and $NaHCO_3$-1,5,7 waters. The PACl dose was 2.5 mg-Al/L. The coagulation pH was 7.0. Error bars indicate 95% confidence intervals.

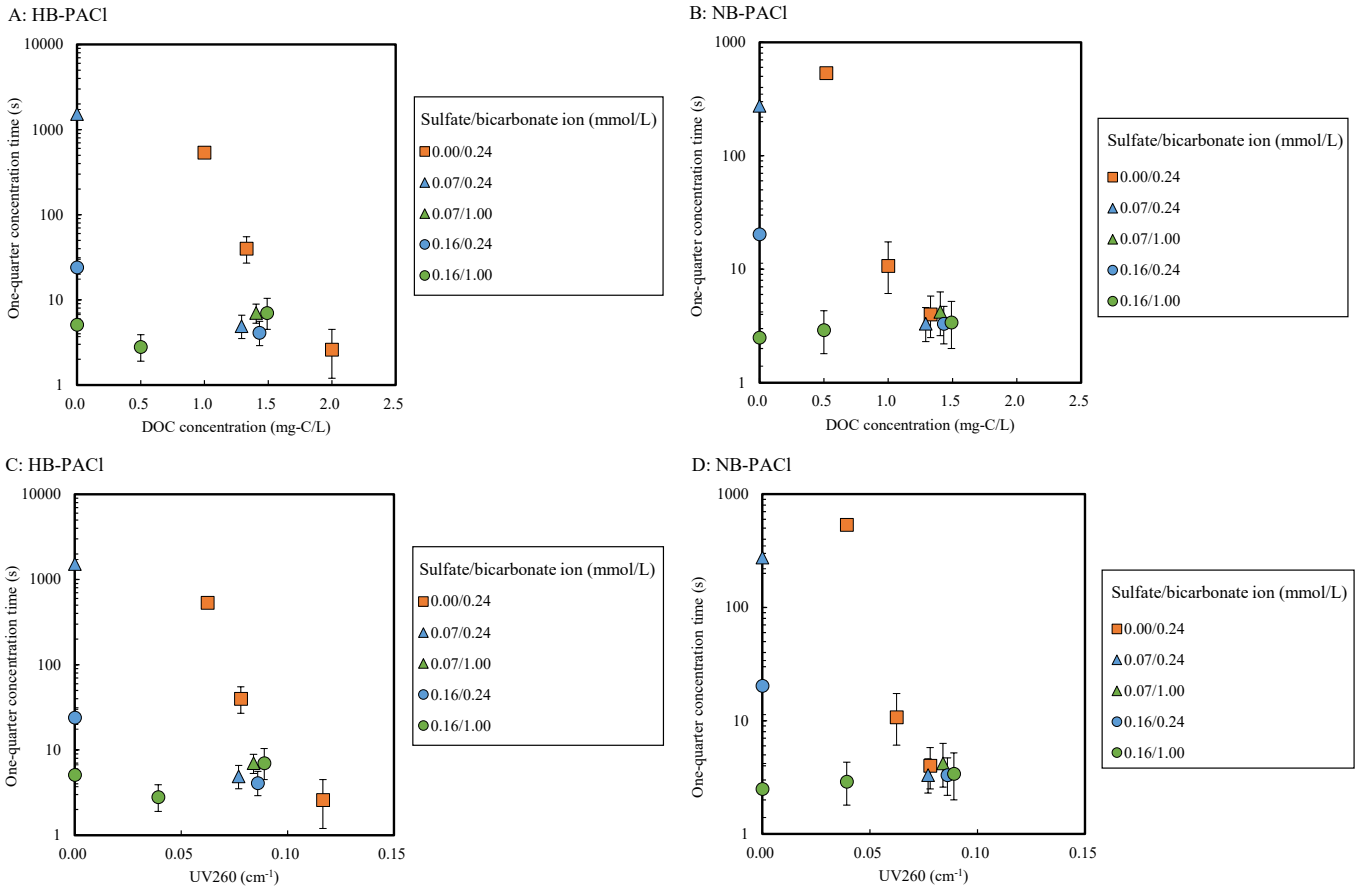

Fig. S16. One-quarter concentration times for various concentrations of NOM (DOC in Panels A and B, UV260 in Panels C and D), sulfate ions, and bicarbonate ions. Panels A and C; HB-PACl was used in SRNOM-3–5,7–10 and Na_2SO_4-2,3,6,8 waters. Panel B and D: NB-PACl was used in SRNOM-2–5,7–9, and Na_2SO_4-2,3,6,8 waters. The coagulation pH was 7.0. The PACl dose was 2.5 mg-Al/L. Numerical values in the legends indicate the concentrations of sulfate ion and bicarbonate ion. Error bars indicate 95% confidence intervals.

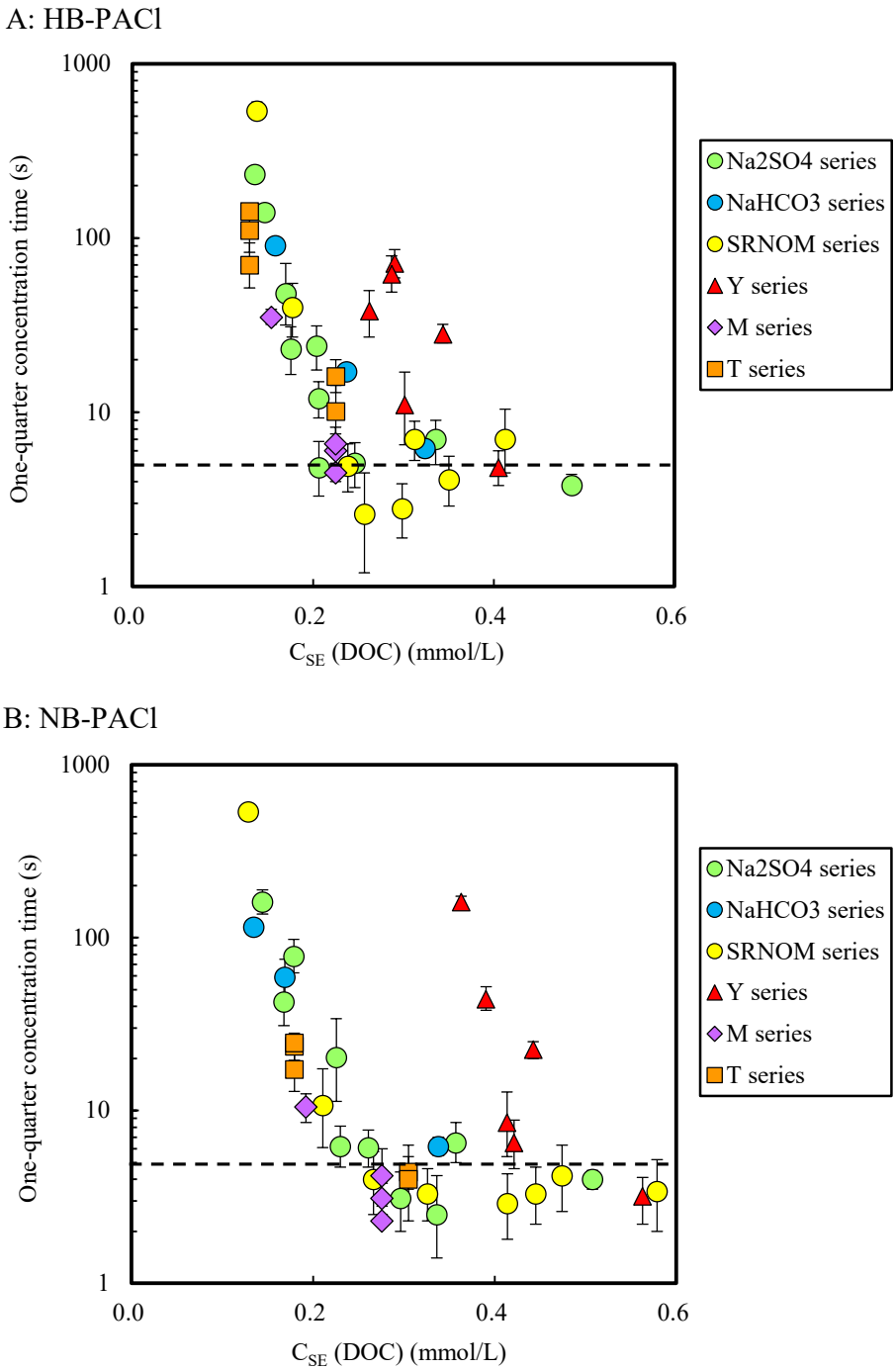

Fig. S17. One-quarter concentration times versus C_{SE} values, where DOC was used instead of UV260 for the NOM concentration. Panel A shows the data for HB-PACl in Na_2SO_4-1,2,4,6,8–13, $NaHCO_3$-3,5,6, SRNOM-3–10, Y-1–6, M-1,2, and T-1,2 waters, and Panel B shows the data for NB-PACl in Na_2SO_4-1,2,4,6,8–13, $NaHCO_3$-1,5,7, SRNOM-2–9, Y-1–6, M-1,2, and T-1,2 waters. The PACl dose was 2.5 mg-Al/L, but doses of 1.5 and 3.5 mg-Al/L were also used in the experiments with M-1,2 and T-1,2 waters. The coagulation pH was 7.0. Error bars indicate 95% confidence intervals.

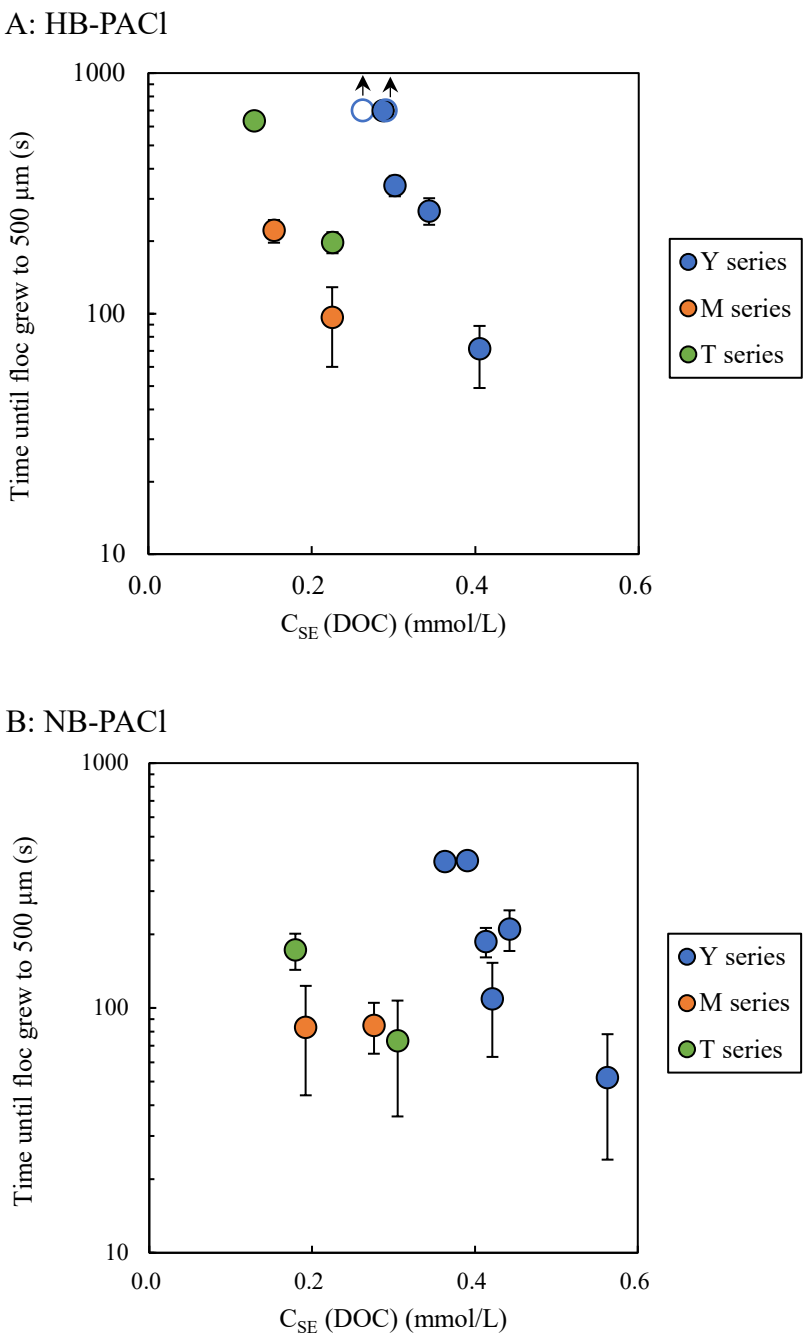

Fig. S18. Plots of the time until floc grew to 500 µm for HB-PACl (Panel A) and NB-PACl (Panel B) against C_{SE}, where DOC was used instead of UV260 for the NOM concentration. Y, M, and T series waters were used. The coagulation pH was 7.0. The PACl dose was 2.5 mg-Al/L. The open circles with an arrow in Panel A indicate that the floc size did not increase to 500 µm during the experiment, therefore the y-axis values were above that point. Error bars indicate 95% confidence intervals.

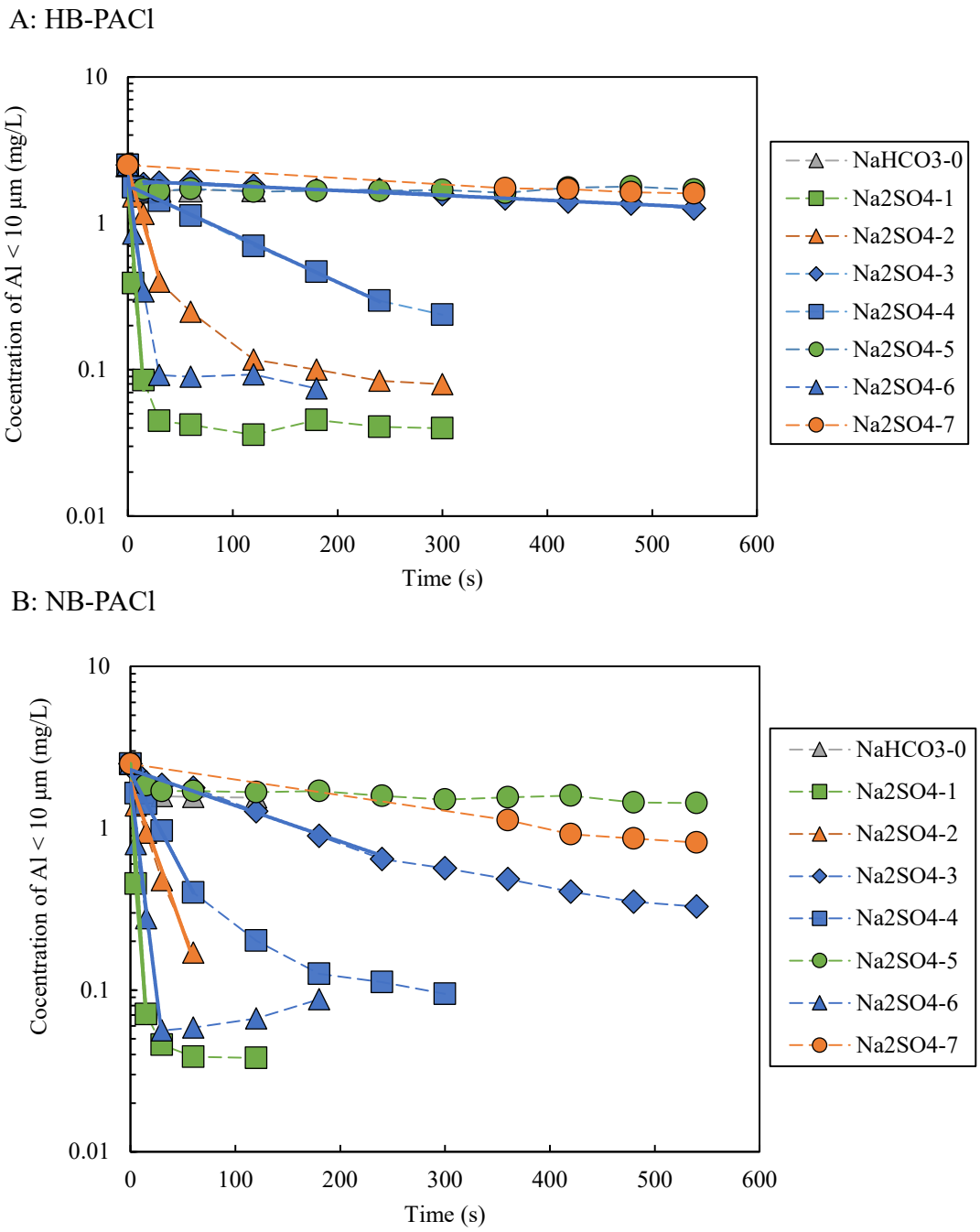

Fig. S19. Change of concentration of aluminum that passed through a membrane with a 10-µm pore size in a test of hydrolysis rates. The results for HB-PACl are shown in Panel A. The results for NB-PACl are shown in Panel B. $NaHCO_3$-0 and Na_2SO_4-1–7 waters were used. The PACl dose was 2.5 mg-Al/L. The pH during the experiment was 7.0.

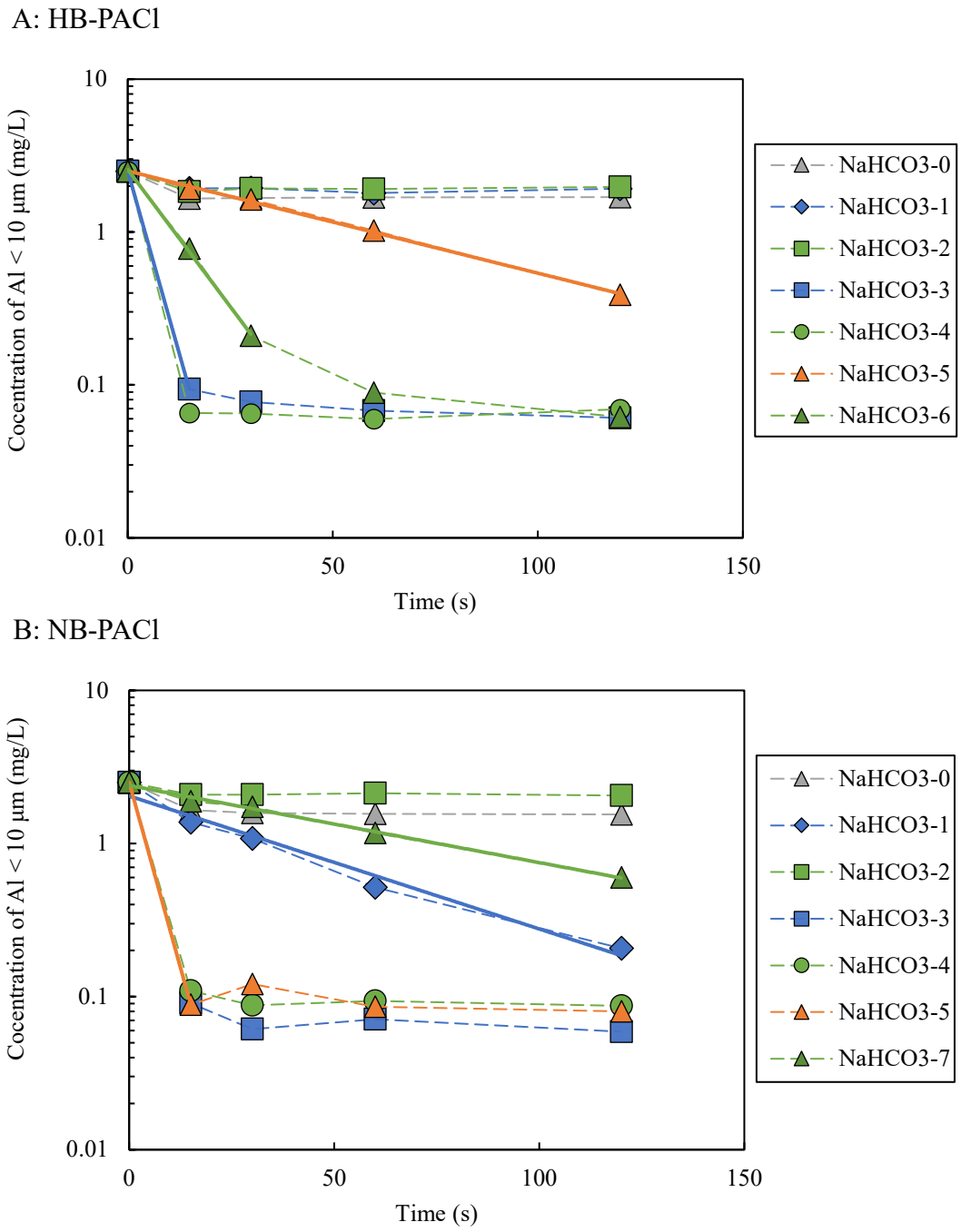

Fig. S20. Change of concentration of aluminum that passed through a membrane with a 10-µm pore size in a test of hydrolysis rates. $NaHCO_3$-0–7 waters were used. The results for HB-PACl are shown in Panel A. The results for NB-PACl are shown in Panel B. The PACl dose was 2.5 mg-Al/L. The pH during the experiment was 7.0.

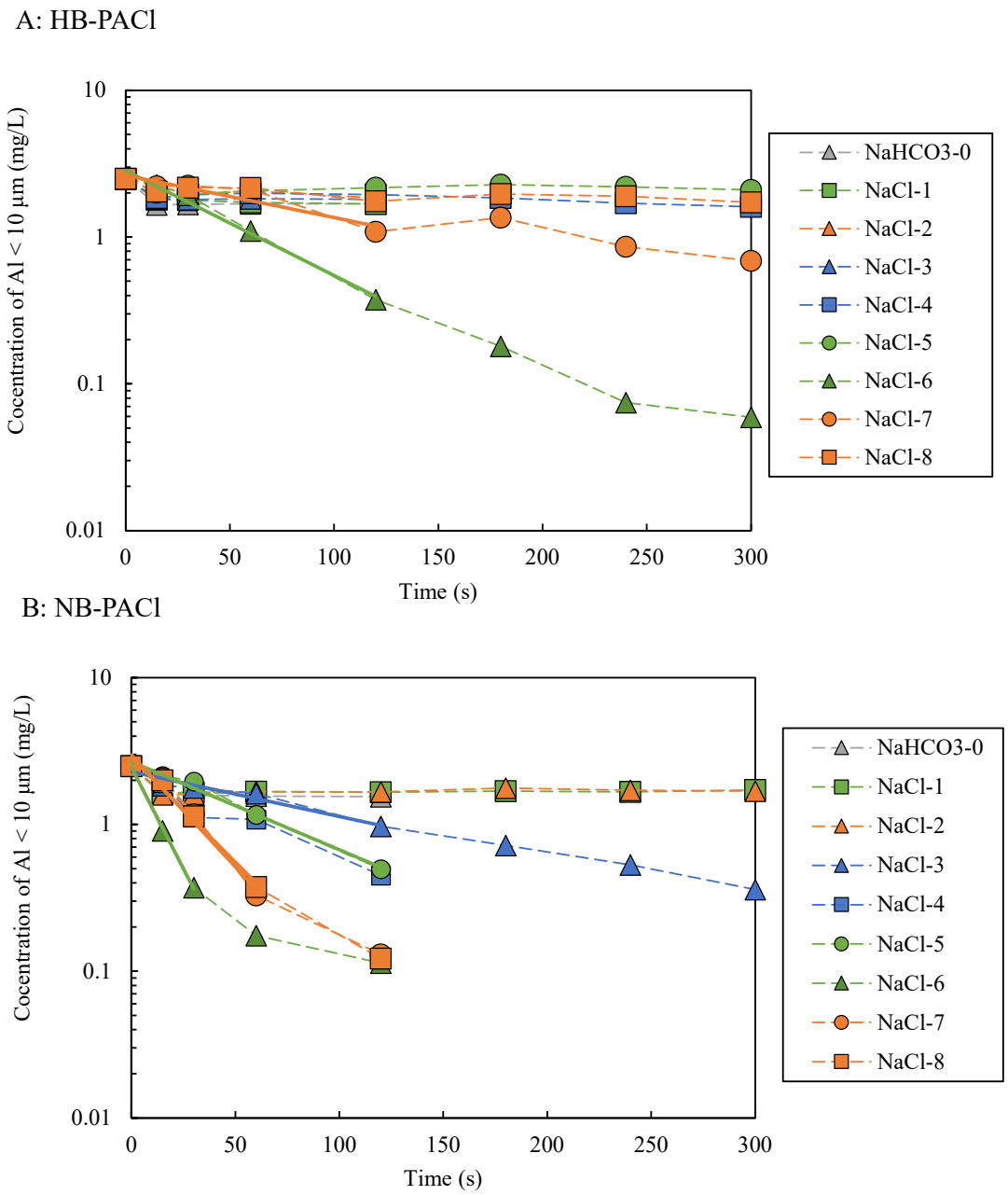

Fig. S21. Change of concentration of aluminum that passed through a membrane with a 10-µm pore size in a test of hydrolysis rates. $NaHCO_3$-0 and NaCl-1–8 waters were used. The results for HB-PACl are shown in Panel A. The results for NB-PACl are shown in Panel B. The PACl dose was 2.5 mg-Al/L. The pH during the experiment was 7.0.

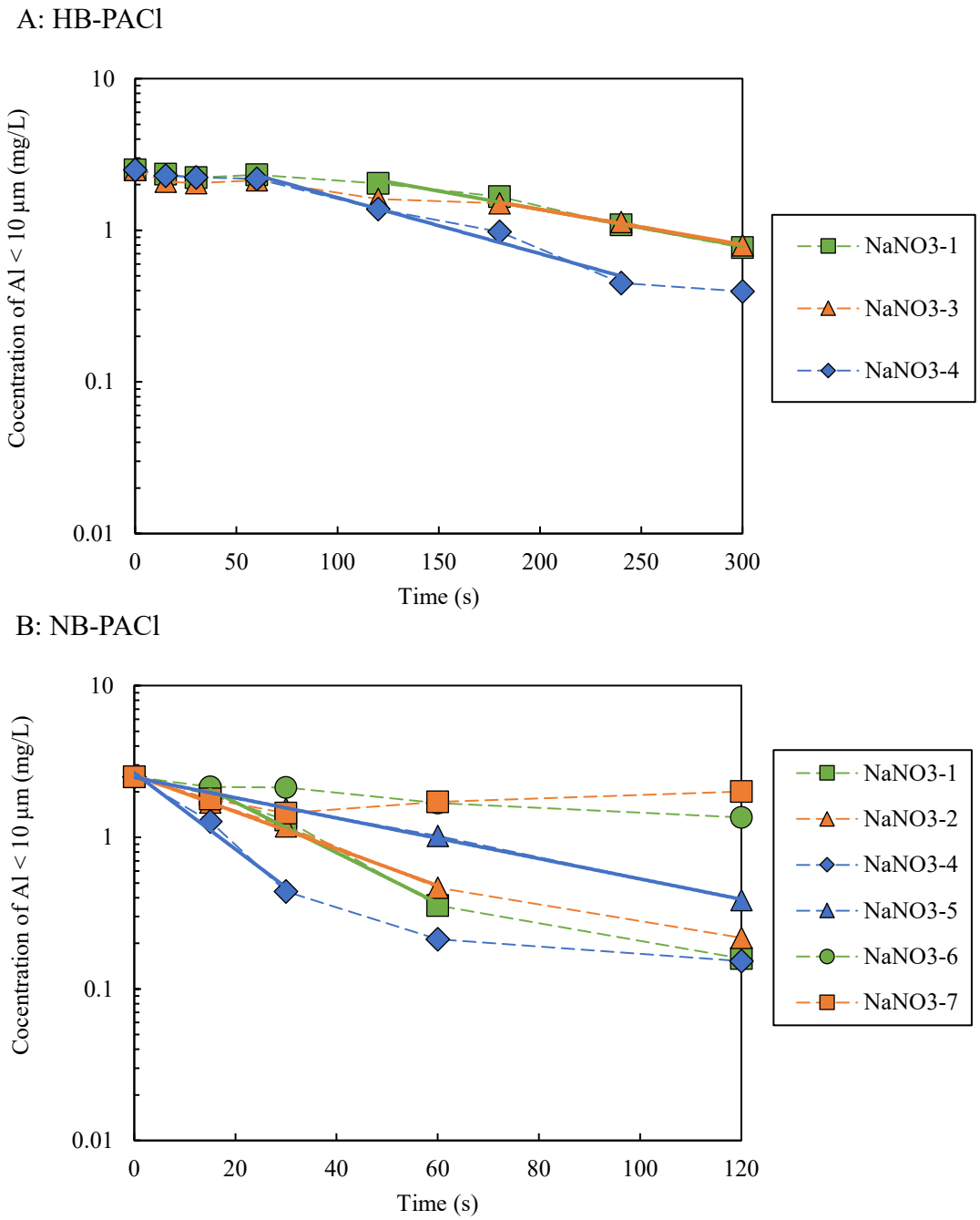

Fig. S22. Change of concentration of aluminum that passed through a membrane with a 10-µm pore size in a test of hydrolysis rates. $NaNO_3$-1–7 waters were used. The results for HB-PACl are shown in Panel A. The results for NB-PACl are shown in Panel B. The PACl dose was 2.5 mg-Al/L. The pH during the experiment was 7.0.

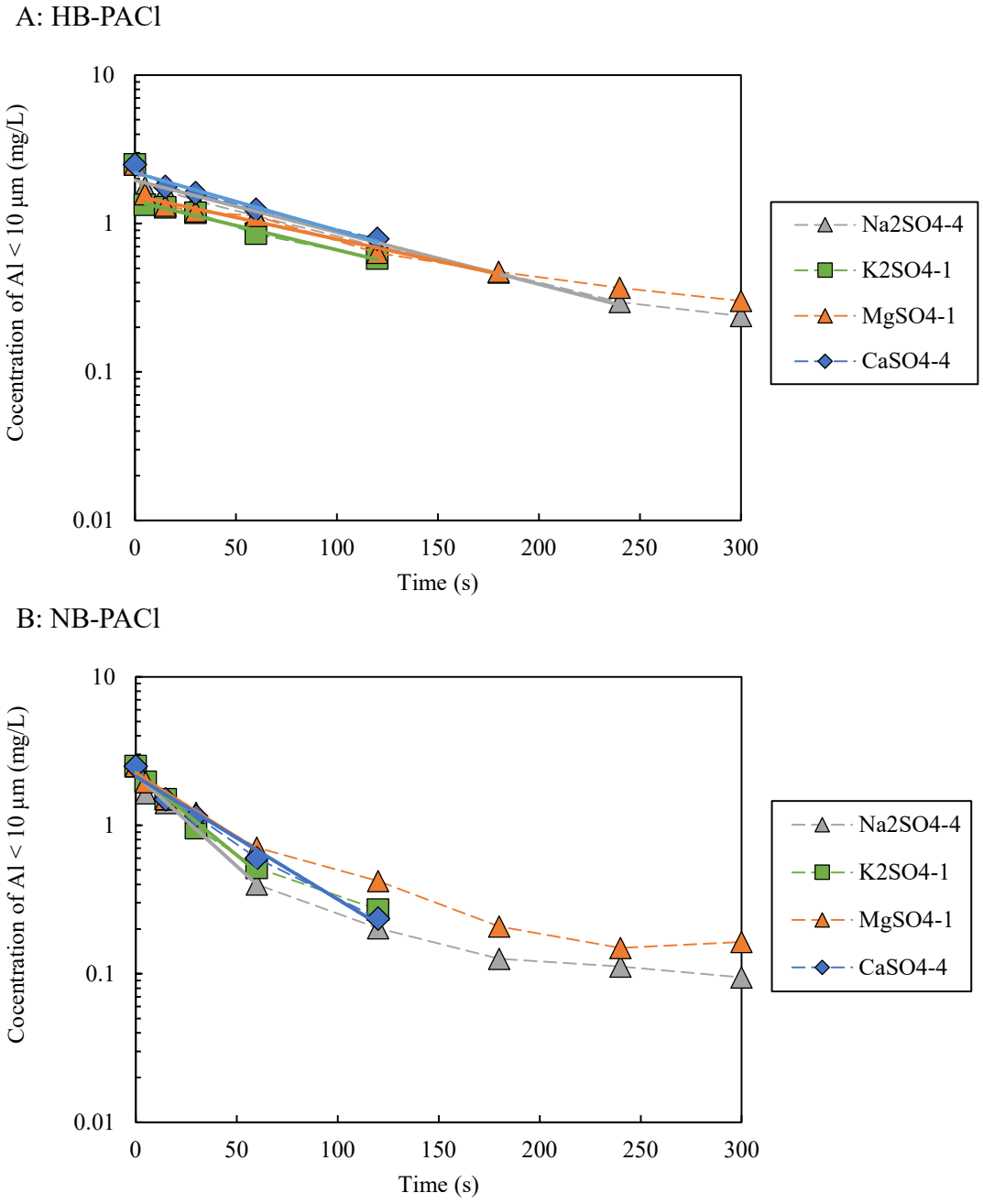

Fig. S23. Change of concentration of aluminum that passed through a membrane with a 10-µm pore size in a test of hydrolysis rates. $CaSO_4$-4, Na_2SO_4-4, K_2SO_4-1, and $MgSO_4$-1 waters were used. The results for HB-PACl are shown in Panel A. The results for NB-PACl are shown in Panel B. The PACl dose was 2.5 mg-Al/L. The pH during the experiment was 7.0.

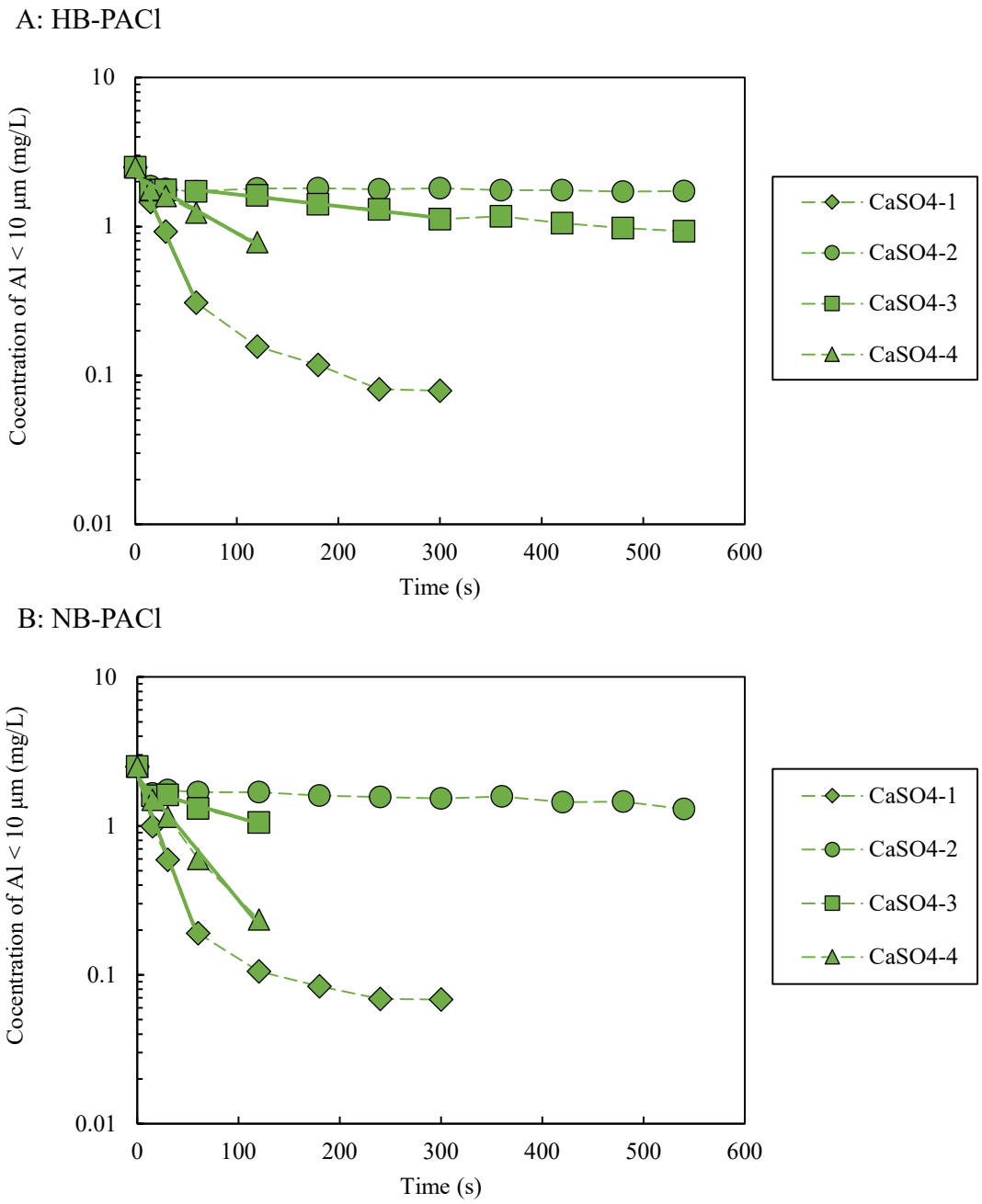

Fig. S24. Change of concentration of aluminum that passed through a membrane with a 10-µm pore size in a test of hydrolysis rates. $CaSO_4$ series water $CaSO_4$-1–4 were used. The results for HB-PACl are shown in Panel A. The results for NB-PACl are shown in Panel B. The PACl dose was 2.5 mg-Al/L. The pH during the experiment was 7.0.

.

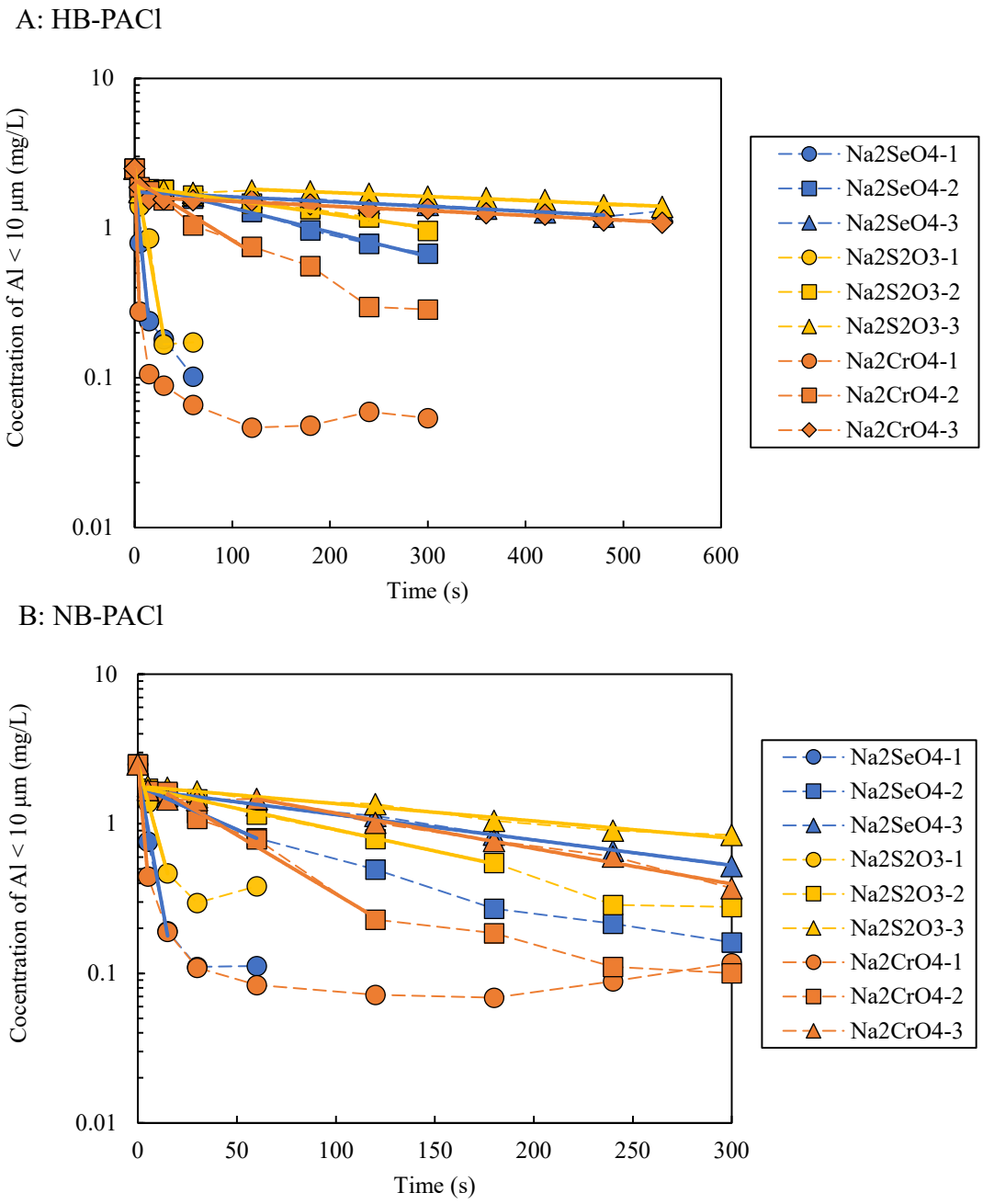

Fig. S25. Change of concentration of aluminum that passed through a membrane with a 10-µm pore size in a test of hydrolysis rates. Na_2SeO_4-1–3, $Na_2S_2O_3$-1–3, and Na_2CrO_4-1 waters were used. The results for HB-PACl are shown in Panel A. The results for NB-PACl are shown in Panel B. The PACl dose was 2.5 mg-Al/L. The pH during the experiment was 7.0.

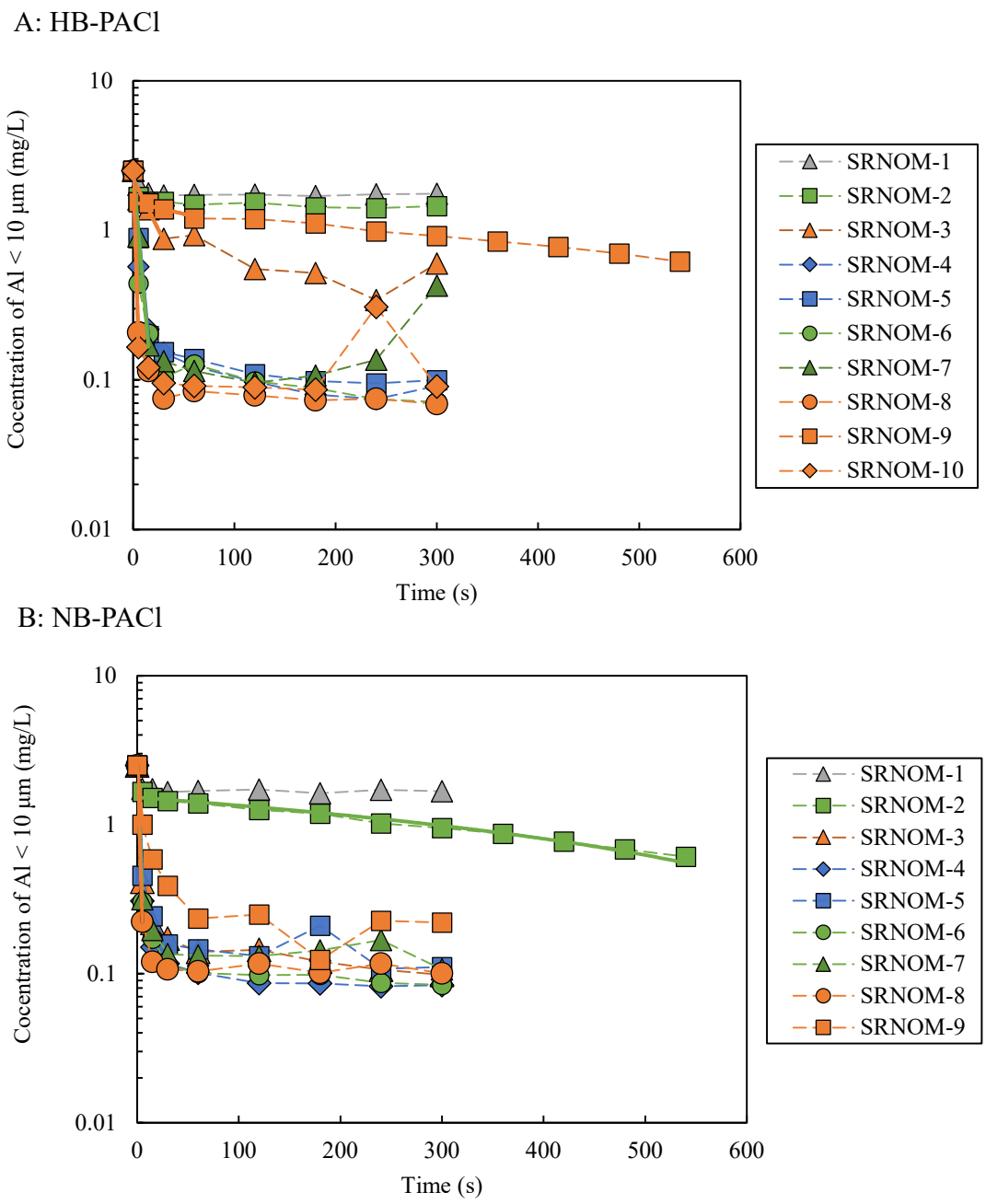

Fig. S26. Change of concentration of aluminum that passed through a membrane with a 10-µm pore size in a test of hydrolysis rates. SRNOM-1–10 waters were used. The results for HB-PACl are shown in Panel A. The results for NB-PACl are shown in Panel B. The PACl dose was 2.5 mg-Al/L. The pH during the experiment was 7.0.

A: HB-PACl

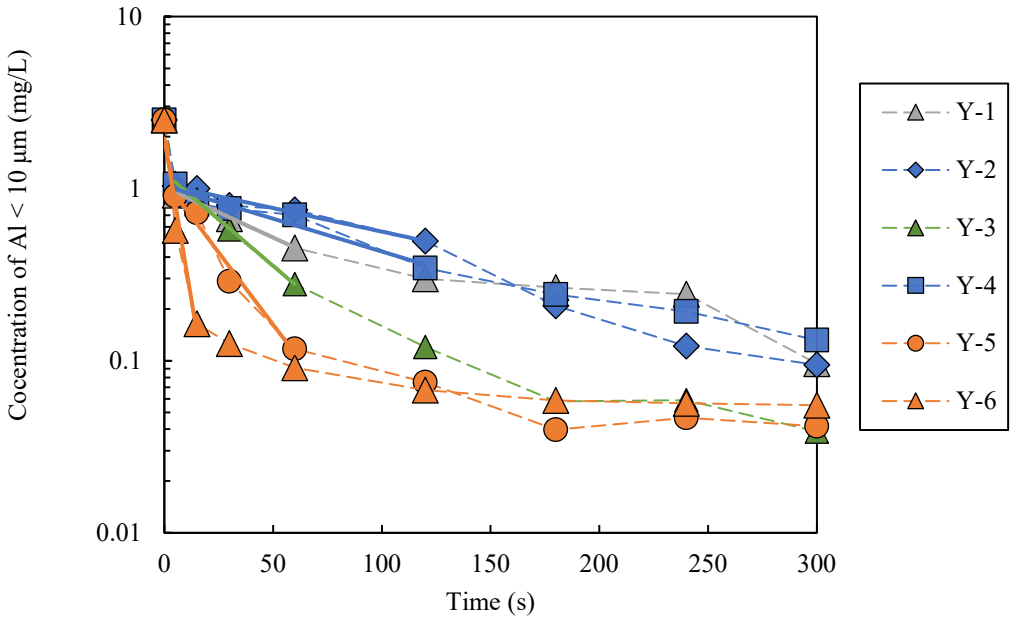

B: NB-PACl

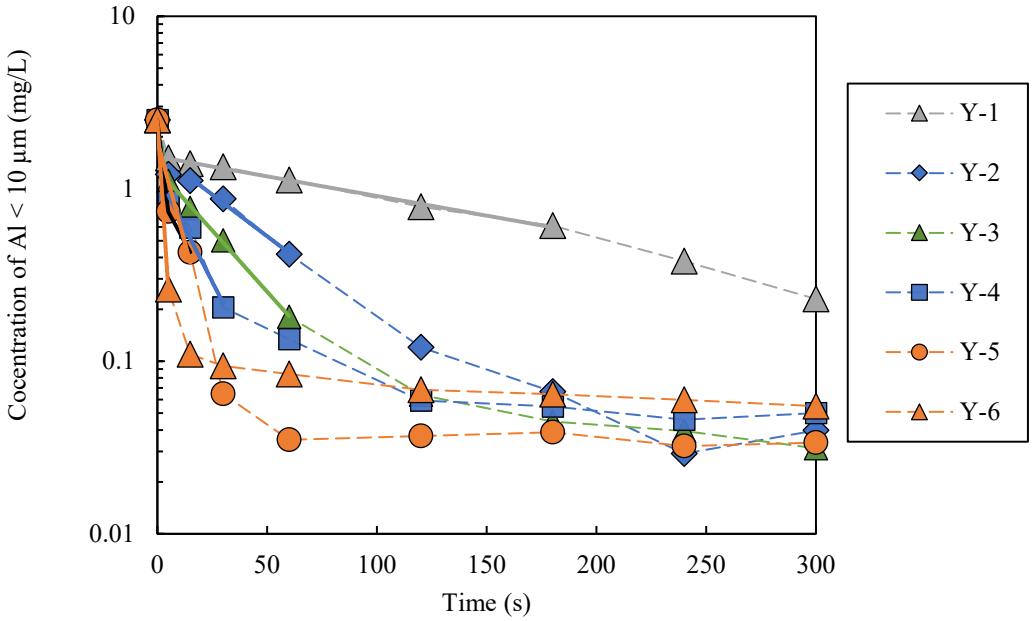

Fig. S27. Change of concentration of aluminum that passed through a membrane with a 10-µm pore size in a test of hydrolysis rates. Y series Y-1–6 waters were used. The results for HB-PACl are shown in Panel A. The results for NB-PACl are shown in Panel B. The PACl dose was 2.5 mg-Al/L. The pH during the experiment was 7.0.

A: HB-PACl

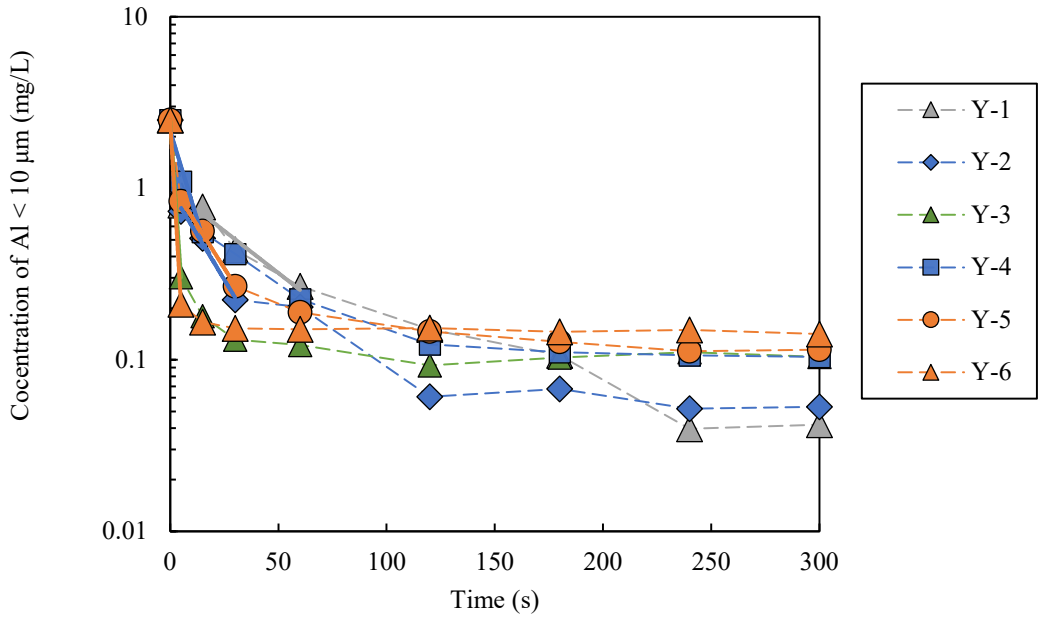

B: NB-PACl

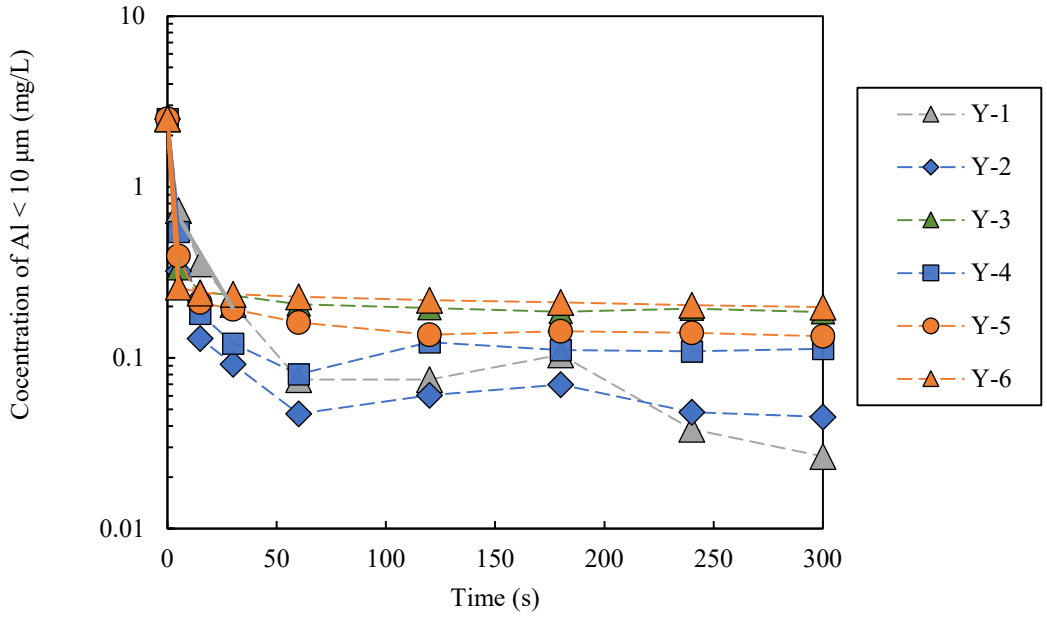

Fig. S28. Change of concentration of aluminum that passed through a membrane with a 10-µm pore size in a test of hydrolysis rates. Y series Y-1–6 waters were used. The results for HB-PACl are shown in Panel A. The results for NB-PACl are shown in Panel B. The PACl dose was 2.5 mg-Al/L. The pH during the experiment was 7.5.

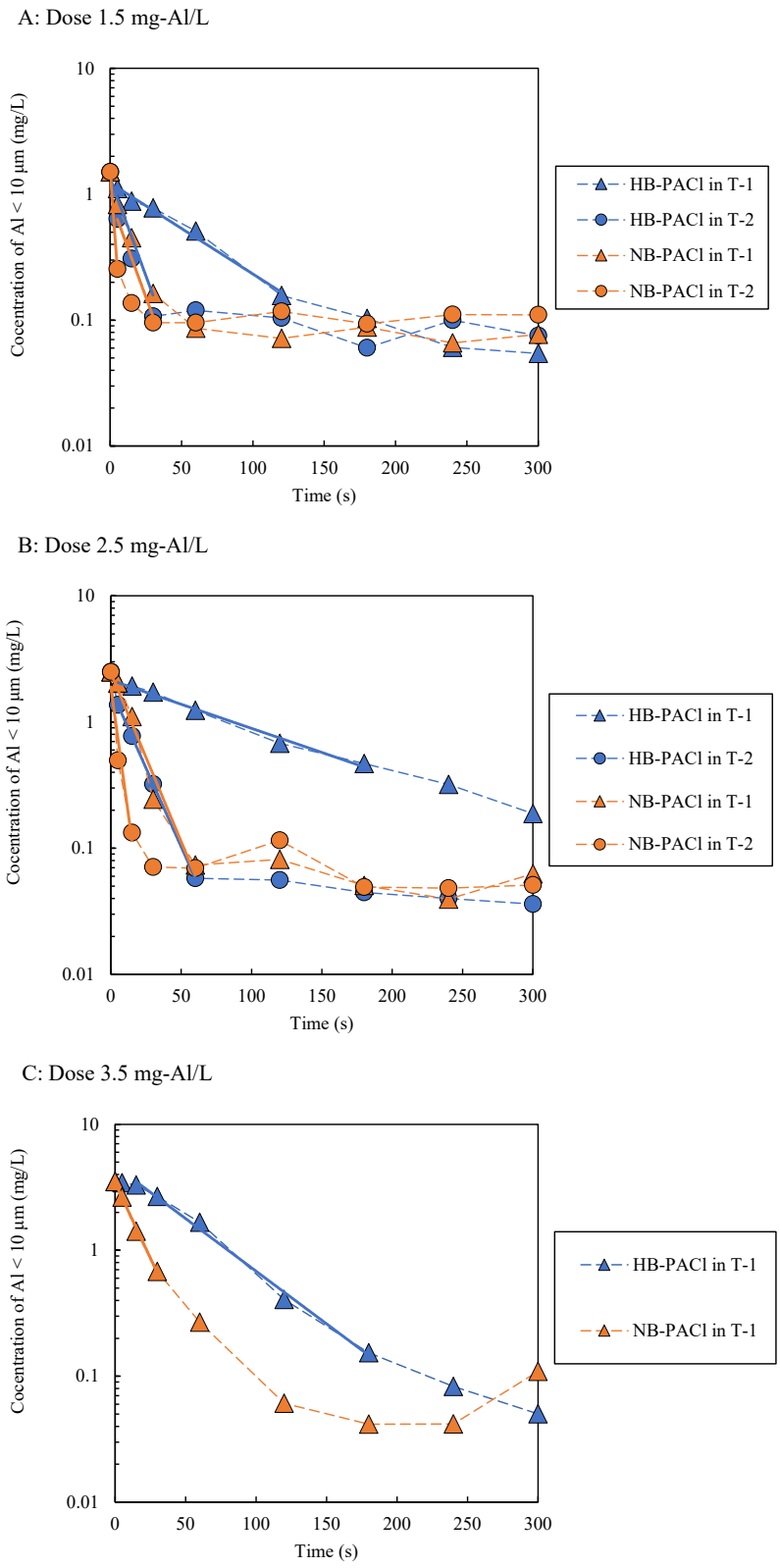

Fig. S29. Change of concentration of aluminum that passed through a membrane with a 10-µm pore size in a test of hydrolysis rates. T series waters were used. The results for PACl doses of 1.5 mg-Al/L, 2.5 mg-Al/L, and 3.5 mg-Al/L are shown in Panel A, B, and C, respectively. The pH during the experiment was 7.0.

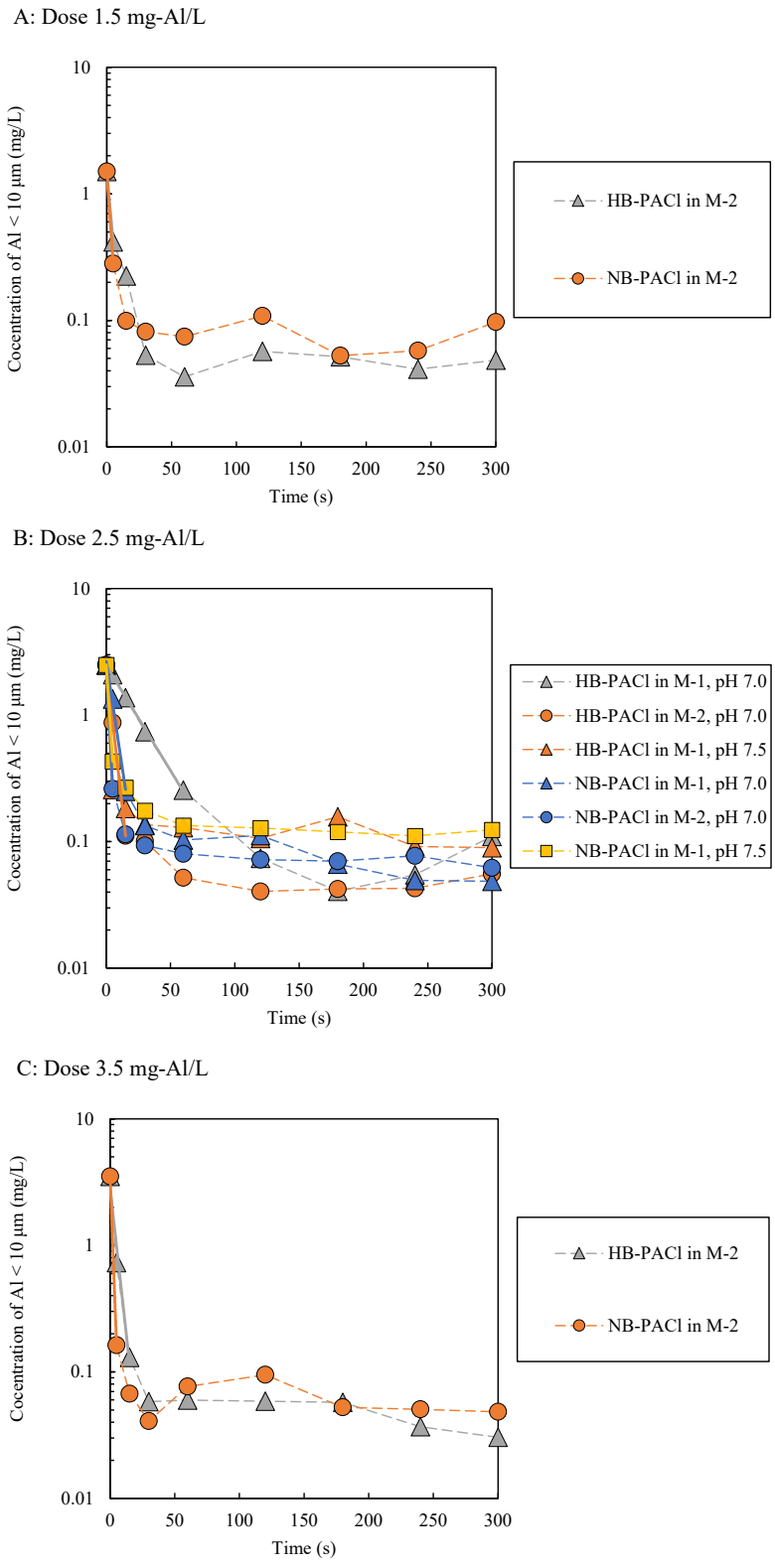

Fig. S30. Change of concentration of aluminum that passed through a membrane with a 10-µm pore size in a test of hydrolysis rates. M-1,2 waters were used. The results for PACl doses of 1.5 mg-Al/L, 2.5 mg-Al/L, and 3.5 mg-Al/L are shown in Panel A, B, and C, respectively. The pH during the experiment was 7.0 unless otherwise noted.

References

Chassagne, C., 2021. A simple model to study the flocculation of suspensions over time. Chem. Eng. Res. Des. 172, 302–311. https://doi.org/10.1016/j.cherd.2021.06.006

Chen, Y., Nakazawa, Y., Matsui, Y., Shirasaki, N., Matsushita, T., 2020. Sulfate ion in raw water affects performance of high-basicity PACl coagulants produced by Al(OH)3 dissolution and base-titration: Removal of SPAC particles by coagulation-flocculation, sedimentation, and sand filtration. Water Res. 183, 116093. https://doi.org/10.1016/j.watres.2020.116093

David R. Lide, 2004. CRC Handbook of Chemistry and Physics, 84th Edition Edited by David R. Lide (National Institute of Standards and Technology). CRC Press LLC: Boca Raton. 2003. 2616 pp. $139.95. ISBN 0-8493-0484-9., Journal of the American Chemical Society. American Chemical Society. https://doi.org/10.1021/ja0336372

Kimura, M., Matsui, Y., Kondo, K., Ishikawa, T.B., Matsushita, T., Shirasaki, N., 2013. Minimizing residual aluminum concentration in treated water by tailoring properties of polyaluminum coagulants. Water Res. 47, 2075–2084. https://doi.org/10.1016/j.watres.2013.01.037

Macintyre, J.E., Daniel, F.M., Stirling, V.M., 1992. Dictionary of Inorganic Compounds, Chapman & Hall chemical database. Chapman & Hall.

Matsui, Y., Shirasaki, N., Yamaguchi, T., Kondo, K., Machida, K., Fukuura, T., Matsushita, T., 2017. Characteristics and components of poly-aluminum chloride coagulants that enhance arsenate removal by coagulation: Detailed analysis of aluminum species. Water Res. 118, 177–186. https://doi.org/10.1016/j.watres.2017.04.037

Nakamura, H., 2009. FT-NMR data processing by computer, Secong edi. ed. Sankyo Shuppan.

Wang, D., Sun, W., Xu, Y., Tang, H., Gregory, J., 2004. Speciation stability of inorganic polymer flocculant-PACl. Colloids Surfaces A Physicochem. Eng. Asp. 243, 1–10. https://doi.org/10.1016/j.colsurfa.2004.04.073

Wang, D., Tang, H., Gregory, J., 2002. Relative importance of charge neutralization and precipitation on coagulation of kaolin with PACI: Effect of sulfate ion. Environ. Sci. Technol. 36, 1815–1820. https://doi.org/10.1021/es001936a

Yan, M., Wang, D., Qu, J., He, W., Chow, C.W.K., 2007. Relative importance of hydrolyzed Al(III) species (Ala, Alb, and Alc) during coagulation with polyaluminum chloride: A case study with the typical micro-polluted source waters. J. Colloid Interface Sci. 316, 482–489. https://doi.org/10.1016/j.jcis.2007.08.036